Operational Impact of Ammonia as Marine Fuel

A MILP model for an Ammonia-Powered Shipping Network

F. T. Boersma

Delft University of Technology

TUDelft

Thesis for the degree of MSc in Marine Technology in the specialization of
Maritime Operations and Management

Operational Impact of Ammonia as Marine Fuel

A MILP model for an Ammonia-Powered Shipping Network

by

F. T. Boersma

to obtain the degree of Master of Science
at the Delft University of Technology,
to be defended publicly on Wednesday, February 28, 2024 at 15:00 PM.

Thesisnumber:	MT.23/24.008.M	
Project duration:	February 13, 2023 – February 28, 2024	
Thesis committee:	Dr. ir. J. F. J. Pruyn,	TU Delft, supervisor
	H. Naghash	TU Delft
	Prof. E. B. H. J. van Hassel	TU Delft, University of Antwerp

Cover: Crude Tanker - Agios Fanourios I (Modified) from: http://cache.eastmedmla.com/vessels/tankers/46.jpg

An electronic version of this thesis is available at http://repository.tudelft.nl/.

TU Delft

Abstract

The consequences of climate change are becoming more and more visible. A significant cause of this is CO2 emissions; the shipping sector is responsible for 3% of global CO2 emissions. As a result, the Fourth IMO GHG Study 2020 presents pathways to reduce the GHG emission of the shipping industry by 50% by 2050. Recent IMO goals have overtaken this to reduce net emissions to zero by that year.

As a result, research in renewable energy sources has grown in significant interest, offering a wide range of potential solutions. Recently, (green) ammonia (NH3) has been added to these pools, as it is carbon-free and has a higher storage density than liquid or pressurized hydrogen. However, when comparing ammonia to the current conservative fuels, its energy density is still not at the same level, and more fuel volume would be required to deliver the same amount of energy. There are two ways to address this challenge. More frequent bunkering or larger volumes for the fuel tanks on board at the cost of cargo space and thus income. This is a difficult choice to make in the pre-design as it depends on the choices of other owners as well.

This report investigates the impact of a fuel switch to ammonia on the ship design and bunkering pattern based on the current operational profile of 1025 seagoing ships. A mixed integer linear programming model will establish the optimal fuel tank volume and bunkering strategy for each vessel. This model considers rerouting for trips that are not feasible and two approaches for the bunker strategy. Besides, a port model will establish the ammonia bunker pricing based on the resulting demand in each port. The estimated ammonia bunker prices are implemented in the bunker strategy model. This is repeated till a balance is found. The two models represent an Ammonia Powered Shipping Network considering a homogeneous shipping market. The report presents the results and key factors influencing the balance between the fuel tank volume and the sailing range. The simulated bunker strategies show different possibilities for finding this balance and reducing the operational impact caused by the transition to ammonia.

Preface

This research was undoubtedly the most challenging project of my academic career so far. Finishing this thesis has been an educational and fascinating journey. However, it wasn't all smooth sailing. I definitely underestimated how time-consuming some aspects of this research would be. Especially developing a model from scratch, along with collecting the raw data - including a set of 1025 ships and 644 ports - and transforming this into suitable input data and then writing down all these efforts in a structured report.

In the end, overcoming these bumps in the road led me to complete my master's with this thesis, as well as improving my Python skills significantly. This only makes me more excited to share my research, which hopefully will contribute to reducing the use of fossil fuels and will make the maritime industry a little bit more sustainable. Knowing that my research could be part of a bigger picture was an important source of motivation.

During this process, I wasn't completely left on my own. I would like to thank my parents. Their support, feedback, and numerous walks encouraged me to stay focused. Not at the least, I want to thank my sisters and brother, who have helped me to stay down to earth during the last months.

Above all, I would like to thank Jeroen Pruyn and Hesam Naghash for their supervision and patience throughout this project. Their assistance in finding useful data sources for the model and providing me with the AIS dataset has supported me in developing the model for my research.

This thesis marks the end of my time as a student, and I couldn't be more grateful to have studied in Delft. Over the past eight years, I have not only had the privilege of getting an excellent education, but I have also built meaningful and long-lasting friendships in my student house and in and around the university. These experiences have significantly enriched my academic and personal growth, leaving an unforgettable mark on this chapter of my life.

F. T. Boersma
Rotterdam, February 2024

Contents

Acronyms

AIS Automatic Identification System. 23, 29, 32, 37–42, 49, 50, 53, 57, 74
APSN model Ammonia Powered Shipping Network model. 19–21, 32, 41, 48, 53, 60, 69, 71–74

BS model Ammonia Bunker Strategy Optimization model. 17, 19, 20, 22–27, 29, 30, 58, 59, 62, 63
BS-model Ammonia Bunker Startegy Model. 22

CAPEX Capital Expenditures. vii, ix, 16, 20, 26–28, 71, 72
CO_2 carbon dioxide. 1, 2, 4, 13, 37

DLCOA Delivered Levelized Cost Of Ammonia. 26
DNV Det Norske Veritas. 5
DWT deadweight tonnage. 5, 8, 31–33, 72

EC European Commission. 1
EM Engine Margin. 35
ETC Energy Transitions Commission. 16
ETS Emissions Trading Systems. 1, 70
EU European Union. 68, 74

fcm fuel consumption per nautical miles. 22

GHG greenhouse gasses. 1, 2, 5, 6, 70

H_2 Hydrogen. 1, 2
HFO Heavy Fuel Oil. 5, 36

ICE Internal Combustion Engine. 36
IEA International Energy Agency. 4
IMO International Maritime Organisation. 1, 2, 5, 38, 75
IRENA International Renewable Energy Agency. 4, 5, 70

KPF Key Performance Factors. 15

LH_2 Liquified Hydrogen. 2
LHV Liquified Heat Value. 36
LNG Liquified Natural Gas. 1, 2, 5, 33, 58
LWT lightweight tonnage. 32

MAGPIE sMart Green Ports as Integrated Efficient multimodal hubs project. 5, 7, 50, 68, 70, 74
MBM Market-based Measures. 70
MCDM Multi-Criteria Decision-making. 15

MCR Maximum Continuous Rating. 34, 53

MDO Marine Diesel Oil. 5

MFO Marine Fuel Oil. 5, 15

MILP mixed-integer linear programming. 19, 20, 24

N_2 Nitrogen. 2

NH_3 ammonia. 1, 6

NO_x Nitrogenoxides. 1, 2, 12

OPEX Operating Expenditures. vii, 13, 16, 20, 24, 26–28, 42

PEM Proton Exchange Membrane. 3

PLCOA Production Levelized Cost Of Ammonia. 15, 26, 43

Port model Ammonia Bunker Port model. 17, 19, 20, 26, 27, 30, 58, 60, 62, 64, 65, 71

Ro-Ro Roll on Roll off. 5, 70

SIN Shipping Intelegence Network. 29, 38, 41, 42

SO_x Sulfoxides. 1, 2

SOFC Solid Oxide Fuel Cells. 36

TEU Twenty-feet Equivalent Unit. 33

THETIS-MRV The Hybrid European Targeting and Inspection System for Monitoring, Reporting, and Verification. 29, 31, 32, 37, 38, 40, 41, 48

TTW Tank-to-wake. 1

UK United Kingdom. 3

UN/LOCODE United Nations Code of Trade and Transport Locations. 37, 42, 71

UNFCCC the United Nations Framework Convention on Climate Change. 1

USA United States of America. 3

VLSFO Very Low Sulphur Fuel Oil. 43

WFR World Fleet Register. 29, 31–34

WPI World Port Index. 29

WTT Well-to-take. 2

List of Figures

List of Tables

1 Introduction

In 2015, the United Nations Framework Convention on Climate Change (UNFCCC) adopted the Paris Agreement. This agreement states that the participating parties must cut their emissions by 50% by 2030 to prevent global warming of more than 1.5 °C (UNFCCC, 2015). The Paris Agreement also includes maritime shipping, which is responsible for almost 3% of the carbon dioxide (CO_2) emissions worldwide in 2018, according to research presented in the *Fourth IMO GHG Study 2020* (International Maritime Organisation (IMO), 2021). A significant part of these emissions can be accounted for by international shipping (2% of the worldwide CO_2 emissions); thus, the maritime industry can play an essential role in the development of climate change (IEA, 2022). Therefore, the IMO presented a strategy to reduce the total annual greenhouse gasses (GHG) emission from international shipping by at least 50% by 2050 compared to 2008 (International Maritime Organization, 2018), which recently is enhanced to 80%. As a result, multiple organizations implemented new regulations for emissions to encourage the industry to reduce their emissions and develop more sustainable alternatives. For example, the European Commission (EC) introduced the EU Emissions Trading Systems (ETS), which makes shipowners pay for emissions, including carbon dioxide, methane and nitrogen dioxide, and the FuelEU Maritime Initiative, which sets specific GHG intensity limits on energy used onboard vessels (European Commission, 2021). The main reason for the emissions is that fossil fuels are still the most significant energy source in the shipping industry. Therefore, the shipping industry must transition to alternative fuels that produce lower or zero emissions to exert a substantial impact.

In recent decades, the research of alternative low and zero CO_2 emission fuels and their potential to replace existing fuels has significantly increased. This resulted in technical developments and sustainable innovations for the realistic implementation of alternative fuels. Currently, the high potential alternative fuels can be divided into two categories, low-carbon fuels like methanol, Liquified Natural Gas (LNG) and biofuel and zero-carbon fuels like ammonia (NH_3) and Hydrogen (H_2) (Pruyn et al., 2022; DNV, 2021; Al-Enazi et al., 2022). Ammonia and hydrogen produce no carbon emissions, and for that reason, these two fuels have an advantage over the other alternative fuels.

Due to its high hydrogen content, several sources suggest that ammonia could be a future fuel option for shipping (McKinlay et al., 2020). Like hydrogen, ammonia could be burned or used in a fuel cell. A third option would be to use ammonia as a hydrogen carrier. Transport of hydrogen contained in ammonia molecules is far more efficient than directly compressing hydrogen in fuel containers. Therefore, ammonia is gaining more interest from the industry (European Maritime Safety Agency, 2022, Hansson et al., 2020), with zero Nitrogenoxides (NO_x), Sulfoxides (SO_x) and CO_2 emissions (Al-Enazi et al., 2022), as the energy density of ammonia is higher compared to the other alternative fuels. For example, the energy density of pressured liquid hydrogen, at a pressure of 70 MPa, is three times lower than for ammonia in the same condition (Valera-Medina et al., 2018). Therefore, less storage space is required for the same amount of energy and, therefore, will have less effect on the cargo storage capacity of vessels (McKinlay et al., 2021).

When green ammonia is used as a marine fuel, not only the Tank-to-wake (TTW) process is carbon-free, but the Well-to-take (WTT) process can reduce GHG emissions as well. This makes ammonia a high potential marine fuel in the challenge to reduce GHG emissions with 80% by 2050 (familyDNV, 2023). Last year, several companies in the industry announced to invest in ammonia production plants and import in Europa (Cepsa and Fertiberia, 2023; FLUOR, 2023; OCI, 2022; HES International et al., 2022; Orsted, 2021). The prognosis is that blue and green ammonia will increase to 42% of the market share in maritime fuels, starting to substitute LNG and fossil fuels from 2035 (Wu et al., 2022). Therefore, proper and extensive research on ammonia as a marine fuel and its impact on the maritime sector is required.

1.1. Ammonia as Marine Fuel

Ammonia is a carbon-free chemical compound consisting of one Nitrogen (N_2) and three H_2 atoms, bonded to 2 NH_3, as described in equation 1.1. Ammonia is a colourless gas with a boiling point of -33°C at atmospheric pressure (1 bar) and can be liquefied at 20°C when compressed to 0.8 MPa. This makes ammonia a more accessible fuel to store compared to other renewable fuels, like hydrogen. Its gravimetric energy density (22.5 MJ/kg) is comparable to methanol (22.7 MJ/kg), ethanol (29.7 kJ/kg), which are carbon-containing fuels and is lower than natural gas (55 MJ/kg), diesel (45 MJ/kg), and hydrogen (142 MJ/kg) (Al-Aboosi et al., 2021). However, the volumetric energy density of ammonia (9.45 MJ/L) is 2.5 higher than compressed hydrogen (3.73 MJ/L) (Snaathorst, 2022). The flammability of ammonia is negligible to zero (Klerke et al., 2008), which is much lower than hydrogen and methanol (Foretich et al., 2021; National Fire Protection Association, 2017; Ji et al., 2021). This makes it possible to store ammonia safely onshore and onboard. The carbon-free fuel has a toxicity over three orders of magnitude higher than comparable fuels such as methanol or diesel (McKinlay et al., 2020). According to Al-Enazi et al. (2022), ammonia produces no NO_x-, SO_x- and CO_2-emissions, which makes ammonia an attractive fuel regarding the IMO sustainability goals.

Like hydrogen, ammonia could be burned and used in a fuel cell. A third option would be to use ammonia as a hydrogen carrier (McKinlay et al., 2020). Besides, ammonia contains more hydrogen than pressurised or Liquified Hydrogen (LH_2) itself and can be stored under more manageable conditions, either liquified under pressure (10 bar at 25°C) or refrigerated (boiling point -33°C) (Butler et al., 2023). At the same time, hydrogen has a liquefaction temperature of -253°C (ABS, 2020). For onshore and onboard ammonia tanks, it is cheaper and safer when stored in refrigerated form (Butler et al., 2023).

Production Process

The production of ammonia as a hydrogen carrier is comparable to the production of hydrogen. However, the ammonia production is expanded with an extra step to transform the hydrogen into ammonia. A standard method to realise this last step is the Haber-Bosch process. The Haber-Bosch process is a synthetic manufacturing technique to produce ammonia and takes place under high pressure (15-20 MPa) and temperatures of 400°C to 500°C. Equation 1.1 shows the chemical process in this method (Al-Aboosi et al., 2021).

$$N_2 + 3H_2 = 2NH_3 \,(-91.8\, kJ/mol) \tag{1.1}$$

To realise the Haber-Bosch process, a large amount of hydrogen is required, and therefore, ammonia production highly depends on hydrogen production. Hydrogen can be provided from fossil fuels, like natural gas, or green electricity from wind and solar energy. This results in three production processes to obtain ammonia, resulting in grey, blue or green ammonia, also known as e-ammonia.

Today, ammonia production mainly consists of grey ammonia, produced with energy input from fossil fuels. For grey ammonia, the required hydrogen is obtained from natural gas, and the next step is methane reforming to prepare the hydrogen for the Haber-Bosch process. The CO_2 emissions are significantly higher than other fuels during this process. The process for blue ammonia is similar to that for grey ammonia, except that in this process, the carbon emissions in hydrogen production are captured before the Haber-Bosch process. Therefore, the production of blue ammonia can be used to reduce carbon emissions in the production process. However, this reduces a significant part of the CO_2-emissions; it is not 100% carbon-free (Butler et al., 2023). In figure 1.1, the production process of green ammonia is demonstrated, including the Haber-Bosch process.

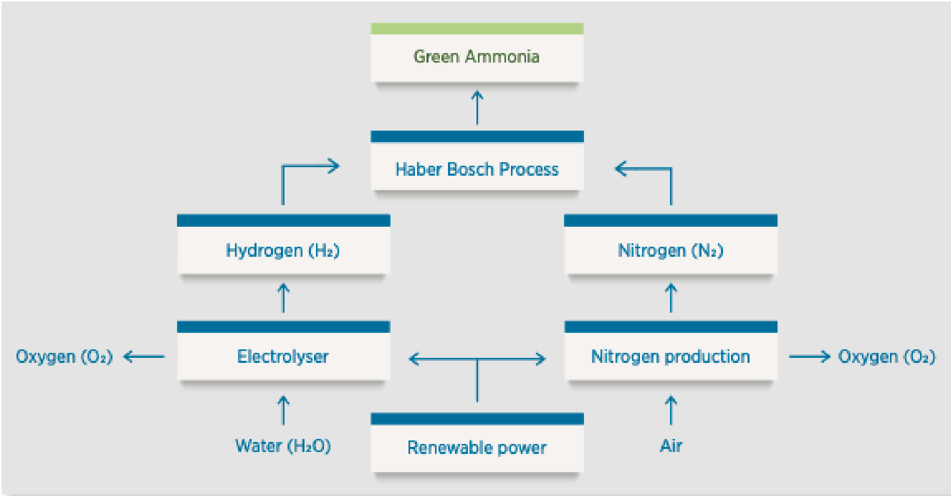

Figure 1.1: Renewable e-ammonia production process via Haber-Bosch process (IRENA, 2021)

Green ammonia is the cleanest production process for ammonia production, with 0% carbon-emission. In this process, the energy input is obtained by green energy power plants like solar panels, wind turbines and hydropower (Armijo and Philibert, 2020). Using this green electricity and electrolysis, water is split in an electrolyser to produce the hydrogen required for the Haber-Bosch process. Commonly used electrolysers are an alkaline electrolyser, an Proton Exchange Membrane (PEM) electrolyser, or a solid oxide electrolyser. The technology for green ammonia production is still under development. Following in promising results of green ammonia pilot plants converting solar and wind energy into ammonia and producing 20-30 kg/day (Japan and United Kingdom (UK)), or 25 tons/year (United States of America (USA)) (Al-Aboosi et al., 2021). Besides the promising results and the proof of concept, green ammonia has not been developed for large-scale production. Next to the onshore ammonia production development, recent research is also looking into opportunities for offshore hydrogen and ammonia power plants to expand the future demand for ammonia (Salmon and Bañares-Alcántara, 2022).

Ammonia Market

Ammonia is not a novel stock on the global market. For decades, ammonia has been transported overseas as a commercial good and is mainly used to create fertiliser in agriculture (McKinlay et al., 2020). According to Valera-Medina et al. (2021), the global ammonia production in 2021 amounts to 146 million t/year, with primary production locations in China (48 Mt/year), Russia (12 Mt/year), India (11 Mt/year), and the USA (9 Mt/year). The report from ALFA LAVAL et al. (2020) estimated the annual global production of 180 million tons, including an overcapacity of 60 million tons. This report suggests an ammonia fuel price of $13.5 per gigajoule (GJ).

The infrastructure for ammonia distribution already exists globally, and 120 ports are equipped with ammonia trading facilities (ALFA LAVAL et al., 2020). Besides the existing ammonia ports, the global ammonia trade indicates the experience of safely storing ammonia onboard vessels. This confirms the potential feasibility of ammonia-fueled vessels and an ammonia bunker network.

However, an ammonia-powered shipping industry of 40% of the global shipping market suggests by Scarbrough et al. (2022) requires the ammonia demand for the shipping industry will be 150 to 200 million tons per year (ALFA LAVAL et al., 2020). Besides, the shipping industry is not the only market for ammonia, as it will also be used for industrial demand, power generation, cracking into hydrogen and fertiliser (Butler et al., 2023). Considering this, the supply chain for ammonia has to increase. Nayak-Luke and Bañares-Alcántara (2020) establish a selection of 534 potential locations for green ammonia production, shown in figure 1.2.

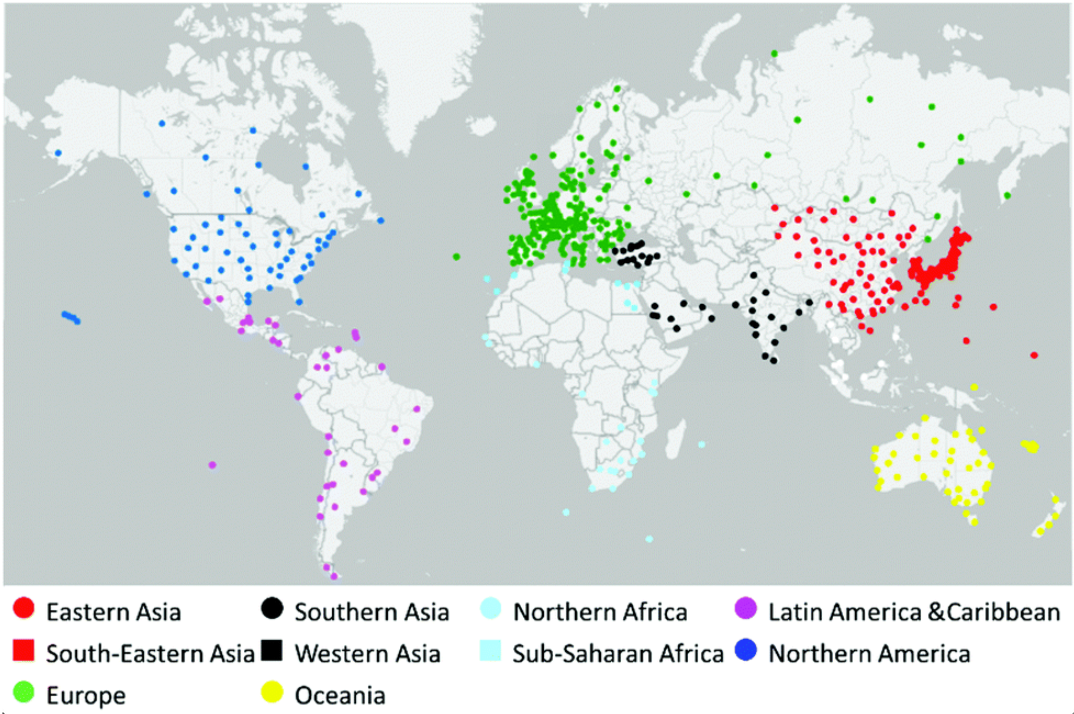

Figure 1.2: Potential location for green ammonia production, grouped by geographical region (Nayak-Luke and Bañares-Alcántara, 2020).

The reports of IEA (2021) and IRENA (2021) confirm that ammonia will expand to be a significant contributor to the marine fuel market. The IRENA report suggests that ammonia will be responsible for 40% of the global fuel demand in 2050, according to the plausible pathway. This pathway considers the scenario where global warming is limited to an increase of 1.5°C and brings CO_2 emissions closest to net zero by 2050. In figure 1.3, the development of the energy demand according to the 1.5°C scenario from IRENA (2021) is shown.

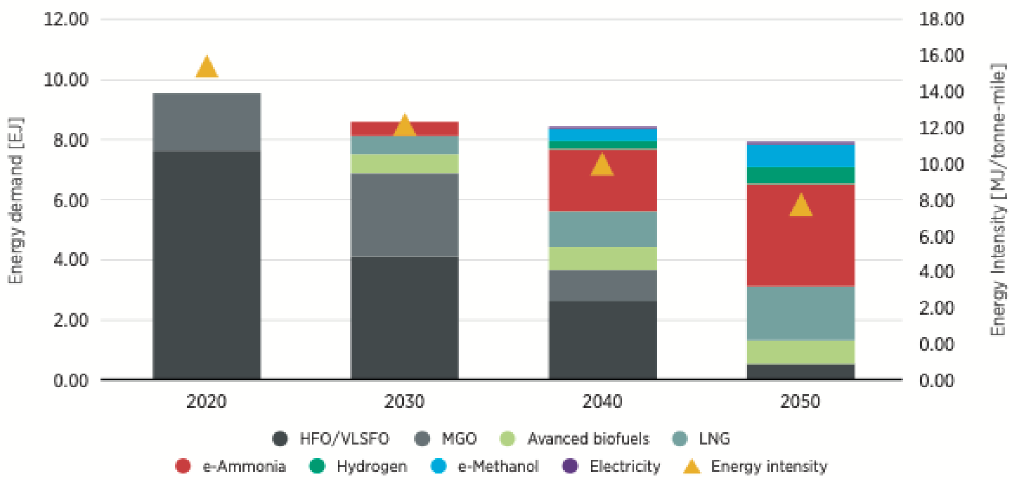

Figure 1.3: The energy demand development considering the 1.5°C Scenario energy pathway 2018–2050 from IRENA (2021)

Ammonia and shipping

The opportunities of ammonia as a marine fuel are broadly recognized in the maritime industry. Multiply organizations, like the International Renewable Energy Agency (IRENA), International Energy Agency

(IEA), and Det Norske Veritas (DNV), drawn pathways suggesting ammonia will become the marine fuel of the future, become responsible for 30 to 40 % of the total marine fuel market in 2050. Their confidence in the high potential of the zero-carbon fuel is mainly based on ammonia's environmental and energy transfer advantages. Several companies have already relied on the fuel's potential and have invested in large ammonia production power plants.

The promising character of ammonia as a renewable fuel for the maritime industry enforces the significant increase in research on this topic, both academically and from the industry itself. Multiple studies have investigated the design and performance changes required for a ship to be powered with ammonia. These studies discuss a wide variety of ships, among others: LNG carriers (McKinlay et al., 2021), containerships (Wu et al., 2022), bulk carriers (Sommer, 2023) and tankers (Snaathorst, 2022). These four studies acknowledge that the lower energy density of ammonia will increase the required fuel tank volume of the ships to maintain the same energy output compared to Heavy Fuel Oil (HFO), Marine Diesel Oil (MDO) and other conservative fuels.

According to Yang and Lam (2023), fuel tanks of an ammonia-powered ship require 1.6-2.3 times more volume than conventional Marine Fuel Oil (MFO) powered ships. For ships powered with LNG, the tank volume needs to increase with 50% of the fuel tank to provide the same amount of power (Machaj et al., 2022). This will impact the ship design (larger ship sizes or decreased cargo space) and the bunkering pattern (smaller sailing range or bunker more frequently) or both. Secondly, ammonia is known to be a highly toxic substance. This is considered a main issue for ammonia as a marine fuel (ABS, 2020). Therefore, it is recommended that strict safety regulations be developed and specific crew training should be provided before implementing the fuel.

Next to this, a switch to ammonia as a marine fuel is not only affecting the ship's design and performance. In the prospect of the suggested pathway towards 2050 by IRENA, the ammonia-powered ships will also have an impact on the shipping network in general. Supply possibilities, like bunker location and supply capacities, have an impact on ship design and other considerations. The operational aspect of the ammonia-powered shipping network has been inadequately addressed in recent research, in contrast to the technology and environmental impact. However, the sMart Green Ports as Integrated Efficient multimodal hubs project (MAGPIE) project is exploring the bunker supply possibilities for green energy carriers, like ammonia.

The MAGPIE project is a European-orientated project with the goal of reducing the GHG emissions in the transport sector, including seagoing transport. Part of this project focuses on investigating alternative fuels in several transport methods. According to their last deliverable, ammonia came forward as one of the future fuels for seagoing ships, especially for trips of more than one day (Pruyn et al., 2022). More specifically, ammonia is the most suitable fuel for larger vessels, >25000 deadweight tonnage (DWT), including container vessels, Roll on Roll off (Ro-Ro) vessels, bulk carriers, tankers and miscellaneous. The report assumes these vessels will use ammonia for trips of 2 to 4 days from 2040 on. From 2050 on, ammonia is also suited for trips longer than five days (Pruyn et al., 2022). This conclusion is supported by other research, which acknowledges that ammonia as a fuel will be most relevant for seagoing shipping (Christodoulou and Cullinane, 2022; McKinlay et al., 2021; Wu et al., 2022). According to the IRENA (2021), "Large and very large ships are responsible for about 85% of net GHG emissions associated with the international shipping sector". Considering this statement, a fuel switch to ammonia would be even more effective to reach the climate goals purposed in the *Fourth IMO GHG Study 2020* for IMO (2021).

All in all, ammonia is a promising fuel to reduce the GHG emissions in maritime shipping. Research has shown the technical and environmental possibilities of ammonia (van Veldhuizen et al., 2023) and the required safety regulations for the use of ammonia as a fuel onboard and onshore (ABS, 2020; National Fire Protection Association, 2017). However, the impact of ammonia on the operational aspects of the maritime industry and what is required to implement ammonia as a bunker fuel in the current shipping network is not investigated in prior research. Therefore, this report presents research on the operational feasibility of an ammonia-powered shipping network, considering related challenges regarding the increase in fuel volume for ammonia.

2 Problem Statement

Recent research shows promising theoretical results for ammonia as a marine fuel, especially for seagoing ships. This fuel could contribute as a potential solution to reducing the GHG emissions in maritime shipping (van Veldhuizen et al., 2023). The published research about ammonia is mainly attracting the technical and environmental possibilities of ammonia and the required safety regulations of the use of ammonia as a fuel onboard and onshore (ABS, 2020; National Fire Protection Association, 2017). However, the operational impact of ammonia on the operational aspects of the maritime industry and what is required to implement ammonia as a bunker fuel in the current shipping network has not been investigated in prior research. Two operational challenges emerge when implementing ammonia as a marine fuel in the global shipping market. The increasing fuel volume required to deliver the same amount of energy impacts the ship's design and performance, and the non-existent ammonia bunkering network introduces uncertainties regarding the reliability of the supply.

2.1. Energy Density of Ammonia

The first operational challenge regarding ammonia as a marine fuel occurs as a result of the lower energy density of the fuel compared to conservative fuels, like fuel oil, as shown in table 2.1. To provide ships with the same amount of energy, the required fuel volume will increase significantly. This implies that the fuel tanks of ships have to be expanded to realize the switch to ammonia, which impacts the ship's design. Increasing the fuel tanks results in a reduction in the cargo capacity of the ship and, therefore, a reduction in the income of the ship operators. Alternatively, the required fuel volume of the ships can be cut by lowering the fuel consumption. Fuel consumption is related to the ship's performance, depending on, among other things, the ship's sailing speed and the range at which it sails. Considering these relations, a lower sailing speed or shorter distances can reduce the expansion of the fuel tanks for ammonia-powered ships. Combining these possibilities to deal with this challenge can result in a minimal impact on the design and performance of the ship. According to the student, no studies have been published yet regarding this challenge on a global scale.

Table 2.1: The volumetric energy density (ρ_{VE}), gravimetric energy density (ρ_{ME}) and density (ρ) of Fuel Oil and Ammonia (IRENA, 2021; Snaathorst and Pruyn, 2022)

	Volumetric energy density [MJ/L]	Gravimetric energy density [MJ/kg]	Density [kg/L]
Contained Fuel Oil	33.20	29.65	1.12
Uncontained Fuel Oil	35.70	41.00	0.87
Contained Ammonia	9.45	11.70	0.81
Uncontained Ammonia	12.70	22.00	0.58
Contained ratio NH_3/FO	3.51	2.53	1.38
Contained ratio NH_3/FO	2.81	1.86	1.5

Recent research shows that the fuel tank onboard the ship has to change significantly when the fuel switches to ammonia. The volume and the weight of the fuel can increase by 50% and 100%, respectively (McKinlay et al., 2021;Wu et al., 2022). This affects the total weight and space consideration in the ship design. Considering that the fuel tank of the ship requires more space, there is less space left for cargo, or the ship needs to be larger. Another way to deal with this is to make a compromise in the sailing range of the ship or to find a way to reduce fuel consumption (Foretich et al., 2021; Prussi et al., 2021). Considering that most merchant ships are designed with fuel tank volumes that fit 2.5 times the required amount of fuel oil for their trips, the ships can bunker at the ports with the lowest bunker prices on their route (Snaathorst, 2022). This overcapacity can contribute to decreasing the impact of the energy density of ammonia on the ship design. Therefore, a balance should be found between the increase of the fuel tank volume and the reduction of the sailing range.

2.2. Uncertain Bunker Supply

Secondly, there are still uncertainties regarding the availability and supply of the fuels, which are related to the bunker price and uptake of ammonia in the market (Prussi et al., 2021). Several developments are going on, but most of them have not been realized and proven in practice. Regarding the availability of ammonia supply ports, an estimation of the future demand for ammonia in ports is required to generate a feasibility analysis for investing in ammonia supply facilities in ports. This uncertainty makes it difficult to indicate the prospection of the fuel price for ammonia, which is significantly higher than conservative fuels. However, by switching from conservative fuels to ammonia, ship operators can avoid possible carbon taxes due to the carbon-free character of ammonia.

2.3. Research Questions

The two challenges posed in sections 2.1 and 2.2 both reflect on the operational feasibility of ammonia as a marine fuel and will be investigated in this research. Therefore, the objective of this research is to develop a model for an ammonia-powered shipping network. The model has to examine the operational performance of the ships considering a fuel switch to ammonia. This includes the effect of the design and performance parameters of ships. Besides, the model has to explore the opportunities for ammonia bunkering. In order to obtain the research objective, the main research question this report will answer is:

What is the operational impact on the ship design, performance and bunker port network when switching to ammonia as a marine fuel, considering a homogeneous shipping market?

Sub questions

To answer this main research question, the following research questions are established:

1. What parameters have a significant influence on the operational performance of seagoing vessels, like the fuel consumption and bunkering pattern?
2. What are the model requirements to simulate the operational impact of ammonia on the ship design and performance and the bunker port network?
3. What is the impact on the **fuel tank volume** of seagoing vessels with an economical and operational feasible ammonia bunker strategy?
4. What is the impact on the **sailing speed** of seagoing vessels with an economical and operational feasible ammonia bunker strategy?
5. What is the impact on the **sailing range** of seagoing vessels with an economical and operational feasible ammonia bunker strategy?
6. Which **ports** are suitable to be part of an ammonia bunker port network, which is economical and operationally feasible?

The objective of this research derives from the results in *Deliverable 3.1* and *Deliverable 3.6* from the MAGPIE project and the growing interest in the potential of ammonia as a marine fuel (Pruyn et al., 2022; Butler et al., 2023). Therefore, this research is performed within the scope of the MAGPIE project. The research presented a model for an ammonia-powered shipping network that is EU-oriented and specified for seagoing ships with a DWT larger than 25000 tonnes. Besides, it is assumed that the ammonia-powered shipping network is implemented as a homogeneous shipping market for ammonia.

2.4. Methodology

This section briefly describes the methodology that was followed for this research. Figure 2.1 shows a schematic overview.

Figure 2.1: The five steps perform in the research.

Literature Research

Firstly, literature research is performed to determine the relations between the main design and performance parameters regarding bunker strategies and the consequences of ammonia as a marine fuel. Besides, current studies on bunker strategy models and port choice models are researched to establish the model requirements. The literature research also includes a further investigation to determine the requirements and expenses for bunker ports to supply ammonia.

Data Collection

By performing a case study, the operational impact of ammonia can be studied in a realistic simulation of an ammonia-driven shipping network. The data for the simulations is obtained from the Clarkson World Fleet Register and the EU MRV-THETIS database. MarineTraffic.com provided the AIS port call data of the selected ship. The port data used in the case study is obtained from the World Port Index and complemented manually based on port data from MarineTraffic.com.

Data Processing

The available data cannot be adopted directly and is partly incomplete. Therefore, the data has to be transformed to be suitable and plausible input data for the model. In this process, the AIS data has to be cleaned to ensure a consistent sequence of port calls. Next to that, the ship data requires an extension to provide the required ship parameters for the model, and all data sets need to be merged.

Modelling

A model is established to examine the operational feasibility of an ammonia bunkering network. This model contains two parts. Firstly, an ammonia bunker optimization is developed to minimize the ship's loss of income based on fuel consumption. The optimization is performed in Python based on mixed integer linear programming. The model will generate an economic optimal balance between the changes in the fuel tank volume, the sailing range and speed. This model also indicates the ammonia demand in each port. The second part of the model estimates the fuel price of ammonia in each port and considers the demand and the costs to provide port facilities for ammonia supply. Modelling is done in Python with the use of the shortest route package from `networkx`.

Research Results

The results are presented in different scenarios that give a quantitative output of the costs, revenue, and port attractiveness of ammonia fuel demand and prices. These results are for the larger part presented per fleet type.

3
Literature Research

This chapter gives an overview of the recent developments regarding the effect of ammonia on ship performance, which is the result of the literature research. In section 3.1, the relationships between significant performance and design parameters are explained. These parameters will set the core structure of the model that is developed in this research. In section 3.2, the optimization approaches for a bunker strategy model are discussed. In section 3.3, the important considerations for port choice models and the formulation of the ammonia production price are described. This literature research establishes the main structure of the model. In section 3.4, the model structure is presented, as are the model requirements and assumptions.

3.1. Ship Parameters

In this section, the effect of ammonia on the design and performance parameters is described. The parameters that will be elaborated on are volume and mass, speed, fuel consumption, and sailing range. These parameters are assumed to be most relevant regarding a transition to ammonia. The parameters are elaborated individually, and their relation to other parameters is explained. Other parameters that are appointed in this section are emissions, ship deployment, ammonia and operational expenses. An overview of the relation between the parameters is summarized in table 4.3.

Weather conditions are a factor that affects the ship's performance. However, the implementation of weather conditions in a model requires a large dataset and depends on the exact location of the ship. This results in very detailed fluctuation in the performance. Therefore, the weather conditions in this research are neglected.

3.1.1. Volume and Mass

On this matter, Snaathorst and Pruyn (2022) studied the design and powering impact of alternative fuels, including ammonia, for three ship types. This study develops a parametric design tool, which provided the results shown in table 3.1 for using ammonia as fuel. The results describe the impact of ammonia on the ships by an indication of the change regarding fuel oil for six design parameters: total installed power ($\Delta P_{B,TOT}$), main engine brake power ($\Delta P_{B,ME}$), overall internal volume (ΔV_{INT}), lightweight ship (Δm_{LIGHT}), deadweight tonnage (ΔDWT) and length-beam ratio ($\Delta L/B$).

Table 3.1: Design and power impact results for bulk carriers, tankers, and container ships using ammonia w.r.t. fuel oil. (Snaathorst and Pruyn, 2022)

ship Type	$\Delta P_{B,TOT}$	$\Delta P_{B,ME}$	ΔV_{INT}	Δm_{LIGHT}	ΔDWT	$\Delta L/B$
Bulk carriers	+3.7%	+4.4%	+5.3%	+21.8%	+2.2%	+1.0%
Tankers	+3.2%	+4.2%	+5.2%	+9.6%	+2.5%	+1.9%
Container ships	+4.9%	+5.9%	+7.4%	+18.5%	+5.5%	+2.4%

An ammonia-powered ship requires more space for its fuel tank volume and propulsion system. There are two alternatives to implement this in the ship design. The size of the ship stays the same, and the cargo capacity of the ship reduces, or the size of the ship increases, equivalent to the increase in the fuel tank volume and propulsion system. An alternative design consideration is to obtain a balance between increasing the fuel tank volume and bunkering more frequently. These considerations are simulated in the scenarios of this research.

Fuel Tank Capacity

As mentioned before, one of the main issues of ammonia as a marine fuel is its lower energy density (Valera-Medina et al., 2018). As a result of which, the fuel volume required for the same energy content will be larger. Therefore, the fuel tank volume of the ship is an important element to analyze. Using ammonia requires adjustments to the size and mass of the propulsion system.

Lagemann et al. (2022) compared eight fuels on their performance for two trips of a LNG carrier with 73000 t deadweight (dwt) and 290 m length and 2700 m^3 fuel oil tank volume. This study indicates that the fuel tank volume of the ship using ammonia needs to be 32% to 35% larger compared to an HFO-powered ship. For the total fuel tank mass, the difference between ammonia is even bigger, 48% more weight for ammonia. These results are relevant in the context of the impact of ammonia on the ship design. Both the ammonia tank volume and the ammonia fuel mass are parameters that are taken into account in the modelling in this research.

Energy System Requirements

Implementing new engine systems, like SOFC, involves changes in the design of the ship (ABS, 2020). According to Wu et al., 2022, the volume of an ammonia SOFC has to be 2.5 times larger than the HFO ICE systems. The expected lifetime of the SOFC for ammonia is five to ten years, and 20 years for HFO ICE. The CAPEX of the system is about 50% higher compared to the engine system for HFO ICE. This includes the replacement of the SOFC after seven years. They also did an estimation for the OPEX of the ammonia SOFC system, based on the annual energy consumption, which is over 80% more expensive than an HFO-powered container carrier with the same operation profile. Important to mention is that next to the OPEX, the paper calculates the expected extra costs following the ETS regulation and includes an extra carbon tax in the OPEX for the HFO system.

Solid oxide fuel cells (SOFC) can be used to convert the hydrogen stored in ammonia directly to electricity. These SOFC systems are estimated to be 1.5 times bigger and heavier than diesel engines, producing the same power amount (Machaj et al., 2022).

3.1.2. Speed

Ships are designed with a design speed. This is the optimal speed for the installed propulsion system. This speed depends on the ship type, size, and the purpose of the operation. In general, the design speed operates at 80% of the engine power of the propulsion system. Nevertheless, the ideal speed of the ship can change during operation due to weather conditions, technical reasons or economic reasons. The latter refers to the economic speed and is based on fuel efficiency.

The economic speed of a ship is interesting, so we should have a closer look at the operational profile of the ships. For example, from the shipowners' perspective, it can be more attractive to lower the speed when the fuel price gets higher (Wen et al., 2017). So, the fuel consumption is reduced, and the operational expenses do not increase too much. Economic speed represents the speed that ensures the optimal balance between operational costs and revenue for the ship's operation.

It can also be eligible to sail faster than the design speed to avoid penalties for being late or providing special service by fast delivery. Higher speed implies a larger amount of fuel consumption, whereas it is also shorter transit time and a smaller number of ships required to deliver the same service (S. Wang and Meng, 2015). More bunker consumption results, in general, in higher operational expenses because fuel costs are a main element. In contrast, freight rates are responsible for shipowners' revenues.

However, speed reduction is an upcoming interest in terms of emission reduction. Lower speeds reduce the fuel consumption and, therefore, the emission of the ships (Lindstad and Eskeland, 2015). This can be part of the solution for fuel tank volume challenges that arise from a transition to ammonia.

Correspondingly, the research of Kouzelis et al. (2022) analyses the impact of alternative fuels on economic speed. According to this research, lower sailing speeds are the result of the switch to alternative fuels in maritime shipping. The consequence is that more ships are required if ships operate at lower speeds, considering that the ship size remains constant. The downside of this is that the transit time of the ship will increase, and it can result in less sufficient service to the clients or lower freight rates. Sailing speed is taken into account in this research model.

3.1.3. Fuel consumption

In the prior subsection, the relation between speed and fuel consumption is already explained. Higher sailing speeds result in more fuel consumption. However, more fuel consumption does not necessarily imply an increase in the sailing speed because fuel consumption depends on more factors.

Speed and the frequency of rotation of the engine have the most effect on the fuel consumption per mile (Işıklı et al., 2020). Other factors that impact the fuel consumption are distance, draught, and cargo load. The draught and cargo load depend on the operational mode of the ship, laden or ballast. Işıklı et al. (2020) also considers wind and sea waves as environmental effects on fuel consumption. To implement the environmental conditions of the trips, the ship's route must be known. The route of the ship is not determined as input data for the model because part of the problem is assigning the potential ammonia bunker ports. Therefore, it is not useful to implement these factors in the model. Besides, applying environmental factors to the model includes a large data set and probabilistic distributions, which complicates the model and increases the solving time. For this research, the relevance of the factors does not benefit compared to the complexity.

Fuel consumption has two approaches: the fuel consumption per mile and the total fuel consumption of a trip. The latter depends mainly on the sailing distance of the ship. If the required total fuel consumption of a trip is higher than the fuel capacity of the ship, the ship cannot complete the trip. This is a possible scenario, considering the energy density of ammonia, which results in large fuel volumes to provide the same energy content. Speed reduction can offer a solution to reduce fuel volume, which is elaborated in the subsection Speed.

The fuel consumption is directly related to the fuel costs of the ships. Fuel costs are a significant component of the shipowner's operational expenses. Therefore, it is indirectly related to the fuel price of ammonia. When the fuel price increases, it is more profitable to reduce the fuel consumption in order to manage the increase in fuel costs.

There are multiple concepts to collect fuel consumption data. Christodoulou and Cullinane (2022) applied the MRV database to their model. The MRV database monitors the fuel consumption per ship per year. Prussi et al., 2021 compared the results of an MRV-based model with the results of the POTEnCIA model (JRC, 2019) to derive more representative results for fuel consumption. Fuel consumption is taken into account in this research model.

3.1.4. Sailing Range

Following the strong correlation between fuel consumption and the sailing range of a ship, the sailing range represents an important performance parameter regarding ammonia as a marine fuel. The fuel consumption and the fuel tank volume of the ship define the ship's range. Considering the volume increase of the fuel tank in the ship design, the sailing range of the ship remains the same. This requires arrangements in the ship design.

An alternative to address the increase in fuel tank volume is to reduce the sailing range of the ship. As a result, the required amount of fuel decreases, which implies a smaller fuel tank is required. Shorter sailing routes are suggested to reduce the fuel consumption of the ship when fuel prices increase (Wen et al., 2017). Therefore, this can be a method to obtain this effect. Regarding this measure, it is essential to consider the distance between ammonia supply bunker ports. The sailing range of the ship has to be larger than this distance, and otherwise, it is not feasible to operate with an ammonia-powered ship.

As the total fuel consumption appears to be an important parameter in relation to the sailing range, the fuel consumption per mile affects the sailing range as well. In parts Speed and Fuel Consumption, the relation between those parameters is elaborated. In combination with the relation between the sailing range and fuel consumption, this results in an indirect relation between the sailing range and the speed of the ship.

There is research considering the relation between fuel consumption and range (Lagemann et al., 2022; Lagemann et al., 2023). The downside of this research is that it focuses on the required amount of fuel for a fixed range, which results in a large increase in the fuel capacity. However, concerning the ship design, limitations in the fuel tank volume can occur. Considering the limitation in the fuel tank volume of ships and including renewable fuels, like ammonia, further research is relevant to obtain an optimal balance between the fuel tank volume and the sailing range of the ship. The sailing range and reduction of trip distances through rerouting are taken into account in the model of this research.

3.1.5. Other performance parameters

Emissions

Recent research in the operational performance of ships applies the scope not only to the economic aspects of optimal ship performance but also to the environmental aspects. This results in a broad range of models that, besides minimalizing the costs, aim to maximize the emission reduction. Related to regulation as the EU ETS and levy for (carbon-)emissions, this is an important competency to include in the models.

Although ammonia is a zero-carbon fuel, there is no carbon emission during the operational stage. Ammonia still causes NO_x emissions, and therefore emission fees can be considered. However, the impact of emissions will be less relevant. On the other hand, ammonia-powered ships can have a lower OPEX compared to low-carbon fuels because of this (Lindstad et al., 2015).

Especially regarding green and blue ammonia, the advantage of no carbon emission can be significant. Green and blue ammonia are produced with wind and solar energy; therefore, even the production process is carbon-free. As a result, the wake-to-tank (WTT) and the tank-to-wake (TTW) are carbon-free and avoid carbon taxes (Armijo and Philibert, 2020).

This could suggest that the impact of emission reduction is not very relevant in the case of ammonia. However, this can be a significant difference when comparing the operational expenses of ammonia to the costs of ships powered by fossil or low-carbon fuels. Therefore, emission does not directly impact the performance of an ammonia-powered ship. However, it is recommended that this advantage be mentioned in terms of economic and environmental aspects in comparison to other fuels.

Ship deployment

The operational profile of a ship depends on the ship's deployment by the shipowner. The operational profile shows the different operational modes of the ship and the time it takes to complete the operation. Wu et al. (2022) considered three operational modes in his research;

1. the transit mode, when the ship is sailing from destination A to destination B,
2. the in port mode, when the ship is at berth in port or anchorage and,
3. the manoeuvring mode, when the ship is manoeuvring in and out of the port.

With ship deployment, the shipowner manages the time the ship operates in each mode, referring to transit time, port time, and manoeuvring time. As discussed in the subsection Speed, the transit time depends on the sailing speed of the ship. The relation between these two parameters contains an increase in transit time for lower speeds. As a result, the time to complete a trip is longer, and therefore, the shipowner can assign the ship to fewer trips. To maintain the same service, more ships are required (Kouzelis et al., 2022). Alternatively, changing the trip and route selection for the ship can be a solution. Regarding ammonia, the locations of the ammonia bunker ports will impact this consideration.

Considering that the time required to manoeuvre in and out of the port remains the same, increasing the transit time results in less time left in the port. When a ship is in port, the purpose of its stay differs, among others, from bunkering, cargo handling maintenance, or the ship is idle. Therefore, more transit time does not directly result in fewer trips. The extra time used in transit mode can be compromised with the time a ship is not deployed. This flattens the impact of speed reduction on the deployment of the ship. To define the relevance of this theory, more research on the distribution of transit time and in-port time is recommended. An analysis based on AIS data can provide a clear indication of this topic.

Furthermore, the cargo capacity of the ship is related to ship deployment. The cargo capacity depends on the fuel tank capacity of the ship. In the case of ammonia, the fuel tank volume of the ship increases, and the cargo capacity decreases, assuming the ship size remains constant. In other words, the DWT capacity of the ship remains the same, as well as the total capacity of the fuel tank and the cargo. As a result, the transport service offered by the shipowner contains less cargo capacity. The shipowner can consider deploying more ships to continue the same service.

Operational cost of the ship

The maritime transport sector is a commercial industry. Therefore, costs and revenue are important parameters to the shipowners. This literature research is focused on the operational aspect of the shipping industry; thus, in this part, the costs regarding this are elaborate, in other terms, the operational expenses or OPEX. The OPEX contain (Merien-Paul et al., 2019;Gore et al., 2022):

1. bunker costs,
2. port fees,
3. emission fees (carbon tax),
4. cargo inventory costs,
5. crew salaries, and
6. maintenance expenses

The bunker costs influence the OPEX the most and depends on the fuel price of the bunker port (Lashgari et al., 2021). Besides the shift from fossil fuels towards ammonia, no significant changes are assumed regarding the other five categories. In contrast, the ammonia bunker price is expected to be higher than the conservative fossil fuel (Prussi et al., 2021). This is without the adoption of potential emission fees. Wu et al. (2022) suggest the bunker price for green ammonia in 2030 is 700 USD/1000 kg and will decrease towards 580 USD/ 1000 kg in 2050. The fuel price for blue ammonia is estimated at 475 USD/ 1000 kg and remains constant between 2030 and 2050. Currently, there are no ammonia-powered ships in operation and ammonia as a large-scale marine fuel will be used from 2040 (Pruyn et al., 2022). The timeframe generates a large uncertainty regarding the estimation of the fuel price for ammonia.

Reducing the energy consumption of ships can be done by reducing the speed of the ship. Lindstad and Eskeland (2015) present the potential of this theory for three scenarios: high fuel cost (900 USD per ton), moderate fuel cost (600 USD per ton) and low fuel cost (300 USD per ton). The performed speed optimization shows for all scenarios that the cost in USD per ton transported is minimal at a speed around 1.5-2 knots lower than the ballast speed. For high fuel costs, the effect of speed reduction is three times more than for the low fuel cost. Lowering the speed of the ship results in longer travel times, so Lindstad included cargo inventory cost in the speed optimization and took a fourth scenario to include the effect of CO_2 emission fees of 100 USD per ton. This results in the optimal speed increasing back to the design speed in the case of the low and moderate fuel cost scenarios. For the high fuel cost and CO_2 emission fees scenarios, the optimal speed increases as well, but it is still lower than the design speed.

The uncertainty related to fuel price is addressed in several distributions in prior research. Y. Wang et al. (2018) address the fuel prices by using distribution-free fuel prices based on fundamental descriptive statistic information, including the lower and upper bounds, means, and covariances. Whereas, Lagemann et al. (2023) choose to implement the fuel price as a stochastic distribution because of the fluctuation charter of fuel prices. Besides, fuel prices vary between bunker ports.

To determine the feasibility of an assigned trip, the shipowner prefers to estimate the OPEX and the revenue of the trip. The revenue depends on the freight rates of the transported cargo and the amount of cargo transported (Jensen and Ajspur, 2022). Therefore, the cargo capacity is a significant parameter in the ship design. The cargo capacity of an ammonia-powered ship becomes smaller due to the increase in the fuel tank volume. The consequence is that the revenue of the ship decreases compared to that of the HFO ship. When the revenue of the trip is lower than the OPEX of the ship, it is unlikely the shipowner decide to deploy the ship on the trip. This suggests the relevance of the correlation between the OPEX, net revenue, and ship design regarding ship performance.

3.1.6. Parameter Overview

Overall, there are direct and indirect relations between the factors mentioned above. Table 3.2 provides an overview of the relations between the factors. The direct relations are indicated with an (x). For example, an increase in the fuel price results directly in higher OPEX. For an indirect relation, factor A affects factor B due to the effect of factor A on factor C, which is a between factor A and B, or there is a second circumstance required to obtain the relation between two factors. Indirect relations are indicated with a minus sign (-). The relations between the parameters are used to optimize the ship's performance and generate the optimal bunker strategy.

Table 3.2: Overview of direct (x) and indirect (-) impact of the design and performance parameters regarding the operational profile of a ship.

	Speed	Fuel Consumption	Sailing Range	ship Deployment	Emissions	OPEX	Fuel Price	Freight Rates	Fuel Capacity	Cargo Capacity	Implementation Ammonia
Speed		x	-	x	-	-			-		
Fuel Consumption	-		x	-	x	-	-		x	-	-
Sailing Range	-	-		x	-	-			x	-	-
ship Deployment	x	-			-	x	-		-	-	-
Emission	-	x		x		x	-				x
OPEX		x	-	x					-	-	-
Fuel Price	-	x	-	-	-	x					-
Freight Rates	-	-	-	-					-	x	
Fuel Capacity	-		x	-	-	x	-			x	-
Cargo Capacity				-	-			-	x		
Implementation of Ammonia	-	x	-	-	x	x	-		x	-	

3.2. Ports and Supply network

To realize the transition from fossil fuels to ammonia, the shipping network will be affected in two ways. The implementation of ammonia will not only affect the ship design and performance arrangements alone; the supply of ammonia in bunker ports is also required. In this section, the impact of ammonia on bunkering strategies is elaborated.

The operational profile of the ship is significantly related to the bunker management of the shipowner. Performance parameters such as sailing range, ship deployment and fuel consumption are directly related to the distance between two bunker ports, the port time and fuel availability in a port. Therefore, this section determines the important parameters regarding bunkering strategies and the correlation between port choice decision-making and ship operation.

When developing a bunkering strategy, it is relevant to have a clear picture of the shipping network design. A shipping network consists of ports and shipping routes. Shipping networks can be regarded as hybrid hub-and-spoke networks (Ghane-Ezabadi and Vergara, 2016). Therefore, the ship can sail directly from one port to the other port, and the ship is not required to visit all ports in the network. This literature research assumes a ship will only visit a port if the ship requires new bunker fuel. As a result, the cargo transported on the ship is loaded and unloaded in bunker ports. However, the shipowner has to consider which bunker ports are optimal regarding the operational profile of the ship.

Research developed port choice decision-making models to support the shipowner. Choosing an optimal bunkering port that minimizes the increase in the operating costs in a hub and spoke system is a Multi-Criteria Decision-making (MCDM) problem (Tuljak-Suban, 2019). Next to the fuel price, this MCDM model considers the cargo on board and the port characteristics, including bunkering policy. The important Key Performance Factorss (KPFs) considered in the research of Tuljak-Suban (2019) are:

- Bunker price
- Bunker quality
- Port time
- Safety of bunkering
- Fuel availability
- Efficiency of bunker supply
- Geographical advantage
- Port bunker fuel capacity
- Port tariffs

Comparing these KPFs with the important operational parameters, one factor is not included in this list: the location of the port. Considering the challenge regarding the fuel capacity of the ship and the sailing range, the distance between two ports has a significant impact on the performance of the ship. Therefore, the port location and the distance to the next port should be included in the KPFs.

In this research, the port model is focused on the economic feasibility of providing ammonia bunker facilities. The scope of the research considers a homogeneous market. Therefore, no other fuel options are considered, and the level of the bunker facilities is equal in all ports. It is assumed that the technology is available to realize ammonia bunker facilities without further issues, and there are no capacity limits in the ports. The port tariffs are considered to remain the same for the transition to ammonia and, therefore, are not affected by the fuel switch. The KPFs adopted in the Port model are the bunker price and geographical advantage.

Ammonia Bunker Supply Facilities

One of the KPFs is the fuel availability; regarding ammonia, this is a significant criterion. Currently, ammonia is not implemented as a fuel in the maritime industry. Therefore, ports do not supply ammonia to a bunker fuel today. Nevertheless, ammonia is transported on a large scale as bulk. Worldwide, 88 ports are equipped with storage facilities for ammonia (Pruyn et al., 2022). Therefore, the implementation of supply infrastructure for the port is present.

To evaluate the system performance of the bunker supply chain for ammonia bunkering, Yang and Lam developed a model which considers the supply and demand dynamics of ammonia bunkering (Yang and Lam, 2023). The simulation model studies the economic and operational aspects of the ammonia bunker supply chain, which is seen as a discrete event system. They compared marine fuel oil MFO bunkering to pure ammonia bunkering and ammonia-MFO dual fuel bunkering in their case study, looking at different numbers of supply vessels, capacity of the supply vessels and flow rates of ammonia bunkering. The model investigates three impact parameters: the number of ammonia bunker supply vessels, the capacity of ammonia bunker supply vessels and the ammonia bunkering flow rates. The latter has the most impact on the bunkering and bunker strategies of the ships. The annual operational cost of the bunker and supplier is most affected by the number of ammonia-powered ships. This is an important parameter for port operators to take into account when considering supplying ammonia as a bunker fuel for maritime shipping.

The ammonia production price is required to determine the bunker price of ammonia. This production price of green ammonia strongly depends on the price of the hydrogen, as this is a large substitute for ammonia. Salmon et al. (2021) and Nayak-Luke and Bañares-Alcántara (2020) established models to simulate the Production Levelized Cost Of Ammonia (PLCOA) based on the production location and the local availability of green energy sources like wind and solar energy. The second study included a data set for the estimated PLCOA for 534 locations in 70 countries in 2030. This data set is used as a baseline for the ammonia bunker price calculation in the Port model. It applies as the main indicator of the OPEX for the ammonia bunker port.

For bunker ports to be a part of the transition to ammonia, they have to invest in bunker facilities to supply ammonia. This contains an ammonia storage tank and an ammonia supply chain to provide the port with ammonia. There are two supply chain methods considered to be applicable for ammonia. Ammonia can be transported to the ports by ships, or a pipe system supplies the ammonia (Salmon et al., 2021). Next to this, the size of the ammonia storage tanks define the CAPEX of the ammonia bunker ports. *The First Wave* report for ETC (2020) presents the expected CAPEX for ports in transition to renewable energies, including ammonia. The report provides an indicant for the CAPEX for three different sizes of storage tanks, as listed in table 3.3. The calculation for the CAPEX in the Port model is based on the results in this report. Besides, the Energy Transitions Commission (ETC) suggests a discount of 50% on the CAPEX for ports that are equipped with cargo facilities for ammonia.

Table 3.3: Capacity and CAPEX of ammonia storage tank in ports (ETC, 2020).

Size	unit	Small	Medium	Large
Storage Tank Capacity	[t]	7000	20000	30000
Storage Tank CAPEX	[USD]	800000	2600000	3500000

3.3. Bunker Strategy Models

In section 3.1, the significant design and performance parameters are defined and the relations between the parameters are explained. Those relations are useful for optimization problems. For example, the optimal balance between the sailing range and the fuel tank volume on one side versus minimizing the OPEX and maximizing the revenue of the ship's performance. According to the author's knowledge, no published research considers these three aspects in an optimization problem regarding ammonia as a marine fuel. Nevertheless, extensive research has been done regarding the optimization of sailing speed and fuel consumption. Besides, recent research on this topic aims to reduce ship emissions. An effective measure to achieve that is reducing fuel consumption. This approach has shown similarities regarding the relations that arise in the prior subsection.

Mixed-Integer Programming (MIP)

Mixed-integer programming is a frequently used optimization method and can solve problems with continuous and discrete variables. The MIP models regularly apply a solver to complete the optimization (S. Wang et al., 2013). The solver is required to reduce the computational time of the model. MIP can be divided into two subcategories: mixed-integer linear programming (MILP) and mixed-integer nonlinear programming (MINLP).

The parameters explained in section 3.1 will be applied in the optimization model. Considering the relations, these will add nonlinear terms to the model. Therefore, the MINLP approach could be more suitable for this optimization problem. However, the efficiency of the MINLP model is lower than the MILP problem because of the complexity caused by the nonlinear constraints in MINLP models (S. Wang et al., 2013). This results in long computations, which is not eligible for this research. The nonlinearity of the model does not prescribe that MILP cannot be applied in this research. MILP approaches consider nonlinear terms in the model. These nonlinear terms need to be transformed into linear terms before they can be implemented in the model.

Bunkering Strategy and Port Choice Decision Models

The models for bunkering strategies and port choice decisions published in the research show parallels with the optimization models. Decision-making problem models generally contain an optimization problem to find a balance between two or more main factors. Optimization models for shipping performance are mostly economical-driven. For example, the model is designed to optimize sailing speed and fuel consumption. To achieve this, a suboptimization is implemented to minimize operational expenses, including fuel costs (von Westarp and Brabänder, 2021). Other optimization models minimize emissions or service time or maximize the revenue of the ship (Wen et al., 2017). This subsection elaborates on two bunker port selection models for the bunkering strategy, including port selection, for published research.

Wang and Meng (2015) developed a mathematical model for the robust bunker management (RBM) problem in liner shipping networks (S. Wang and Meng, 2015). The model first optimizes the joint speed and bunkering for the liner shipping network and considers the difference between the planned sailing time and real sailing time. At first, the RBM model was very complex due to many nonlinear terms and both continuous and discrete decision variables. To overcome the complexity and improve the usability, the model was transformed into a mixed-integer linear programming (MILP) formulation.

Ursavas et al. (2020) also developed a MIP model regarding bunker port selection. Therefore, it can be concluded that bunker management and port selection problems can be solved with the MIP approach. Reflecting on the research review in the literature research, an MIP approach is most suitable for this research. The research of Ursavas et al. (2020) provides a model for inland waterway bunkering of LNG. This mixed integer programming model shows the dynamics between ports regarding bunkering port selection. Events or changes in one port affect the demand in other ports and how this influences bunkering strategies.

3.4. Conclusion

The models that are described in this chapter mainly aim to optimize the bunker strategy of the ships, which matches the objective of the model that will be developed in this research. However, there are a number of differences between the models in this research. Firstly, the reference models are not developed for an ammonia-powered shipping network, resulting in different constraints regarding the fuel used. Secondly, these models consider the port bunker prices to be independent of the demand resulting from the bunker patterns of the participating ships. Besides, none of the models is performed for a worldwide fleet of over 1000 ships. Lastly, the model to develop in this research does not have a fixed route and gives the possibility to reroute to suggest a more suitable route.

In order to identify the impact of ammonia on the significant ship parameters, fuel tank volume, sailing speed and sailing range, a model is developed as an Ammonia Bunker Strategy Optimization model (BS model). A second model is added to implement as the Ammonia Bunker Port model (Port model). This model handles the non-linearly in the ammonia bunker price estimation. In figure 3.1, the research approach is illustrated, including the structure between the data collection, the models and the final results.

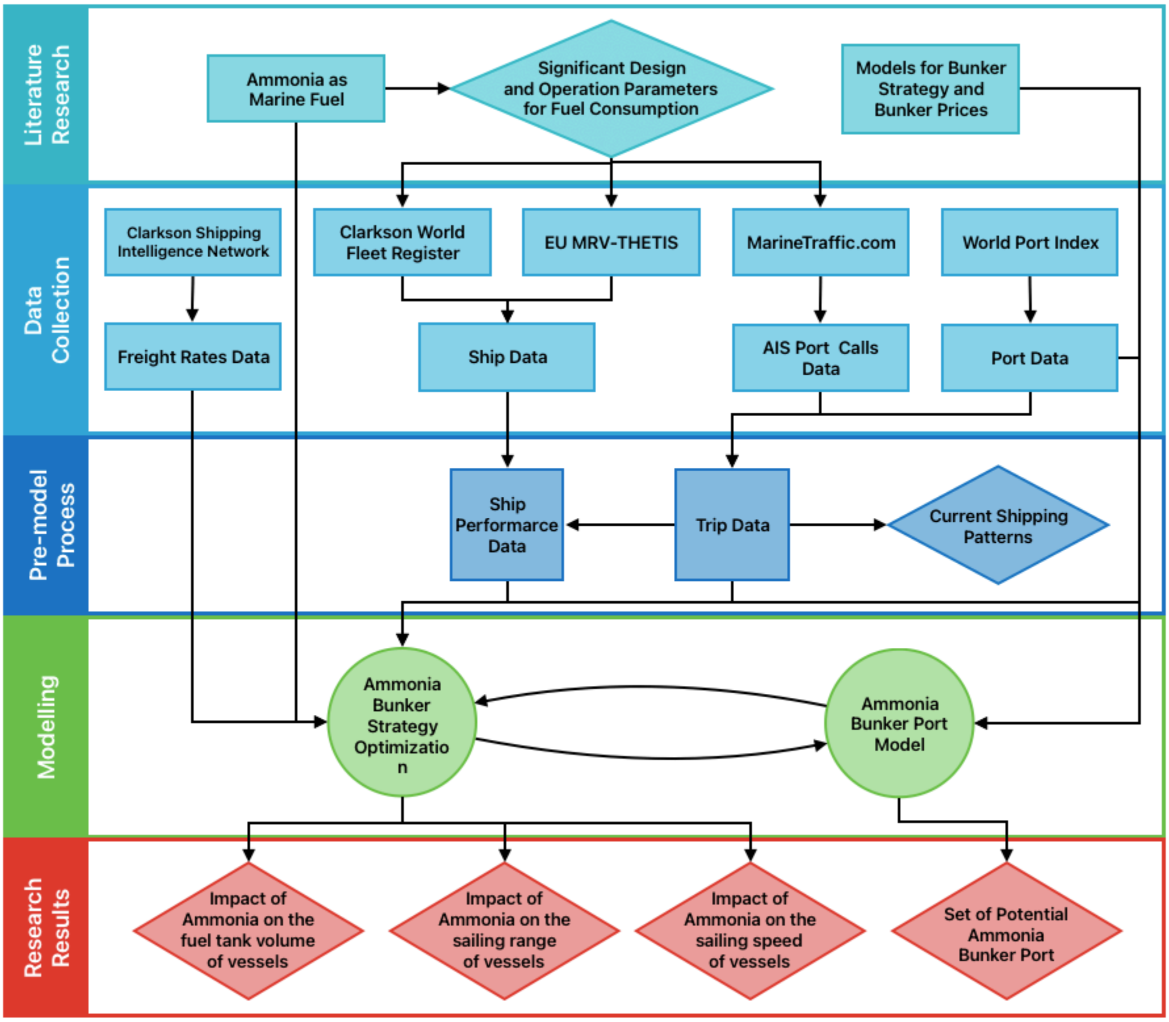

Figure 3.1: Overview of the research structure

4

Ammonia Powered Shipping Network Model

This chapter describes the Ammonia Powered Shipping Network model (APSN model) model developed to quantify the operational impact of ammonia on the design and performance of the ships and the bunker port network. The structure of APSN model is demonstrated in the figure 4.1. The green boxes represent the two sub-models, the BS model and the Port model. The BS model is the main model of the APSN model and includes two extension modules. The implementation of this model is explained in section 4.1. The BS model is formulated as a mixed-integer linear programming (MILP) model to simulate the bunkering pattern of ammonia-powered ships in a global shipping network, as elaborated in section 4.2. The MILP is developed with extended modules for rerouting and the bunker strategy. These modules are elaborated in section 4.2. Finally, the port model is applied to address the non-linearity of the ammonia bunker price implementation to the shipping network, as described in section 4.3.

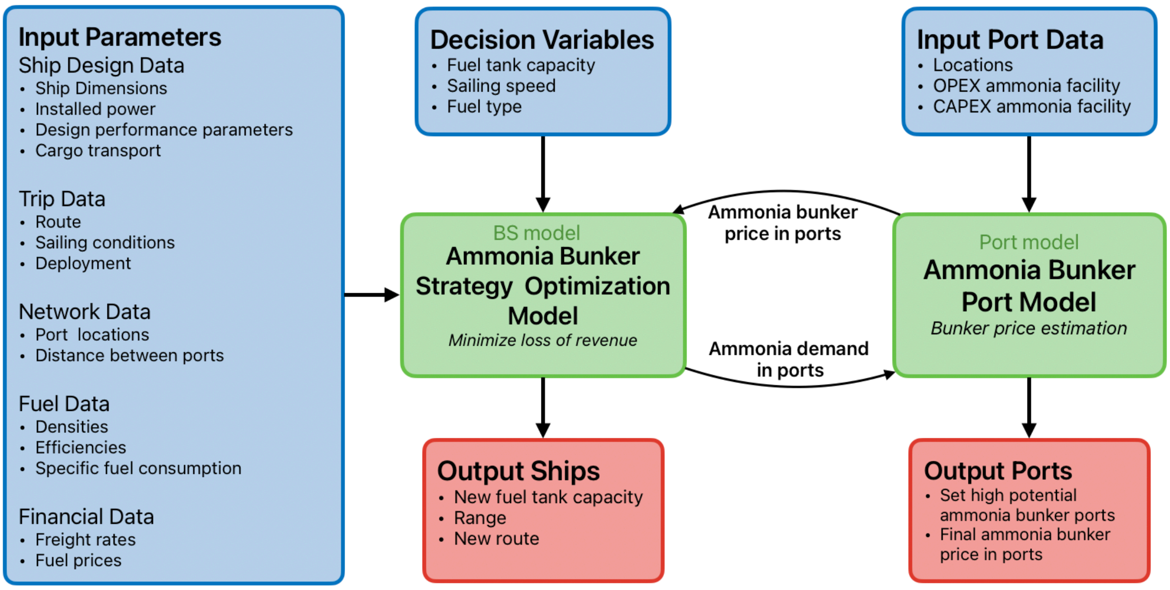

Figure 4.1: The framework of the Ammonia Powered Shipping Network model developed in this report.

In figure 4.1, the coherence of the BS model and the Port model is visualized. The BS model and the Port model cooperate to generate market dynamics for the supply and demand of ammonia. The

APSN model assumes that the ships are dominant to the port due to the fixed set of ports they have to visit. Firstly, the BS model optimizes the bunker strategy for each ship individually. This results in a route containing the assigned ports, including the chosen bunker ports for the ship. The bunker strategies of the total fleet generate the ammonia demand for each port based on the route assigned to the ships. Next, the Port model estimates the ammonia bunker price of each port based on the demand output of the BS model and the CAPEX and OPEX to expand the port with ammonia bunker facilities. The new ammonia bunker prices will be used as new input data to improve the BS model. These steps are repeated until a balance in the output is found. The balance is approved when the difference in the output data between two iterations is minimal or the results switch between the same values. The reviewed output includes the improved fuel tank capacity, the related maximum range and the new route for the ships. For the Port model, the output contains the final ammonia bunker price and demand in each port. The output of the model is shown in the red boxes in figure 4.1.

The blue squares represent the input data of the models. In chapter 5, the process to generate suitable input data for the models is elaborated. The input data creates the structure of the bunker network, including the selected ships, their design and performance specifications, the ports, their location and facilities. The parameters following from that data are referred to as the input parameters in figure 4.1.

4.1. Ammonia Bunker Strategy Optimization Model

An ammonia bunker strategy optimization is developed to indicate the balance between the size of the ship's fuel tank and the maximum sailing range, considering the influence of the sailing speed. This balance depends on the fuel consumption and the bunker strategy of the ship. The goal of the model is to indicate the impact of ammonia on the three parameters. The fuel consumption is linear to the fuel costs of the ship, which is assumed as the dominant factor for the OPEX of the ship. Next to this, the size of the fuel tank is related to the cargo capacity of the ship, which defines the income of the ship. Therefore, the indication of the impact of ammonia on the ship is developed to minimize the loss of revenue per year. The model considers that the revenue of the ship (R) is equal to the cargo income (I) minus the fuel costs (C). The optimization of the loss of revenue is formulated as a MILP model, as suggested in Chapter 3 and is described in section 4.2.

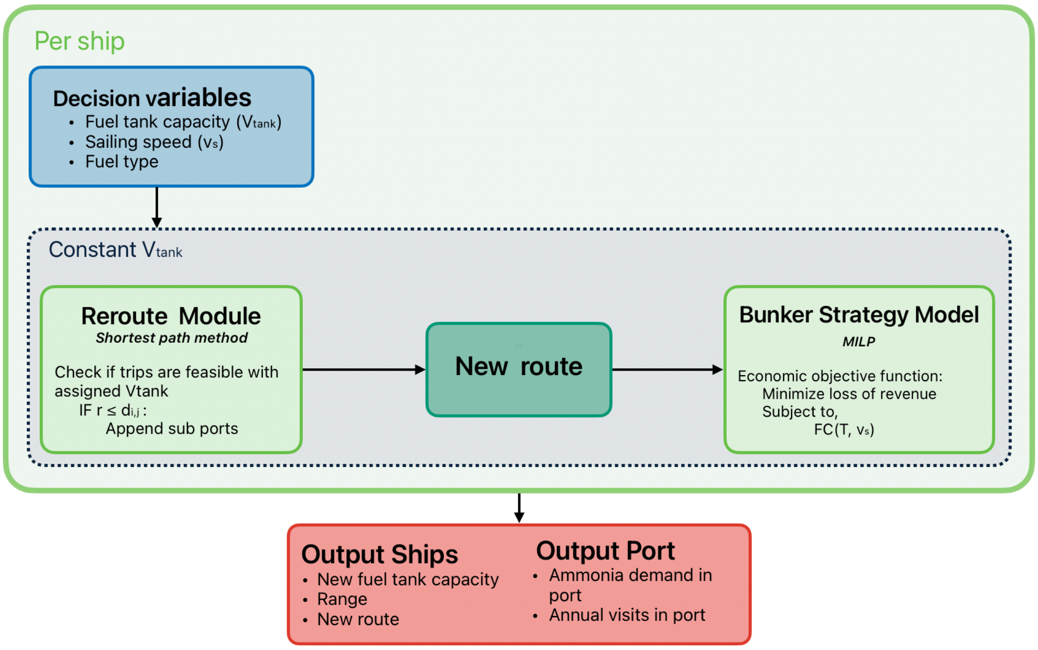

Figure 4.2: The structure of the ammonia bunker strategy optimization model representing the reroute module and the bunker strategy model.

In addition to the bunker strategy optimization, an extended module is developed to ensure that the ship is capable of performing its original trips. This module is referred to as the rerouting module. The rerouting module provides the most profitable alternative route between two ports if the range of the ship is smaller than the distance between the ports. The sub-ports in the alternative route are added to the original route, resulting in the new route. The new route is applied in the bunker strategy module. The relation between the rerouting module and the bunker strategy optimization is displayed in figure 4.2. The rerouting module is described in more detail later in this section.

In this research, the APSN model is used to investigate the impact of a switch to ammonia on the design and performance parameters of the ships with ten scenarios. These scenarios have two different bunker strategies: trip bunkering and forward bunkering. The bunker strategy model is applied to both bunker strategy approaches: trip bunkering and forward bunkering. The bunker strategy determines whether to bunker in a port on the route. For both approaches, it is assumed that the ship has to bunker at least the amount of fuel required for the first trip and the fuel margin of 10% of the fuel tank capacity. The fuel margin is the extra fuel present in the fuel tank for unforeseen events.

Trip bunkering

Trip bunkering assumes that the ship always bunkers the amount of ammonia required for the trip in the departure port related to the trip. During the trip, the fuel tank only contains the fuel required for that trip and the fuel margin. Figure 4.3 depicts a hypothetical illustration of the flow of the fuel level in the bunker tank is depicted. The red dots represent the ports where the ship bunkers. Considering this bunker strategy, a reduction of the fuel capacity of the ship will not cause significant challenges because the fuel level is not higher than 50%.

However, this approach limits the freedom of bunker port choice, and therefore, the shipowner has to bunker in each port on the route, even when the bunker price at the port is substantially high. This can result in higher fuel costs, and therefore, the revenue will decrease.

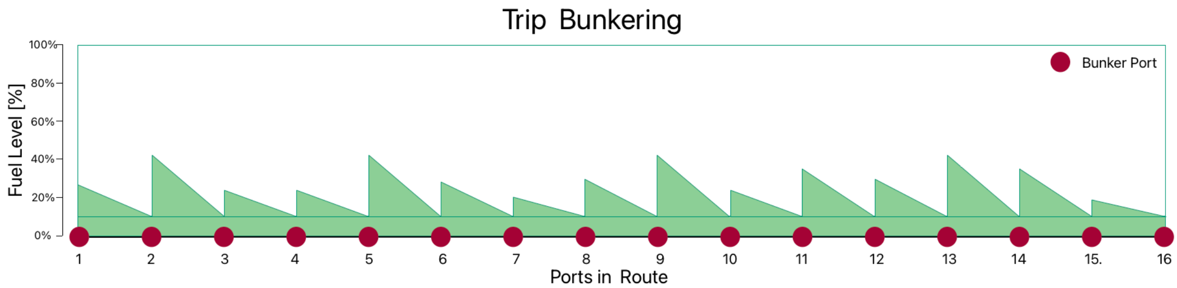

Figure 4.3: A hypothetical illustration of the flow of the fuel level in the fuel tank of the ship, considering the trip bunkering approach.

Forward bunkering

The forward bunkering approach assumes that the ship bunkers the amount of ammonia required to perform the bunker strategy to minimize the total annual bunker expenses. The bunker port selection is based on the maximum fuel capacity and the ammonia bunker price in the port, including the shipping route. The model limited the set of ports contained in the determined route after the reroute module and could not deviate from this route to minimize costs even more. However, the rerouting model is based on the shortest path theory and is modelled to find the cheapest alternative route between the two ports. Therefore, it can be assumed that the route after rerouting is the cheapest.

In each port, the model examines which port with its range has the lowest bunker price for ammonia. If a port within the range of the ship supplies ammonia for a lower price than the current port, the ship will bunker the amount of ammonia to reach the cheaper port. This is the next bunker port for the ship. However, if there is no cheaper port within the range of the ship, the ship bunkers the amount of ammonia needed to fill up the fuel tank. In this case, the next bunker port is the port with the lower ammonia bunker price after the current port. When the ship arrives in the next bunker port, the consideration is applied again. Figure 4.4 depicts a hypothetical illustration of the flow of the fuel level in the fuel tank of the ship considering this approach. The red dots mark the bunker ports of the route, and the blue dots are ports with only cargo handling.

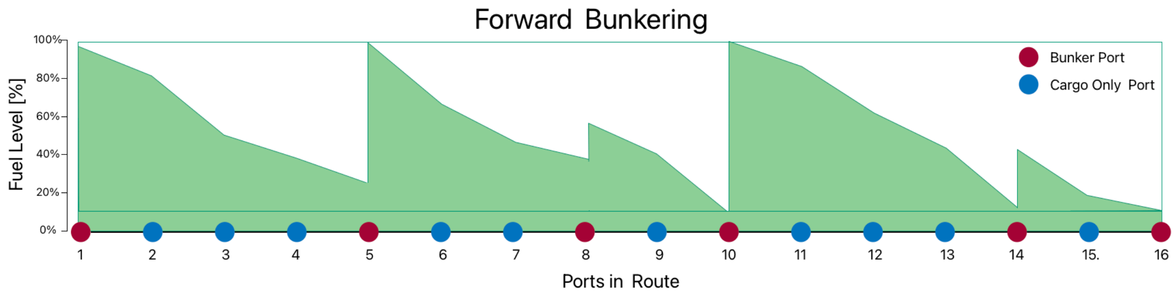

Figure 4.4: A hypothetical illustration of the flow of the fuel level in the fuel tank of the ship, considering the forward bunkering approach.

The figure shows that the fuel capacity of the ships is used more optimally with the forward bunker strategy compared to the trip bunker strategy. Besides, the forward bunker strategy provides the possibility of avoiding ports with high ammonia bunker prices. This suggests that a larger fuel tank results in lower fuel costs and, therefore, higher revenue. However, a larger fuel tank reduces the cargo capacity of the ship and, thus, the cargo income. The BS model proposes the optimal balance between these two parameters. To ensure that the ship does not bunker more fuel than required for the total trips, the total bunker amount of ammonia in the forward bunkering module should be equal to the amount of ammonia bunker in the trip bunkering approach.

4.1.1. Rerouting module

This section describes the implementation of the rerouting module. Before the Ammonia Bunker Startegy Model (BS-model) minimizes the loss in annual revenue of the ships, the rerouting module is applied. The rerouting module tests if the ship can complete the assigned trips in the ship's route. The sailing range (r) of the ship has to be larger than the distance between the start port *hk* and the end port *hk+1* to satisfy the feasibility test. The ship's sailing range depends on the fuel tank capacity and fuel consumption. The maximum fuel tank capacity is assumed to be 90% of the ship's fuel tank volume (V^T). The fuel consumption is calculated based on the formula 4.5 in chapter 5. The fuel consumption is determined by the sailing speed (v_s) and the ship's draught during the trip. The decision variables, V^T and v_s, are based on the performed scenario. Considering the assigned route of the ship, the reroute module decides if rerouting is required. When the range of the ship is more extensive or equal to the distance between the start and end port ($r > d_{hk,hk+1}$), the ship can complete the assigned trip. In this case, rerouting is not required, and the ship will sail straight from port *hk* to port *hk+1*. However, when the sailing range of the ship is smaller than the distance between the start and end port of the trip ($r < d_{hk,hk+1}$), the rerouting process begins.

The rerouting module considers all alternative routes within the ship's sailing range between the start port and the end port of the trip. It is based on the shortest path optimization and *Dijkstra's algorithm* (Aardal et al., 2020). The rerouting module is developed using the `networkx` module in Python. The shortest path is formulated as the route with the lowest fuel costs. The fuel costs of the alternative routes are estimated by multiplying the fuel consumption of the sub-trip by the ammonia fuel price at the start port. The fuel consumption of the sub-trips is equal to the trip distance multiplied by fuel consumption per nautical miles (fcm) of the original trip. A port entry fee was introduced to avoid endless extra subtrips. To ensure it is not preferable to visit more ports than needed, the port entry fee is applied as the large number M. The output of the rerouting module is a set of ports to cover the trip distance, starting with the start port *k*, followed by the sub port and finally the end port *k+1* of the original trip. The extra ports are added to the ship's route and are included in the [rest] of the model.

In figure 4.5, the implementation of the rerouting sub-model is demonstrated. Here, the solid blue circles refer to ports in the original route (P_1), and the smaller empty circles are the added sub ports after rerouting ($'P_{1.1},' P_{1.2},' P_{3.1}$). In this example, the trips P_1 — P_2 and P_3 — P_4 have to cover a distance without their maximum sailing range, and therefore the ship has to divert to an alternative route. As figure 4.5 implies, the ship can visit more than one extra port between the trip's start and end port when required, or it results in the cheapest alternative route.

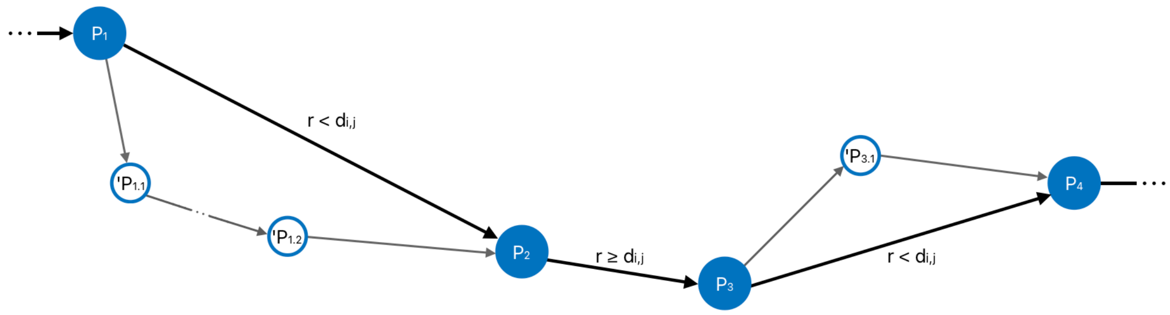

Figure 4.5: The visualization of the application of the rerouting module.

Due to the implementation of the shortest path method, it is assumed that the output of the rerouting sub-model is the best alternative route for the ship in the applied scenario. Therefore, it cooperates with the main objective of the ammonia bunker strategy model to minimize the loss of ship annual revenue.

4.2. Bunker Strategy Model

4.2.1. Notations

The BS model minimizes the loss in revenue for a set of 1025 ships (S), and the optimization is applied for each ship individually. The ammonia shipping network includes a set of 644 ports (H). The ships are assigned to complete a route based on the port calls for the Automatic Identification System (AIS) data. This results in a subset of trips that the ship has to perform (K_s). Each trip has a departure port (hk) and an arrival port ($hk+1$), which correspond to a port in the ammonia shipping network. Each ship transported a specific cargo (G) with different freight rates and densities. The sets, variables, and parameters used in the BS model are presented in tables 4.1, 4.3, 4.2 and 4.4.

Table 4.1: Notations of sets

Set	Definition
G	Set of cargo types transported in ammonia shipping network, indexed by g
H	Set of all ports in the ammonia shipping network, indexed by h
K_s	Set of trips in the route performed by ship s in the ammonia shipping network, indexed by k
S	Set of ships in ammonia shipping network, indexed by s

Table 4.2: Notations of decision variables

Variable	Definition
V^T	Volume of the fuel tank (m^3) of ship s
v_k	Sailing speed (kn) of ship s during trip k
x_{ks}	1 if ship s transports cargo during trip k, 0 otherwise
y_{hks}	1 if ship s bunkers ammonia in port h for trip k, 0 otherwise

Table 4.3: Notations of dependent variables

Variable	Definition
dwt_k	Total deadweight (t) during trip k
$FC_{ks}(v_k, T_k)$	Fuel consumption (t) required for trip k based on the trip speed and trip draught
$fcm_{ks}(v_k, T, k)$	Specific fuel consumption per nautical miles (t/nm) of ship s during trip k
m_k^C	Mass of the cargo transport (t) during trip k
m_k^T	Mass on fuel tank (t) including bunkered ammonia during trip k
$Q_{hk,i}^B$	Amount of ammonia bunker (t) in departure port hk of trip k according to bunker strategy i
Q_{hk}^{rem}	Amount of ammonia left in fuel tank (t) when arriving in departure port hk
Q_k^{req}	Amount of ammonia (t) required for ship s to complete trip k
$Q_s^{res}(V^T)$	Amount of ammonia (t) reserved for unpredicted events in ship s based on the fuel tank volume
Q_{hk}^T	Amount of ammonia (t) present in the fuel tank of ship s at departure port hk
Q_{max}^T	Maximum fuel tank capacity (t) is ship s based on the fuel tank volume
r_{ks}	Range (nm) of ship s for trip k
V_k^C	Volume of the transported cargo (m^3) during trip k
V_k^{TOT}	Total volume related to the deadweight (m^3) during trip k

Table 4.4: Notations of parameters

Parameter	Definition
$d_{hk,hk+1}$	Distance (nm) of trip k, between departure port hk and arrival port $hk+1$
dwt_s^0	Original deadweight (t) of ship s
FR_g	Freight rate of cargo type g in USD /(unit · nm)
k_1, s	Performance constant related to the design speed and maximum draught of ship s defined in equation 5.25
m_s^{rest}	Mass of other deadweight parts (t) of ship s
$P_s^{AUX,non-PP}$	Auxiliary power (kWh) required for ship s
p_{hk}	Ammonia bunker price (USD/t) in port h in related to departure port of trip k
R_s^{S0A}	Revenue (USD) of ship s in baseline scenario S0A
T_k	Draught (m) of ship s during trip k
$V_{0,s}^C$	Original volume (m^3) of the cargo capacity of ship s
$V_{k,0}^C$	Original volume (m^3) of the transported cargo during trip k
V_{max}^C	Original volume (m^3) of the transported cargo during trip k
V_s^{rest}	Volume of other deadweight parts (m^3) of ship s
V_0^T	Original volume (m^3) of the fuel tank capacity of ship s
V_0^{TOT}	Total volume (m^3) related to original deadweight of ship s
ρ_g^C	Density (kg/L) of cargo type g
$\rho_{NH_3,con}$	Density (kg/L) of contained ammonia

4.2.2. Economic Objective Function

The Ammonia Bunker Strategy Optimization model is a MILP model. The BS model optimization is based on the OPEX and incomes due to the transported cargo. The OPEX considered in this model is limited to the fuel costs of the ship, assuming the other variable costs of the ship are not significantly affected by a fuel switch towards ammonia. The objective function of the BS model is formulated in equation 4.1. This function minimizes the shipowner's annual revenue loss compared to the revenue calculated for the baseline scenario S0A (R_{S0A}). The revenue for ammonia-powered ships is the difference between the income from the transported cargo and the fuel costs. The cargo income is estimated with the freight rate (FR_g) and the transported cargo volume (V_k^C). The fuel costs are calculated with the bunker price of the ports (p_h) and the amount of fuel bunkered in the port (Q_{hk}^{ref}).

$$min\left[R_s^{S0A} - \sum\left[FR_g * V_k^C * x_{ks} - \sum(Q_{hk,i}^B * p_{hk} * y_{hks})\right]\right] \tag{4.1}$$

The annual revenue of the reference scenario S0A (R_{S0A}) is calculated in scenario S0A and refers to the ships powered by fuel oil. The freight rates (FR_g) of the several cargo types and the base bunker prices for ammonia in each port ($p_{h,0}$) are estimated in section 5.3. After the first iteration, the bunker price for ammonia in each port is estimated in the port model and used as input for the BS model. The amount of ammonia bunkered in the port (Q_{hk}^{ref}) depends on the approach of the bunker strategy. The trip bunkering strategy is that the ship only bunkers the ammonia required to have enough fuel onboard to complete the upcoming trip ($\sum(Q_k^{req})_1$). The forward bunkering strategy ensures that the ship bunkers the amount of ammonia required to minimize the total annual fuel costs ($\sum(Q_k^{req})_2$). Besides, the amount of ammonia onboard the ship always has to be the sum of the least amount of fuel required to complete the upcoming trip and the fuel reserve of the ship (Q_s^{res}). The fuel reserve of the ship is equal to 10 % of the fuel tank capacity of the ship.

$$Q_{hk,i}^B = \sum(Q_k^{req})_i - Q_{hk}^{rem} \tag{4.2}$$

$$Q_k^{req} = FC_{ks}(v_k, T_k) + Q_s^{res}(V^T) \tag{4.3}$$

$$Q_{hk}^{rem} = Q_{hk-1}^T - FC_{k-1,s}(v_{k-1}, T_{k-1}) \tag{4.4}$$

$$FC_{ks}(v_k, T_k) = \left(\frac{k_1 * T_k^{2/3} * v_k^3}{v_k} + \frac{P_s^{AUX,non-PP}}{v_k}\right) * d_{hk,hk+1} \tag{4.5}$$

4.2.3. Constraints

The objective function is subject to constraints regarding the bunker and fuel tank volume (4.6 - 4.8), the weight and space of the ship (4.9 - 4.15) and the range of the ship (4.16 and 4.17).

Constraint 4.6 ensures that the amount of fuel in the fuel tank is always equal to or larger than the amount of fuel required to complete the next trip. Constraint 4.7 defines the amount of fuel onboard the ship when leaving the start port, and constraint 4.8 ensures that the volume of the amount of fuel onboard cannot be larger than the volume of the fuel tank of the ship.

$$Q_{max}^T \geq Q_{hk}^T \tag{4.6}$$
$$Q_{hk}^T = Q_{hk}^B + Q_{hk}^{rem} \tag{4.7}$$
$$Q_{max}^T = V^T * \rho_{NH_3,con} \tag{4.8}$$

Constraint 4.9 defines the transported cargo weight during the trip based on the cargo volume and related cargo density. Constraints 4.10 and 4.11 define the total weight of the variable weight components and ensure that it cannot be larger than the ship's deadweight tonnage.

$$m_k^C = V_k^C * \rho_g^C \tag{4.9}$$
$$dwt_k = m_k^C + Q_k^T + m_s^{rest} \tag{4.10}$$
$$dwt_k \leq dwt_s^0 \tag{4.11}$$

Constraint 4.12 imposes the maximum cargo volume the ship can carry according to the increase in the fuel tank volume, and constraint 4.13 states the cargo volume transported during the trip. Constraints 4.14 and 4.15 define the total volume of the variable space components in the ship, and this cannot be larger than the available volume in the ship.

$$V^C_{max} = (V^C_0 + V^T_0) - V^T \tag{4.12}$$
$$V^C_k = min(V^C_{k,0}, V^C_{max}) \tag{4.13}$$
$$V^{TOT}_k = V^C_k + V^T + V^{rest}_s \tag{4.14}$$
$$V^{TOT}_k \leq V^{TOT}_0 \tag{4.15}$$

Constraint 4.17 ensures that the ship cannot perform a trip with a distance that is larger than the range of the ship allows. The range of the ship is defined by constraint 4.16.

$$r_k s = \frac{0.9 * V^T}{fcm_{ks}(v_k, T_k)} \tag{4.16}$$
$$d_{hk,hk+1} \leq r_k s \tag{4.17}$$

4.3. Port Model

The Port model is the second part of the ammonia-powered shipping network model and was developed to solve the non-linear character of the bunker prices. This results in a linear approach for the ammonia bunker price that is implemented in the BS model. The Port model model aims to estimate the ammonia bunker price in the ports based on the demand resulting from the BS model. The demand determines the OPEX and the CAPEX of ammonia bunker facilities in ports. In this section, the structure of the Port model is elaborated, and the considerations are explained. The data applied in the Port model based on the results of the PLCOA and Delivered Levelized Cost Of Ammonia (DLCOA) estimations from Salmon et al. (2021) and Nayak-Luke and Bañares-Alcántara (2020) and the data for the parameters included in the CAPEX calculation are established from *The First Wave* report (ETC, 2020). Besides the expenditure components, the Port model requires a demand input for each port.

Figure 4.6 shows the structure of the port model and the considered costs to estimate the OPEX and the CAPEX of the ammonia bunker facilities in the ports. The estimated ammonia bunker price is used for the next iteration of the BS model.

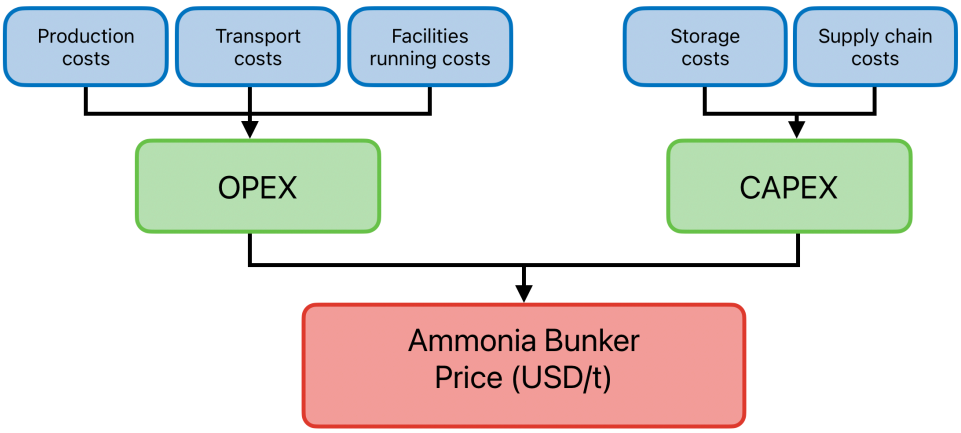

Figure 4.6: Illustration of the port model structure.

To avoid errors in the model for ports with very low annual ammonia demands, the minimum demand of a port is set to 200 tonnes of ammonia. This extension is included in the model to maintain all selected ports available in the shipping network. Otherwise, the ports with a demand lower than 200 tonnes of ammonia are cancelled out and will not be reconsidered in the next iteration. The model does not consider the limitation of the bunker price estimation.

Table 4.5: Notations of parameters

Parameters	Definition
a	Return of investment time for ammonia supply facilities in years
C^{run}	Ammonia storage running costs (USD/h)
$C_h^{storage}$	Costs (USD) for one ammonia storage facility in port h
$C_h^{supplychain}$	Costs (USD) for supply chain for one ammonia storage facility in port h
c_h^{prod}	Production costs (USD/t) for ammonia in port h
c_h^{trans}	Transportation costs (USD/t) for ammonia to port h
$CAPEX_h$	Capital expenditure (USD) for the ammonia supply facilities in port h
n_h	Number of ammonia storage tanks required in port h
n_r	Annual operational hours of the ammonia supply facilities
$OPEX_h$	Operational expenditure (USD) for ammonia supply in port h
P_h^{an}	Annual ammonia supply capacity (t) for one ammonia storage tank in port h
p_h^{new}	New ammonia bunker price (USD/t) in port h
Q_h^{an}	Total volume of annual ammonia demand (t) in port h
Q_{hk}^{B}	Amount of ammonia (t) bunkered in departure port hk for trip k related
r	Discount rate of 0.05%
u_h	Number of existing ammonia cargo facilities in port h

The demand output data of the BS model of all ships is translated to the annual demand in each port by the sum of the ammonia demands related to the port. Equation 4.18 gives a prediction of the ammonia demand in each port. Based on the demand in the port, the number of storage tanks required (n_h) is defined.

$$Q_h^{an} = \sum_S (\sum_K (Q_{hk}^B))_s \tag{4.18}$$

$$n_h = \frac{Q_h^{an}}{P_h^{an}} \tag{4.19}$$

The Port model is simulated based on the equations 4.20 to 4.19, and the adopted parameters are explained in table 4.5. First, the CAPEX of the ammonia bunker facilities to supply the required demand is estimated with equation 4.20. The CAPEX of the port depends on the costs for the realization of the storage tanks and the supply chain. The discount rate considered in this research is 5%, and it is assumed that the return on investment time is 30 years. For the ports which are already equipped with existing ammonia cargo facilities, a discount of 50% for the storage tanks is added to the equation.

$$CAPEX_h = \frac{C_h^{storage} * (n_h - u_h * 0.5) + C_h^{supplychain}}{(1+r)^a} \tag{4.20}$$

The OPEX in the Port model is formulated as the sum of the production costs and transportation costs multiplied by the demand in the port. Next to this, the energy costs of the storage tanks, based on running hours per year, are added to equation 4.21. The transportation costs depend on the transportation mode for ammonia to the port, which is determined in section 5.4.

$$OPEX_h = (c_h^{prod} + c_h^{trans}) * Q_h^{an} + C^{run} * n_r \tag{4.21}$$

Finally, the new ammonia bunker price is calculated in equation 4.21. This is the sum of the CAPEX and the OPEX divided by the annual demand of the port.

$$p_h^{new} = \frac{CAPEX_h + OPEX_h}{Q_h^{an}} \tag{4.22}$$

In this approach, the CAPEX and the OPEX are both related to the demand for ammonia. To illustrate this relation, figure 4.7 depicts the ammonia bunker price as a function of the ammonia demand for the Port of Rotterdam. Besides, the figure includes the trend of the CAPEX and the OPEX.

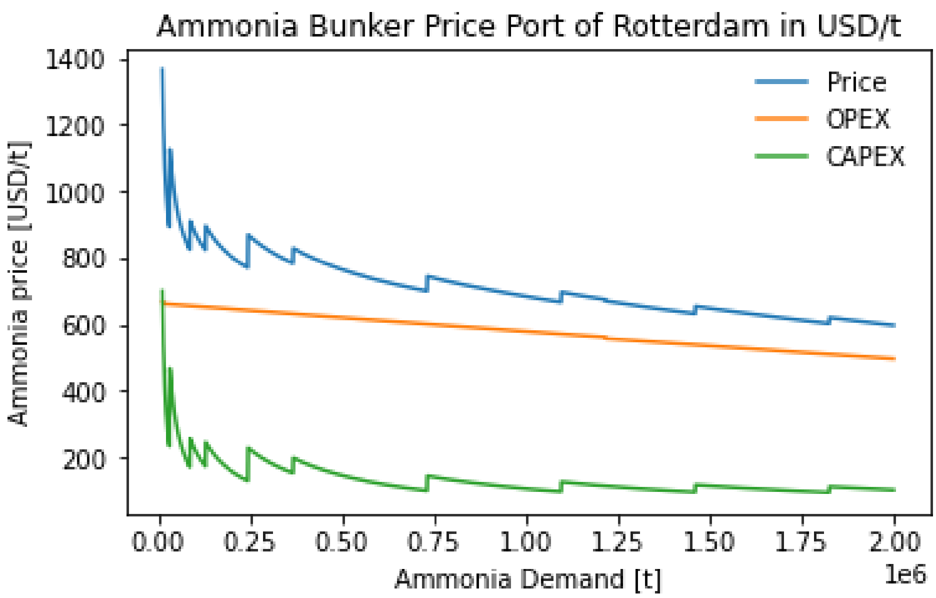

Figure 4.7: Illustration of theCAPEX (green), the OPEX (orange) and the ammonia bunker price (blue) as a function of annual demand in the Port of Rotterdam is used as an example.

5 Input Data

The two models formulated in chapters 4 and 4.3 require a set of parameters representing the ship design, operation, and network characteristics to generate results to indicate the impact of ammonia on the operational performance of the shipping network. In this chapter, the required data for the model is collected and processed to create a suitable dataset for the BS model and the port model. The ship data is mainly obtained from the Clarkson Research World Fleet Register (WFR) in combination with the database of The Hybrid European Targeting and Inspection System for Monitoring, Reporting, and Verification (THETIS-MRV) (Clarkosn Research, 2023b and EMSA, 2023). In section 5.2, a list of obtained parameters for these databases is summarized, followed by an elaboration of the data processing. The trip data is based on AIS port call data and is requested from MarineTraffic.com (MarineTraffic, 2023). An overview of parameters obtained from the AIS data is presented in section 5.3. This section elaborates on the process of transforming the raw data into suitable data for the models. In section 5.4, the obtained network data and processing process is provided. This port data is accessed for the database World Port Index (WPI) (Maritime Safety Office, 2019) and complemented with port data from MarineTraffic.com (MarineTraffic, 2023). Based on port data, the network data is complemented with distance estimation performed with the `searoute` toolkit in Python (Halili, 2023). The freight rates data for Clarkson Research Shipping Intelegence Network (SIN) is used to estimate the freight rates applied in the model (Clarkosn Research, 2023a).

Table 5.1: Data sources.

Data source	Access
Ship data	
Clarkson WFR	TU Delft licence
THETIS-MRV	Open source
Trip data	
AIS history port calls	Purchased dataset on request
`searoute`	Open source
Port data	
World Port Index	Open source
Marine Traffic Port data	Open source
Freight rates data	
Clarkson SIN	TU Delft licence

Besides the ship, trip and network data, the models require data regarding fuel characteristics and ammonia bunker price to provide the economic aspect of the research. The fuel characteristics are adapted from the master thesis from Snaathorst (2022), and the monetary parameters for the ammonia bunker price are obtained in the literature research. The considered data for fuel and monetary parameters is summarized in section 5.4 as suitable input data for the BS model and Port model.

5.1. Ship selection

The goal of the case study is to create a realistic case for an ammonia-powered shipping network. The focus of the research is to address the feasibility of a bunker port network for ammonia, as well as the impact on the operational profile of the ships. Therefore, the case study is performed based on the ship data of a fleet of more than 1000 ships collected for the Clarkson World Fleet Register (WFR) (Clarkosn Research, 2023b). To obtain a suitable selection of the ships, four requirements are established based on the model requirements and the scope of this research. In this section, the requirements are elaborated, resulting in the final ship collection. The ships in the ship collection are characterised by their fleet type. The complete selection contains five fleet types.

5.1.1. Ship Requirments

The ships in the selection have to be seagoing ships in operation in 2022, future-proof, and Europe-oriented.

Seagoing Ships

According to Pruyn et al. (2022), ammonia will be used for seagoing ships larger than 25000 dwt and trips of multiple days. Therefore, the ships need to be at least 25000 dwt. However, considering the challenges regarding the increase in the fuel tanks and the decrease in the sailing range of the ships, it is required that the ships' routes include long distances because these have the largest influence on the limitation of the onboard fuel tank. Therefore, the minimum deadweight tonnage of the selected ships is 50,000 dwt.

Operation in 2022

The reference year of the case study is 2022, as elaborated in Chapter 2. For the selection of ships, the AIS port call data is requested from MarineTraffic.com. To ensure the data is useful for the research, the ships have to be in service during the year 2022, so ships that are idle or in dock in 2022 are filtered for the selection. Next to this, the ship should be built before 2022 to be able to operate during the reference year. This results in a selection of ships that are built in 2021 at the latest.

Future Proof

The lifetime of seagoing ships is 25 to 30 years. Following the reports of Scarbrough et al. (2022) and Pruyn et al. (2022), ammonia will become a marine fuel on a large scale from 2040 and will enlarge its market share to 40% in 2050. Therefore, the choice is made to limit the ship selection to ships that are likely to be still in operation in those years, assuming these are ships built after 2014. Since these ships have recently been built, they are equipped with more innovative technology to reduce emissions than older ships. Besides, these are ships that have to deal with the regulations realised as a result of IMO's aim to reduce 80% of the GHG emissions by 2050 (International Maritime Organization, 2018). Therefore, retrofitting to ammonia-fuelled ships could be a potential solution to comply with these regulations.

Europe-Oriented

The prior three requirements create a suitable set of ships for a realistic display of the global shipping network. However, this research is done in the context of the MAGPIE project, which is Europe-oriented. Therefore, it is eligible for the included ships to visit ports in Europe in 2022. To ensure this, the remaining ships, answering the prior requirements from the Clarkson WFR, are compared, based on their IMO numbers, to the MRV-THETIS data of 2022 (EMSA, 2023). The MRV-THETIS data registers all ships that have visited a port with Member State (MS) jurisdiction, so all ships in this database operated in EU territory during 2022 (DNV.com, 2023). All ships present in both databases compose the final ship selection consisting of 1026 ships meeting all four requirements. The names and IMO numbers of the ships included in the selection can be found in appendix B. In this appendix, some of the main parameters of the ships are also presented.

5.1.2. Five Ship Types

Following the ship requirements, the obtained ships are a broad selection of seagoing ships with a deadweight larger than 50000 dwt. The selection can be characterised into five different fleet types: 112 bulkers, 300 containerships, 313 crude tankers, 125 product tankers and 176 LNG carriers. The total fleet contains 1025 ships with a DWT range from 79274 to 320785 tonnes. In table 5.2, the parameters are collected for each fleet type to understand the context of the ship selection. Besides the DWT range, the average built year and the considered cargo type are included in the table. The total fleet represents a wide selection of ships operating worldwide, as shown in 5.1.

Table 5.2: Main identification parameters for each fleet type.

Fleet Type	Number of ships	DWT range in tonnes	Average Built Year	Cargo Type
Bulkers	112	87665 - 210724	2018	Grain
Containerships	300	79274 - 241960	2017	TEU
Crude Tankers	313	103118 - 320785	2018	Crude
Product Tankers	125	109258 - 156634	2018	Product
LNG Carriers	176	81514 - 98936	2019	LNG

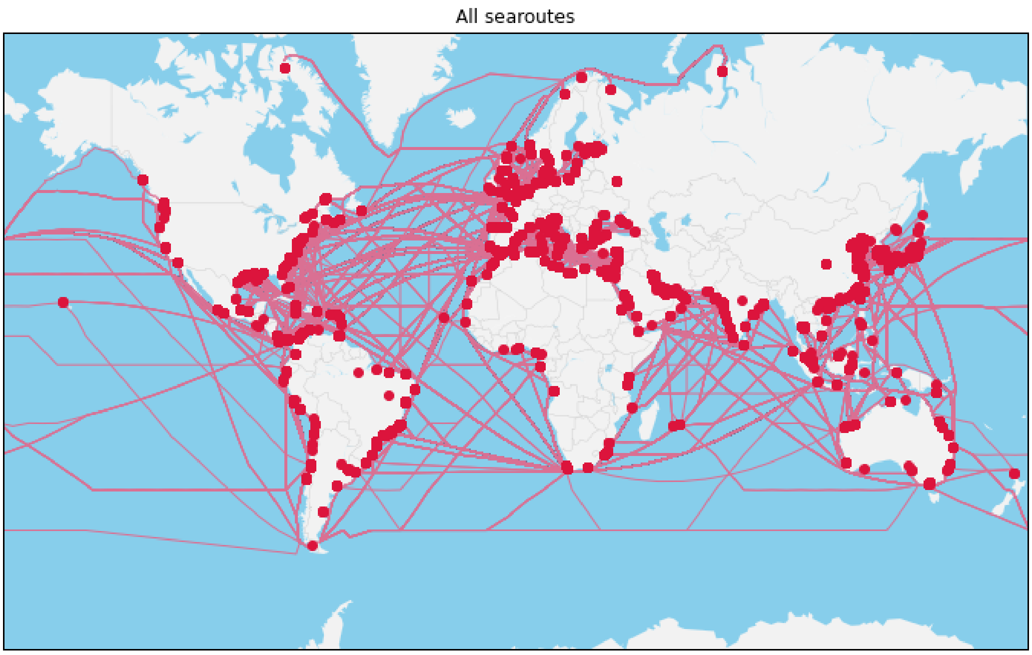

Figure 5.1: Represntation all trips in the shipping network considering in the research.

5.2. Ship data

The data collection starts with the ship data. Chapter 3 elaborates on the significant design and performance parameters that are impacted by a fuel switch for fossil fuels towards ammonia and determine the performance of the ship. The required parameters for the models are collected for the Clarkson Research WFR and THETIS-MRV databases. In this section, the obtained data is translated to a suitable ship dataset. The required input parameters are calculated according to the general design and performance theories to complete the dataset. In table 5.3, a list of all ship parameters is disclosed, including their definitions and sources.

Firstly, the weight and space parameters are achieved, followed by the calculations for the general power and energy estimations of the ships. Next, the fuel consumption calculations are elaborated and translated into one formula that can be implemented in the APSN model. Finally, the THETIS-MRV database is used to provide reference data to validate the operational data for the AIS dataset.

The Clarkson Research WFR database did not include all parameters for all ships. Therefore, the missing data is estimated using linear regression based on the available data from the other ships. This applies to the parameters referring to the footnote in table 5.3.

Table 5.3: Ship design and performance parameters, units, definitions, and sources.

Parameter	Unit	Definition	Source
B	m	Beam midship	Clarkson Research WFR
C_B	-	Block coefficient	Calculated according to equation 5.4
C_D	[-]	Specific delivered power coefficient	Calculated according to equation 5.10
dwt	t	Deadweight tonnage	Clarkson Research WFR
fcm	kg/nm	Fuel consumption per nautical miles	Calculated according to equation 5.24
GT	m^3	Gross tonnage	Clarkson Research WFR
k_1		fuel consumption constant	Calculated according to equation 5.25
L_{pp}	m	Length per pedicular	Clarkson Research WFR
L_{wl}	m	Length waterline	Calculated according to equation 5.3
lwt	t	lightweight tonnage	Clarkson Research WFR*
m^C	t	Mass of related to the cargo	Clarkson Research WFR*
m_{rest}	t	Other mass of related to deadweight	Clarkson Research WFR*
m^T	t	Mass of related to the fuel tank	Clarkson Research WFR*
$P_{AUX,non-PP}$	kW	the non-power plant auxiliary power	Calculated according to equation 5.17
$P_{AUX,PP}$	kW	The power plant auxiliary power	Calculated according to equation 5.16
$P_{AUX,tot}$	kW	Total delivered auxiliary power	Clarkson Research WFR
P_{B,AUX,NH_3}	kW	Auxiliary brake power	Calculated according to equation 5.18
$P_{B,ME}$	kW	Main engine brake power	Calculated according to equation 5.22
$P_{B,tot}$	kW	Total brake power	Calculated according to equation 5.19
P_D	kW	Total installed main engine power	Clarkson Research WFR
P_{MCR}	kW	Total delivered auxiliary power	Calculated according to equation 5.14
sfc	kg/kWh	Specific fuel consumption	Calculated according to equation 5.20
T_{max}	m	Draught midship when loaded	Clarkson Research WFR
v_0	kn	Design speed	Clarkson Research WFR
v_s	kn	Sailing speed	AIS data
V^T	m^3	Fuel tank capacity	Clarkson Research WFR*
V^C	m^3	Cargo volume capacity	Clarkson Research WFR*
W	t	Mass displacement	Calculated according to equation 5.1
∇	m^3	Volume displacement	Calculated according to equation 5.5
∇_{max}	m^3	Maximum volume displacement	Calculated according to equation 5.2

* This data was not available for all ships, and therefore, the missing values are estimated with linear regression.

5.2.1. Volume and Mass

The fuel consumption depends on the volume displacement (∇) of the ship; this represents the underwater volume of the fully loaded ship and refers to the maximum draught of the ship. Firstly, the maximum total weight (W) of a ship is determined to obtain the volume displacement. The maximum total weight is the sum of the deadweight (dwt) and the lightweight tonnage (lwt), equation 5.1. The DWT represents the weight-carrying capacity of the ship, including cargo, fuel, ballast water, fresh water and crew. The lightweight tonnage (LWT) is the weight of the empty ship, representing the steel structure, machinery and outfitting of the ship.

$$W = dwt + lwt \tag{5.1}$$

According to Archimedes' law, the weight of the water displacement is equal to the total weight of the ship. This is called the mass displacement and is calculated by multiplying the volume displacement by the density of seawater (ρ_{sw}) of 1.025 t/m^3.

$$\nabla = \frac{W}{\rho_{sw}} \tag{5.2}$$

The maximum volume displacement (∇_{max})is a function of the ship's length of the waterline (L_{wl}), the beam (B), maximum draught (T_{max}) and the block coefficient (C_B). The L_{wl} has to be estimated because this parameter is not included in the WFR dataset. The length per pedicular is around 96% to 98% of the waterline length of the ship. Therefore, the average of 97% is applied in equation 5.3 (Man Energy Solution, 2018).

$$L_{wl} = \frac{L_{pp}}{0.97} \tag{5.3}$$

Besides, the block coefficient is required to determine the volume displacement. The block coefficient is a constant representing the dimensionless ratio that provides information about the underwater volume of a ship's hull compared to a block with the same overall dimensions. The block coefficient is calculated with equation 5.4.

$$C_B = \frac{\nabla_{max}}{L_{wl} * B * T_{max}} \tag{5.4}$$

The volume displacement is determined with equation 5.5 and represents the maximum water displacement of the ship. For the ship, the length and beam dimensions are fixed, along with the block coefficient. However, the draught of the ship can fluctuate as a result of the loading conditions. Therefore, this equation is applicable to estimate the amount of loaded capacity of the ship, as demonstrated in equation 5.32. Besides, the volume displacement affects the resistance of the ship and, therefore, the required brake power of the ship. This is elaborated further in the next subsection 5.2.2.

$$\nabla = L_{wl} * B * T * C_B \tag{5.5}$$

Furthermore, the Clarkson Research WFR database provides the volumes of specific components related to the DWT, including the fuel tank volume (V^T), the cargo volume capacity (V^C) and the volume of the ballast tanks (V^B). These values are not provided for all ships in the database; for these ships, the missing volumes are approached by linear regression based on the gross tonnage (GT) of the ships. The ballast tanks, fresh water tanks and crew components of the DWT are implemented as one parameter m_{rest} and represent the DWT without the weight of the fuel tank (m^T) and the cargo weight (m^C) in equation 5.6. It is assumed that m_{rest} is constant and will not change as a result of design changes for the fuel tank.

$$dwt = m^C + m^T + m_{rest} \tag{5.6}$$

The cargo capacity measurements depend on the cargo type of the ship. For bulk carriers, LNG carriers, crude and product tankers, the cargo capacity is given in cubic meters, and a containership quantifies its cargo capacity in the amount of Twenty-feet Equivalent Unit (TEU), see equation 5.7. The related densities define the weight of the volumes.

$$1\,TEU = L \times B \times H = 6.1m \times 2.44m \times 2.59m \tag{5.7}$$

This subsection provides the required parameters for the developed ammonia-powered shipping network. Table 5.4 contains the average of main space and weight parameters for each fleet type.

Table 5.4: The average main volume and mass parameters for each fleet type.

Fleet Type	GT [m^3]	DWT [t]	∇ [m^3]	L_{oa} [m]	T_{max} [m]	B [m]	V^T [m^3]	V^C [m^3]
Bulkers	93172	178507	199183	287	18	46	2696	194336
Containerships	161789	165021	209736	363	15	54	5862	15931*
Crude Tankers	93153	175515	198251	279	17	49	2108	187006
Product Tankers	63886	112960	130406	251	15	44	1490	125802
LNG Carriers	117284	92569	126980	295	12	47	3325	173370

* The volume cargo capacity of constainerships is measures in TEU.

5.2.2. Power and Energy Estimation

The total installed power of a ship consists of two components: the total installed main engine power (P_{ME}) and the total installed auxiliary power (P_{AUX}). The main engine power refers to the propulsion system power required to propel the ship and depends on the brake power ($P_{B,ME}$). The brake power depends on the resistance of the ship, which is a function of the sailing speed. The total auxiliary power is the power required for the non-propulsion systems and services onboard the ship and is not directly related to the operational parameters of the ship. The Clarkson Research WFR contains the total installed power of the main engine (P_{ME}) and auxiliary system (P_{AUX}). However, these values cannot be directly applied to the fuel consumption and need to be converted to the brake power.

Propulsion Power

It is assumed the ship is designed to operate at 80% of the Maximum Continuous Rating (MCR) when sailing at design speed (v_0). In this operation mode, the brake power of the main engine is equal to 80% of the total installed power of the main engine (P_{ME}). The delivered power at design speed ($P_{D,0}$) is calculated with equation 5.8.

$$P_{D,0}(v_0) = \frac{P_{B,ME}(v_0)}{\eta_{TRM}} = \frac{0.8 * P_{ME}}{\eta_{TRM}} \tag{5.8}$$

The transmission efficiency (η_{TRM}) represents the losses regarding the power conversion between the main engine and the total delivered power of the propellers and is a combination of the shaft efficiency (η_S) and the relative rotation efficiency (η_R). The shaft losses for ships are typically between 0.5 to 1 per cent, according to Klein-Woud and Stapersma (2002). In *Basic Principles of Ship Propulsion* by MAN Energy Solution, the shaft efficiency is suggested to be 0.99 for two-stroke engines. The ships selected for this research are mainly equipped with two-stroke engines; therefore, a shaft efficiency of 0.99 is applied. The relative rotation efficiency is normally generated from Holtrop & Mennen, a method to provide resistance characteristics and efficiency to predict the resistance of ships. The method has to be performed for each ship individually. Due to the large set of ships handled in the model, applying this method will be a time-consuming process. Besides, the difference in relative rotation efficiency will result in a significant difference in the output of the model. Therefore, the relative rotation efficiency of 0.98 is applied, as suggested by Man Energy Solution (2018). Multiply the shaft and relative rotation efficiencies result in a transmission efficiency of 0.97 and is applied in equation 5.8.

The delivered power (P_D) depends on the displacement (∇) and sailing speed (v_s) of the ship, as demonstrated in equation 5.9. Besides these two parameters, the estimation is based on the specific delivered power coefficient (C_D). The specific delivered power coefficient is calculated according to equation 5.10 (Klein-Woud and Stapersma, 2002), based on the design speed (v_0) and the volume displacement related to the maximum draught ($\nabla(T_{max})$). The relation between the volume displacement and the draught is stated in equation 5.5.

$$P_D = C_D * \rho_{sw} * \nabla(T_i)^{2/3} * v_s^3 \tag{5.9}$$

$$C_D = \frac{P_{D,0}(v_0)}{\rho_{sw} * \nabla(T_{max})^{2/3} * v_0^3} \tag{5.10}$$

Assuming the draught is the only variable parameter in the volume displacement equation, a change in draught (T) impacts the delivered power of the ship. The other parameters in the displacement calculated do not change. Therefore, the actual delivered power estimation is transformed to a function depending on the change in draught and sailing speed; see equation 5.11.

$$\begin{aligned} P_D(v_s) &= P_{D,0} * \frac{\rho_{sw} * \nabla(T)^{2/3} * v_s^3}{\rho_{sw} * \nabla(T_{max})^{2/3} * v_0^3} \\ &= P_{D,0} * \frac{\rho_{sw} * (C_B * L_{wl} * B)^{2/3}}{\rho_{sw} * (C_B * L_{wl} * B)^{2/3}} * (\frac{T}{T_{max}})^{2/3} * (\frac{v_s}{v_0})^3 \\ &= P_{D,0} * (\frac{T}{T_{max}})^{2/3} * (\frac{v_s}{v_0})^3 \end{aligned} \tag{5.11}$$

Consequently, the actual delivered power is converted to the required brake power (P_B) in equation 5.12 with the transmission efficiency (η_{TRM}) as applied in equation 5.8. In equation 5.13, the main engine brake power is formulated as a function of the sailing speed and draught of the ship.

$$P_{B,ME}(v_s) = \frac{P_D(v_s)}{\eta_{TRM}} \tag{5.12}$$

$$P_{B,ME}(v_s) = \frac{P_{D,0}}{\eta_{TRM}} * (\frac{T}{T_{max}})^{2/3} * (\frac{v_s}{v_0})^3 \tag{5.13}$$

It is recommended to include an Engine Margin (EM) in the power estimation to assure a reserve in the installed power for an incidental increase in power demand due to higher sailing speed or extreme weather conditions. Typically, an engine margin of 10 - 15% is applied in equation 5.14 (Man Energy Solution, 2018) and results in the maximum continuous rated engine power (P_{MCR}). The maximum continuous rated engine power is, in general, smaller than the total installed main engine power (P_{ME}) of the ship. The engine margin can decrease in specific and temporary circumstances. However, these are exceptional situations, and therefore, it is not eligible to propose an operational profile with a higher brake power demand than the EM of 15% allows.

$$P_{MCR} = \frac{P_{B,ME}(v_s)}{1 - EM} \tag{5.14}$$

Auxiliary Power

The total installed auxiliary power (P_{AUX}) is independent of the operational parameters like the sailing speed or displacement. It also runs when the ship is in anchorage or port. Considering the energy switch from fossil fuel oil towards ammonia, the total required auxiliary power will change due to the change in the power plant system. Therefore, the total auxiliary power is divided into two components: the auxiliary power for power plant users ($P_{AUX,PP}$) and the auxiliary power of non-power plant users ($P_{AUX,non-PP}$) (Snaathorst, 2022), referring to equation 5.15.

$$P_{AUX,tot} = P_{AUX,PP} + P_{AUX,non-PP} \tag{5.15}$$

The power plant auxiliary power ($P_{AUX,PP}$) is a percentage of the main engine brake power, referring to the energy system used. According to Snaathorst (2022), the power plant auxiliary power is 5% of the main engine brake power (PP_{AUX}) for ships equipped with a diesel Internal Combustion Engine (ICE). For ammonia fuels ships with Solid Oxide Fuel Cells (SOFC), PP_{AUX} is 11% of the main engine brake power. The power plant auxiliary power is calculated according to equation 5.16.

$$P_{AUX,pp} = P_{B,ME} * PP_{AUX} \tag{5.16}$$

The non-power plant auxiliary power is the remaining part of the total auxiliary power, as calculated in equation 5.17. The non-power plant systems and services remain the same when the ship switches the fuel system. Therefore, the non-power plant auxiliary power is based on the reference fuel system, which is fuel oil in this case ($PP_{AUX,FO}$).

$$P_{AUX,non-PP} = P_{AUX} - P_{B,ME} * PP_{AUX,FO} \tag{5.17}$$

For ammonia-powered ships, the total auxiliary brake power is calculated according to equation 5.18, where NH_3 refers to the ammonia SOFC energy system.

$$P_{B,AUX,NH_3} = P_{B,ME} * PP_{AUX,NH_3} + P_{AUX,non-PP} \tag{5.18}$$

Total Power

The total brake power of the ship is the sum of the main engine brake power and the total auxiliary brake power, as formulated in equation 5.19. The total brake power has two components. The first part is variable due to the main engine brake power ($P_{B,ME}$), depending on the sailing speed (v_s) and draught (T) of the ship, and the second part is fixed for the non-power plant auxiliary power of the ship ($P_{AUX,non-PP}$).

$$P_{B,tot} = P_{B,ME} + P_{B,AUX,NH_3} = \underbrace{P_{B,ME} * (1 + PP_{AUX,NH_3})}_{1} + \underbrace{P_{AUX,non-PP}}_{2} \tag{5.19}$$

The deviation of these two components is relevant for the calculation of the fuel consumption in the next subsection. The first part of the equation depends on the performance parameters and fuel choice. The second part is independent of the performance parameters and is assumed to stay the same for all scenarios tested in this research.

Fuel Consumption

The fuel consumption (FC) follows from the total brake power of the ship. First, the specific fuel consumption (sfc) is determined to calculate the fuel consumption, according to equation 5.20. The specific fuel consumption is defined by the efficiency of the power plant (η_{pp}) and the Liquified Heat Value (LHV) of the applied fuel. The power plant efficiency for diesel ICE and ammonia SOFC power plant is 49.34% and 51.33%, respectively, according to Snaathorst (2022). The LHV for HFO is 40.50 MJ/kg and ammonia (NH_3) has an LHV of 18.6 MJ/kg (Klein-Woud and Stapersma, 2002 and IRENA, 2021). The number 3.6 in equation 5.20 represented the recalculation of energy in kilowatt-hours (kWh) to energy in joule (J), 1 kWh = 3.6 MJ.

$$sfc = \frac{3.6}{\eta_{pp} * LHV} \tag{5.20}$$

According to equation 5.20, the specific fuel consumption for fuel oil is 0.180 kg/kWh and for ammonia, it is 0.377 kg/kWh. Thus, the specific fuel consumption for ammonia is more than two times higher compared to fuel oil. This equation only applies when engines are running on 50% MCR or higher. For operations below 50% MCR, the specific fuel consumption increases significantly because the engine becomes lower quickly (Klein-Woud and Stapersma, 2002).

In the BS model, the fuel consumption is calculated per trip, and therefore, the fuel consumption is calculated based on the fuel consumption per nautical mile (fcm). In equation 5.21, the formula for

fcm is defined as a function of the total brake power and sailing speed (Klein-Woud and Stapersma, 2002).

$$fcm = \frac{sfc * P_{B,tot}}{v_s} \tag{5.21}$$

During the trips, the sailing speed (v_s) and the draught (T) of the ship differ, and thus fuel consumption per mile should be formulated as a function of these two parameters. By implementing equation 5.19 into equation 5.21, $fcm(P_{B,ME})$ is a function of the main engine brake power in equation 5.22.

$$fcm(P_{B,ME}) = sfc * \frac{P_{B,ME} * (1 + PP_{AUX,NH_3}) + P_{AUX,non-PP}}{v_s} \tag{5.22}$$

$$fcm = sfc * (\frac{P_{D,0}}{\eta_{TRM}} * \frac{(1 + PP_{AUX,NH_3})}{v_s} * (\frac{T}{T_{max}})^{2/3} * (\frac{v_s}{v_0})^3) + \frac{P_{AUX,non-PP}}{v_s} \tag{5.23}$$

By integrating equation 5.13 into equation 5.22, the fuel consumption per nautical miles is a function of the sailing speed and draught of the ship during the trip; see equation 5.23. The formula for fcm is simplified in equation 5.24, where k_1 is a constant elaborated in equation 5.25.

$$fcm(v_s, T) = \frac{k_1 * T^{2/3} * v_s^3}{v_s} + \frac{P_{AUX,non-PP}}{v_s} \tag{5.24}$$

$$k_1 = sfc * \frac{P_{D,0}}{\eta_{TRM}} * \frac{(1 + PP_{AUX,NH_3})}{T_{max}^{2/3} * {v_0}^3} \tag{5.25}$$

This subsection provides the required parameters for the developed ammonia-powered shipping network. Table 5.5 contains the average of main power and fuel consumption parameters for each fleet type. Next to that, the average annual CO_2 emissions (X_{CO_2}) for each fleet type are included in the table. The CO_2 emissions are estimated by multiplying the average CO_2 per nautical mile, reported in the THETIS-MRV database, by the total sailed distance annually based on the trip data.

Table 5.5: Average power and fuel consumption parameters for each fleet type.

Fleet Type	v_0 [kn]	P_{ME} [KW]	P_{AUX} [KW]	$fcm(FO)$ [kg/nm]	$fcm(NH_3)$ [kg/nm]	X_{CO_2} [t*10^3]
Bulkers	14.8	16820	2887	131.6	244.9	22.2
Containerships	22	53688	15312	368.8	682.3	71.6
Crude Tankers	14.7	17923	3793	147.3	273	20.4
Product Tankers	14.3	14118	3078	132.3	245.9	19.1
LNG Carriers	18.7	31043	7971	260.2	482.3	52.2

The total fleet was responsible for 42.6 million tonnes of CO_2 emissions in 2022, according to the registered average CO2 emissions per distance from THETIS-MRV and the annual distance estimation of the AIS data. This is around 5% of the total annual CO_2 emissions by the total worldwide fleet.

5.3. Trip data

For the selected ships, the AIS history port calls of 2022 are requested from Marine Traffic. This data is used to construct the operational profile of the ships and consists of port and anchorage calls registered by the AIS. Each port or anchorage call is registered with a UTC timestamp, United Nations Code of Trade and Transport Locations (UN/LOCODE), facility type ('port' or 'anchorage'), move type ('arrival' or 'departure') and the minimum, maximum and current registered draught. In this section, the application of this data is elaborated and processed to become suitable data for the BS model. The parameters obtained and discussed in this section are assembled in table 5.6.

Table 5.6: Parameters obtained and based on historical port calls from Marine Traffic.

Parameter	Unit	Definition	Source
$d_{hk,hk+1}$	nm	Trip distance	Calculated with `searoute`
FC_{MRV}	t	Annual fuel consumption	THETIS-MRV
FR_g	USD/(unit·nm)	Freight rate per nautical mile	Clarkson Research SIN
fcm_{MRV}	t	Average fuel consumption per nautical mile	THETIS-MRV
n	-	Number of trips	Based on the AIS data
T_k	m	Draught during trip	Based on the AIS data
t_{hk}	UTC	Port arrival time	Based on the AIS data
$t_{a,anchor}$	UTC	Anchor arrival time	Based on the AIS data
$t_{anchor,k}$	h	Total anchorage time	Calculated in according to equation 5.27
t_{hk+1}	UTC	Port departure time	Based on the AIS data
$t_{d,anchor}$	UTC	Anchor departure time	Based on the AIS data
t_k	h	Trip duration	Calculated according to equation 5.26
t_{port}	h	Total time in port	Calculated according to equation 5.28
t_{sea}	h	Total time at sea	Section 5.3.3
$t_{s,MRV}$	h	Total hours at sea	THETIS-MRV
$t_{tot,anchor}$	h	Total anchorage time	Section 5.3.3
v_{MRV}	kn	Average sailing speed	Calculated according to equation 5.30
v_k	kn	Sailing speed	Calculated according to equation 5.29
V_k^C	m^3	Transported cargo of the trip	Calculated according to equation 5.32
W_k	t	Trip mass displacement	Calculated according to equation 5.31
ρ_g	kg/L	Cargo density	Based on Clarkson Research SIN

5.3.1. Route

The dataset from Marine Traffic contains a large set of port call data and is sorted in chronological order for each ship to create clear port call datasets. However, the dataset shows some distortions, as it appears to have double port calls registered and not all port calls are followed by the expected move type. This means that, for example, arrival port calls are followed by another arrival port call instead of a departure port call as expected. These errors are solved in the data process by examining the disturbing port call to be neglected or adding an extra fictional port call to the data. The consideration is based on the facility type and move type of the prior and later port call.

After the elimination of the distortions, the route assigned to the ship is defined as a set of the trips (K) resulting from the port call referring to the ship's name and IMO number. In this research, a trip is defined as the departure port call followed by an arrival port call, and both port calls refer to the same ship. When an arrival port call does not follow a departure port call, or there is no departure port call prior to the arrival port call, the trip is not considered in the trip data. Each trip in the route has a departure port (hk) and an arrival port ($hk + 1$) and identifies the route of the ship in 2022. The sum of all trips in the route is the number of trips (n) of the ship.

5.3.2. Trip Distance

The trip distance ($d_{hk,hk+1}$) between the departure port and the arrival port is calculated with the `searoute` toolbox in Python (Halili, 2023). This toolbox generates the route between two locations over the sea, and the locations are indicated based on their local coordinates. The route over sea follows a set of coordinates between the two ports, avoiding land and based on the shortest route principle. For the route, the distance is calculated using nautical miles. Before applying this method to the AIS data set, the accuracy of the `searoute` toolbox is tested for ten common routes. The results conform to the estimated distances from other port distance calculation sources. In figure 5.2, the distance calculation with `searoute` and the conservative great-circle route calculation are shown to demonstrate the difference.

Besides, the toolbox contains a feature for restrictions to avoid specific areas on the route, including the Panama and Suez Canal. These two canals have limited depth and width, and therefore, not all ships can pass these canals. The maximum permissible dimensions for the canals are disclosed in table 5.7. Ships that have a wider beam or are sailing with a deeper draught than mentioned in this table have to use another, avoiding the canal. By adding the name of the canal, which has to be avoided, to the restrictions, the `searoute` toolbox will calculate a new route between the two ports. Besides these canals, the toolbox includes a restriction that ensures the route avoids the North West area, referring to the routes going through the Northside of Russia and Greenland. This feature is applied to all routes because it is assumed these routes are inaccessible to the selected fleet.

Table 5.7: Limiting parameters for Panama and Suez Canal

	Panama Canal	Suez Canal
max draught	15.2 m	20.1 m
max beam	49 m	77.5 m
max length	366 m	
max deadweight tonnage	60 -100 t	

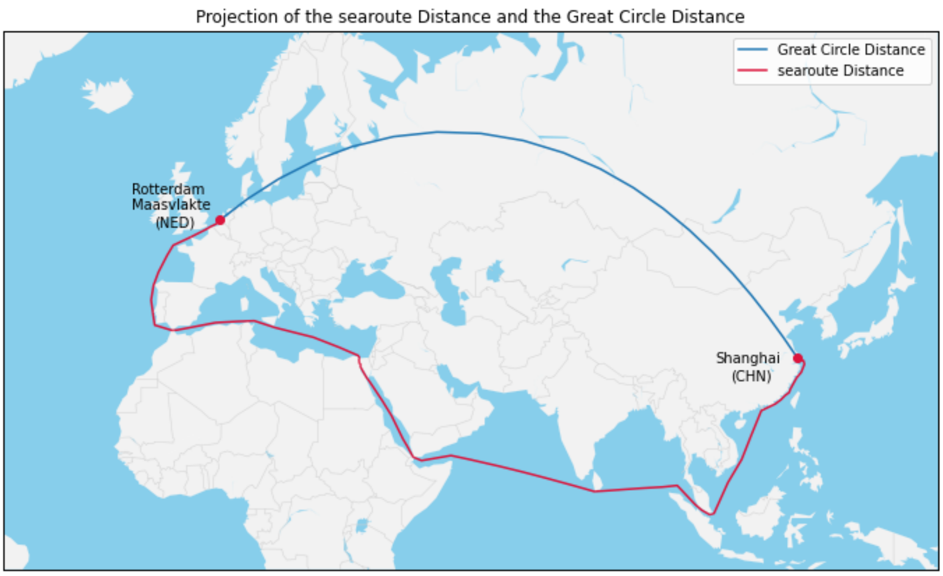

Figure 5.2: Example of the `searoute` distance (10580 nm) compared to the great circle distance (4834 nm) between Rotterdam Maasvlakte (NL) and Shanghai (CN)

The distance calculations from `searoute` perform plausible results that are similar to the real distance between the ports. However, there are two remarks to consider when applying the toolbox. Firstly, the distance calculated between two points is a straight line, and typically, ships do not sail in straight lines due to currents and weather conditions. Another reason to deviate from the shortest path is to avoid unreliable or unsafe areas. Especially for the routes crossing the Pacific and Atlantic Oceans, a straight line across the ocean is not a realistic route. Therefore, this is an optimistic distance calculation, and the routes crossing large waters include an extra margin for the distance calculation.

The second remark is the application of the AIS data The distance calculation is only based on the port calls provided in the AIS dataset The anchorage calls are not included because the locations are not related to a specific UN/LOCODE, and therefore, the position of the anchorage cannot be defined However, a general observation of the AIS data suggests that most of the anchorage calls refer to names that are similar to the nearby ports, which are the ports that are visited right before or after the anchorage call Therefore, it is assumed that neglecting the anchorage position in the distance calculation does not result in significant differences.

5.3.3. Trip Duration

The AIS dataset from Marine Traffic provides a timestamp (UTC) for each registered port or anchorage call. These timestamps are used to determine the duration of the trips, anchorages, and stays in port in hours. The three duration types refer to the three operation modes this research considers: sailing (trip time), anchor (anchorage time) and in-port (port time). The trip time is defined as the time at sea between a port departure call (t_{hk}) and a port arrival call (t_{hk+1}) without the anchor time registered between the two port calls. This estimation is formulated in equation 5.26.

$$t_k = (t_{hk+1} - t_{hk}) - t_{anchor,k} \tag{5.26}$$

For the trips with anchorage calls within the port departure and arrival, the anchor time is calculated according to equation 5.27. It occurs that a ship anchors more than once during the trip, and therefore, the anchor time during the trip ($t_{anchor,k}$) is formulated as the sum of all anchor time within the port calls. In case there are no anchorage calls during the trip, the anchor time is assumed to be zero.

$$t_{anchor,k} = \sum (t_{a,anchor} - t_{d,anchor}) \tag{5.27}$$

All the trip times over the year together are the total annual trip time of the ship and are also referred to as time at sea (t_{sea}). The annual anchor time ($t_{tot,anchor}$) is the sum of all trip anchor times added up. The annual port time is estimated as the remaining time of the year, as shown in equation 5.28. It is assumed that a year is equal to 8760 hours.

$$t_{port} = 8760 - t_{sea} - t_{tot,anchor} \tag{5.28}$$

With the annual port time (t_{port}), annual anchor time and time at sea, the deployment of the ship is determined.

5.3.4. Sailing Speed

The sailing speed of the ship has a significant impact on the ship's fuel consumption and differs during the ship's operations. The available AIS data for this research includes the port and anchorage calls of the ships. However, more specific data regarding the sailing speed during the trip is not included in the dataset. Therefore, the sailing speed during a trip is assumed to be constant for the whole trip, and there is no distinction between sailing operation modes. The sailing speed applied to estimate the fuel consumption is the average sailing speed during the trip. The average sailing speed during the trip (v_k) is approximated based on trip distance and the trip time calculated in equation 5.29.

$$v_k = \frac{d_{hk,hk+1}}{t_k} \tag{5.29}$$

Due to errors in the AIS dataset, there are trips registered with the same start and end port, which results in a trip distance of zero nautical miles. In these cases, there has not been an actual trip to perform for the ship, and therefore, these trips are excluded from the ship's trip data. The average sailing speed is estimated based on trips that remain in the trip data and thus are non-zero.

Next to that, the average sailing speed is estimated with the data registered byTHETIS-MRV. The total distance is approached by dividing the total annual fuel consumption (FC_{MRV}) in tonnes by the fuel consumption per nautical mile in kg/nm. Then, the distance is divided by the total hours at sea to estimate the average sailing speed, as formulated in equation 5.30.

$$v_{MRV} = \frac{FC_{MRV} * 1000}{fcm_{MRV} * t_{s,MRV}} \tag{5.30}$$

The trip sailing speed results in a significant low or high sailing speed for a part of the trip. This can be explained by incorrect registrations and port calls, which result in trips of an unrealistic duration. The obtained AIS data does not provide details regarding the sailing speed of the ship to identify an explanation for this error. Therefore, the trip sailing speeds are corrected to be within the order of 50% to 110% of the design speed. After correcting the average trip sailing speed, the results are in line with the average sailing speed based on the THETIS-MRV database. However, correcting the trip speeds affects the trip duration, considering the trip distance is constant.

5.3.5. Transported Cargo

In addition to the ports and timestamps, theAIS dataset registered the ship's draught at the time of the port call. The reported draught at the departure port is considered trip draught (T_k). This data provides the determination of the mass displacement of the ship during the trip (Δ_k). As suggested in section 5.2.1, the volume displacement is linear and related to the ship's draught, considering the length, beam, and block coefficient are constant. Equation 5.31 calculates the volume displacement during the trip.

$$W_k = L_{wl} * B * T_k * C_B * \rho_{sw} \tag{5.31}$$

The APSN model minimizes the loss of revenue based on the cargo income (I^C) and the bunker costs (C^B). The cargo income depends on the amount of cargo transported by the ship. The transported cargo during the trip (V_k^C) is the main component of the trip displacement and is calculated by equation 5.32. The ρ_g refers to the cargo density of cargo g.

$$V_k^C = \frac{W_k - lwt - m^T - m_{rest}}{\rho_g} \tag{5.32}$$

To estimate the cargo income of the trip, the transported cargo is multiplied by the freight rate. The freight rates for each cargo type are established from the Clarkson Research SIN database. The applied freight rates are balanced over the annual fluctuation of the data. In general, freight rates are related to specific trajectories. Therefore, the original freight rates are divided by the distance of the related traject so that the freight rates can be implemented as USD/(units·nm) and independent from the distance. However, the reported freight rates data for the crude tankers was limited and did not include a reference distance or ship size. Therefore, the freight rate for crude tankers is calculated differently. The final freight rates are shown in table 5.8.

Table 5.8: Freight rates per cargo type.

Cargo Type	Freight Rate	(FR_g)
Grain	0.006224	USD/(t·nm)
TEU	0.5160	USD/(TEU·nm)
Crude	38580	USD/(day)
Product	0.007315	USD/(t·nm)
LNG	0.002318	USD/(m^3·nm)

This section provides the operational parameters for the developed ammonia-powered shipping network. Table 5.9 contains the average of parameters regarding the trip data for each fleet type.

Table 5.9: Average trip performance parameters for each fleet type.

Fleet Type	n [-]	T_{avg} [m]	t_{sea} [h]	d_{TOT} [nm]	v_{avg} [kn]	$V^C_{k,avg}$ [m^3]
Bulkers	11.6	12.9	5533	51611	10.3	90098
Containerships	50.7	13	5760	77349	15.7	11347
Crude Tankers	15.8	11.8	5603	42928	9.9	98100
Product Tankers	17.7	10.9	5329	47245	10.5	60023
LNG Carriers	17	10.5	6484	79386	13.6	136574

* The volume cargo loss of constainerships is measures in TEU.

5.4. Port Data

The port selection is based on ports visited by the considered fleet, as reported in the AIS dataset. In the AIS dataset, the ports are identified by their UN/LOCODE. This results in a port selection of 644 ports worldwide, as shown in figure 5.3. Some big ports have several UN/LOCODE for different areas in their port. In this research, each UN/LOCODE is approached as an individual port. In table 5.10, the required port parameters are defined, including the related units and resources. This section explains the data generation for the port parameters regarding the identification of the port and the input parameter to define the OPEX of the ammonia bunker price.

Table 5.10: The port parameters, units, definitions and sources.

Parameter	Unit	Definition	Resource
C_h	m	Channel Depth of the port	WPI
Lat	°	Latitude location coordinate of port	WPI
Long	°	Longitude location coordinate of port	WPI
N_h	-	Number of port visits	Based on the AIS data
Name	-	Port name	WPI
p_{FO}	USD/t	Bunker price for fuel oil	Clarkson Research SIN
c_h^{prod}	USD/t	Ammonia production cost	Nayak-Luke and Bañares-Alcántara (2020)
c_h^{trans}	USD/t	Ammonia transportation cost	Nayak-Luke and Bañares-Alcántara (2020) & Salmon et al. (2021)
n_h	-	Number of existing ammonia cargo facilities in the port	ALFA LAVAL et al. (2020)
UN/LOCODE	-	United Nations Code for Trade and Transport Locations	WPI

General Port Parameters

Based on the UN/LOCODEs reported in the AIS data, the location of the ports could be obtained from the WPI database. The locations of the ports are defined with the latitude and longitude coordinates. These coordinates are required to calculate the distance between the ports with the `searoute` module in Python, as described in section 5.3. Besides the location of the port, the WPI data provides the official port name and the country of the port. However, the WPI data does not include all the ports reported in the AIS data. Therefore, the location of the missing ports is obtained manually from MarineTraffic.com.

The number of port visits is based on the port calls in the AIS data. This gives a first indication of the participation of the ports in the shipping network. Figure 5.3 depicts the number of port visits for each port based on the AIS data.

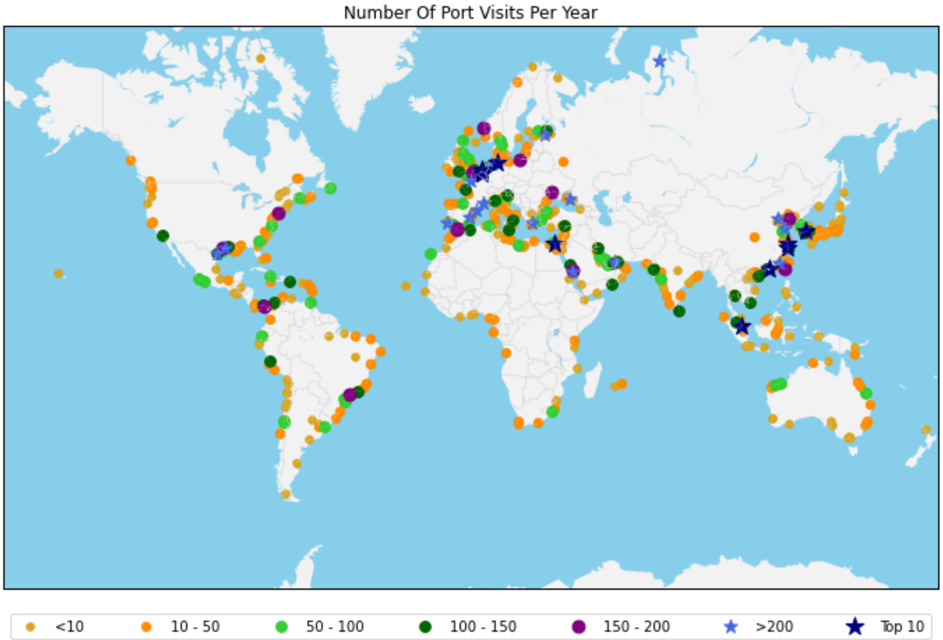

Figure 5.3: The number of port visits at each port location considered in the case study.

Bunker Prices Parameters

The model generates the impact of a transition to ammonia by comparing the operational performance of the ships considering fuel oil and ammonia. Therefore, the bunker prices for this fuel are required. The fuel oil bunker price for each port is estimated based on the Very Low Sulphur Fuel Oil (VLSFO) bunker prices data from Clarkosn Research (2023a). This data provides the global average of bunker prices in 2022 and for specific countries and ports. Considering the variation is the VLSFO bunker price based on the location, the bunker price for fuel oil is determined for each port.

The ammonia bunker price is not obtained from a dataset but is approached using the Port model developed in this research. However, this approach required the production costs (c_h^{prod}) and the transportation costs (c_h^{trans} for ammonia as input data for the Port model. The production costs are approached based on the results of studies Nayak-Luke and Bañares-Alcántara (2020) and Salmon et al. (2021). These studies developed a model to estimate the PLCOA based on the geographical opportunities for green ammonia production, considering the availability of wind and solar energy. Besides, the studies provide an approach to the transportation costs for two modes of transport: by ship and pipeline. The transportation mode for each port is based on the ammonia demand of the port and the region in which the port is located.

Channel Depth

Initially, the bunker strategy model included a third constraint regarding the draught of the ship, equation 5.33. These constraints ensure that the ship can only perform the trip with the draught of the ship being smaller than the channel depths of the departure and arrival ports. If this is not the case, the ship has to reduce its draught by losing cargo or fuel. However, comparing the draughts registered in the AIS trip data to the channel depth of the related ports reported by the WPI, significant errors were found. Most of the ships enter at least once a port with a smaller channel depth than the current ship's draught. Therefore, the constraint is eliminated from the model, and the route is prioritised according to the AIS data. The smallest value of these three parameters is the maximum draught of the ship during the trip, as defined with constraint 5.33.

$$T_{max} = min(T_{max,s}, D_k, D_{k+1}) \tag{5.33}$$

6

Case Study

As a result of the literature study, fuel consumption is a parameter highly impacted by a fuel switch to ammonia. The fuel consumption represents the performance of the ships and depends on the fuel type, draught, sailing speed and the distance travelled by the ship. Besides, the fuel consumption is related to the maximum range of the ship, which is determined based on the fuel tank's volume. Therefore, the three significant design and performance parameters are the fuel type, the fuel tank volume, and the sailing speed. Next to those parameters, the bunkering and rerouting strategies impact the fuel tank volume and vice versa.

This chapter elaborates on the steps taken to investigate the impact of a fuel switch to ammonia on these parameters and strategies. The first section generates a baseline for the ship's operational pattern based on the current ship designs and trip data and compares the fuels, fuel oil and ammonia. In section 6.2, three different speed scenarios are compared, including the trip speed, the design speed and the speed referring to when the ship is operating at 60% MCR. The fuel tank volume of the ship is the following parameter to investigate in section 6.3. Here, the volume of the onboard fuel tank is increased by scaling the tank in three ways based on the density ratio of fuel oil and ammonia: the longest trip and the second-longest trip. The third factor to investigate is the bunker strategy, which includes two strategies. Firstly, in the trip bunkering strategy, the ship always bunkers the fuel required for the upcoming trip at the start port of the trip. Secondly, the forward bunkering strategy is considered to minimize the bunker costs. Besides, the last scenarios apply an integration of fuel tank optimization in the model to generate a fuel tank volume that minimizes the loss of income to the shipowner. This optimization is performed for both considered bunker strategies.

Finally, the ten scenarios are summarised in section 6.5 to provide an overview of the conditions in each scenario and the model process. Besides, the table includes an overview of whether the rerouting module is considered to ensure the route's feasibility.

6.1. Baseline (S0)

This step generates a baseline of the current performance of the ships and their fuel consumption based on their deployment and the trip sailing speed obtained from the trip data. The scenario performed with fuel oil (S0A) is the baseline and is considered the reference data to determine the operational impact of ammonia. The scenario (S0B) considering ammonia as fuel is performed to prove the suggested challenges regarding using ammonia as a marine fuel in the literature research. Besides, the results of this scenario demonstrate the problem statement and, therefore, confirm the relevance of the research.

Besides the different fuels, the two scenarios are performed with the same condition and stay close to the original input data. Therefore, the sailing speed of the ships is the average speed based on the AIS data calculated according to section 5.3 and the volume of the fuel tank onboard is based on the Clarkson WRF data. To retain the baseline simple, it is considered that the ship will always bunker the amount of fuel required for the upcoming trip at the start port of the trip, and rerouting is not considered.

Considering there is no rerouting in scenario S0B, in combination with maintaining the original volume of the fuel tank, it is expected that this will result in unfeasible trips for the ships and therefore, the model will mark the ships with unfeasible trips as failed. However, this scenario aims to provide an insight into the operational challenges that will occur by switching to ammonia as a marine fuel. This will quantify the operational impact of ammonia in the number of trips not feasible in the current operational profile of the ships compared to the fuel oil scenario, S0A.

6.2. Sailing Speed (S1)

In this section, the effect of the ship's sailing speed is studied. The three sailing speed scenarios are the design speed (S1A), the sailing speed when operating on 60% MCR (S1B) and the average trip speed (S1C), based on the AIS data. All scenarios consider ammonia as the fuel and the original fuel tank volume.

With the three sailing speed scenarios, the impact of the sailing speed on the fuel consumption and, therefore, the feasibility of the assigned trips is demonstrated. To prioritise this impact on the ship and the shipping network, the ships will always bunker the amount of fuel required for the upcoming trip at the start port of the trip.

The literature research concludes that higher sailing speeds result in higher fuel consumption and shows that, generally, ships sail at lower sailing speeds than their design speed. Therefore, it is assumed that the fuel consumption of the trips in scenario S1A will be bigger than in scenario S0B. The rerouting sub-model is used in the three sailing speed scenarios to ensure the feasibility of the routes.

The decision to perform these three sailing speed scenarios is established to observe the impact of the sailing speed from the perspective of a fuel switch to ammonia. However, in the context of the obtained data, the sailing speed is estimated based on the AIS data. As elaborated in section 5.3, the unrealistic trip speed resulting from the AIS data is corrected to fit within the range of 50% to 110% of the design speed. This correcting results in a disparity with the registered duration of the time, and therefore, it is assumed that a plausible speed optimization is not attainable.

Hence, the results of these scenarios demonstrate a general impact of the sailing speed on the operational profile of the ships by simulating high, standard, and low sailing speed scenarios to cover the range of potential sailing speeds. Scenario S1A, with ships operating on their design speed, is the upper bound simulation, considering the efficiency of the ship's main engines decreasing for higher speed. Besides, ship operators prefer to sail at an economical speed, which is lower than the design speed in the current market. The lower bound is performed in scenario S1B, with sailing speed defined by the sailing speed related to the ship performance at 60%MCR, assuming that the main engine efficiency decreases significantly for lower MCR, resulting in more fuel consumption. To quantify the impact of the high and low-speed scenarios, the third sailing speed scenario, S1C, is included based on the sailing speed from the trip data. The extension from scenario S0B to scenario S1C is that scenario S1C considers rerouting in contrast to S0B. The other variable conditions are the same in all sailing speed scenarios.

6.3. Fuel Tank Volume (S2)

In this scenario category, the impact of the volume of the fuel tank of the ships is studied in three sub-scenarios. The fuel tank volume scenario is simulated with the sailing speed based on the trip speed for the trip data and is fuelled with ammonia. The bunker strategy for the scenarios is that the ship will always bunker the amount of fuel required for the upcoming trip at the start port of the trip. The scenarios differ in the volume of the fuel tank. Besides, the size of the fuel tank determines if rerouting should be considered.

In the first fuel tank volume scenario, S2A is based on the contained volumetric energy density ratio between fuel oil and ammonia. The volumetric energy density ratio ($R_{\rho_{EV}}$) is 3.51 and is calculated in equation 6.1. Therefore, the volume of the fuel tank of the ships increases by 351% in this scenario. Table 6.1, this is referred to as *Design volume scaled to ammonia*. This is a significant increase in the fuel tank volume. Therefore, no rerouting is considered.

$$R_{\rho_{EV}} = \frac{\rho_{EV}^{FO}}{\rho_{EV}^{NH3}} = \frac{33.2MJ/L}{9.45MJ/L} \approx 3.51 \tag{6.1}$$

Scenario S2B is simulated with a fuel tank volume based on the volume of the amount of fuel required to complete the longest trip of the ship's route. The longest trip refers to the trip that requires the highest fuel consumption, according to the trip data. In this scenario, rerouting is not required because increasing the fuel tank volume to fit the longest trip is coherent with the ship being able to complete all trips. The reroute module applies for trips that are not feasible, considering the maximum sailing range is smaller than the trip distance. In scenario S2B, the fuel tank volume is scaled to fit the longest trip; therefore, the trip distance is always feasible within the range of the ship and rerouting is not required.

The longest trip elimination defines the third fuel tank volume scenario, S2C. In this scenario, the model of the rerouting module is implemented to divide the longest trip into two smaller trips. This implies that the fuel tank volume is scaled to the fuel amount required to complete the second-longest trip or is equal to 75% of the fuel required to complete the longest trip. The smallest volume of the two is the dominant volume for this scenario. Considering the longest trip elimination, the ships cannot complete all their trips. Therefore, the rerouting module is applied in this scenario. This scenario shows the sensitivity of ships with one long trip compared to the other trips in the route. This improves the flexibility of the fuel tank requirements with a minimum change in the routing.

6.4. Bunker Strategy Optimization (S3)

This research includes a broad selection of 1025 large seagoing ships. The selection contains five different fleet types that vary in size and operational area. Therefore, the impact of a fuel switch to ammonia differs for each ship. For example, the preferable fuel tank volume varies for the several ship types. In scenarios S0A to S2C, the ships have a fixed fuel tank volume, which neglects the possibility of varying per ship type to find the most suitable option.

In the two scenarios of S3, the fuel tank volume will vary from 100% to 400% of the original fuel tank volume. The most suitable fuel tank volume for each ship is estimated by pursuing a balance between the fuel tank volume increase and the decrease in cargo volume. The balance is achieved by minimizing the loss of ship annual revenue by applying the bunker strategy model in section 4.1.

This fuel tank optimization is applied for both bunker strategy scenarios, resulting in scenarios S3A and S3B. Scenario S3A simulates that the ships will always bunker the amount of fuel required for the upcoming trip at the start port of the trip. Scenario S3B considers the forward bunker strategy. Both scenarios are simulated for ammonia as fuel, operating on the trip speed and requiring rerouting.

In the bunker strategy scenario S3B, the impact on the ports is studied, and the dynamics between the port choice of the ships, the fuel price and the fuel demand of the ports appear. To generate this, the forward bunker strategy implies that the ship can choose which port the ship bunkers should be in to minimize the total annual bunker costs, and it is not obligated to bunker in each port of the route. The construction and constraints of the forward bunker strategy are further elaborated in section 4.1.

6.5. Overview

This section provides an overview of all the ten scenarios and their related scenario properties. The overview is presented in table 6.1. The table assists the reader in going through the scenarios presented in this report.

Table 6.1: Overview of the simulated scenarios and their conditions and considerations.

Properties	S0		S1			S2			S3	
	A	B	A	B	C	A	B	C	A	B
Fuel										
Fuel oil	✓									
Ammonia		✓	✓	✓	✓	✓	✓	✓	✓	✓
Sailing speed										
Design sailing speed			✓							
Sailing speed with 60%MCR				✓						
Trip sailing speed	✓	✓			✓	✓	✓	✓	✓	✓
Fuel Tank										
Design volume	✓	✓	✓	✓	✓					
Design volume scaled to ammonia						✓				
Required volume the longest trip							✓			
Longest trip elimination								✓		
100% to 400% design volume									✓	✓
Bunker strategy										
Refuel when required one trip	✓	✓	✓	✓	✓	✓	✓	✓	✓	
Refuel forward										✓
Route										
Given route	✓	✓				✓	✓			
Rerouting			✓	✓	✓			✓	✓	✓

7 Validation and Model Testing

In this chapter, the model validation is explained. The results of the APSN model depend on the input data and the structure of the model. Therefore, the validation contains two parts. Firstly, the obtained input data is validated to be a plausible dataset for the model. This validation is described in section 7.1. Subsequently, the APSN model is tested in order to ensure that the model performs as it should by a set of modelling tests, as defined in section 7.2.

7.1. Input Data Validation

The APSN model requires a wide collection of input data, including ship design data, ship performance data, trip data, port data and fuel data. Therefore, the results of the model depend on the reliability of the data. In this section, the validation of the input data is explained. The results for the input data are compared to reports and datasets similar to this research. In table 7.1, the validation method for the data is summarized.

Table 7.1: Input data validation.

Data	Validation Method
Power and Energy Parameters	The results are compared with the results of the power and energy results in the study of Snaathorst (2022), which determines the power of the ships based on Holtrop & Mennen. This research considers smaller ship selection.
Fuel Consumption Results	The fuel consumption is estimated with two approaches, based on the power estimation and based on the THETIS-MRV data of the ships.
Port Distance	The distance estimation from the `searoute` module in Python are recalculated manually for ten random distances.
Trip Speed	The trip speed resulting from the AIS data is compared to the average speed obtained from the THETIS-MRV data, and excessive results are corrected based on the design speed of the ship.
Increase Fuel Volume	The increase of fuel volume for ammonia according to the APSN model shows similar results to the prior research (McKinlay et al., 2021; Wu et al., 2022; Lagemann et al., 2022)

7.2. Model Testing

For the scenario S0, the model was tested with one ship to identify and solve errors. The test ship was the ‘Abliani’, which had a set of 19 trips. In this way, the basic functionality of the model is tested, and results are compared to expected results. In the second step, the complete raw data set is used to evaluate the model and to identify and solve errors that result from the much wider variety of trips and routes. Similar approaches are followed for the other scenarios with a focus on the changes in the simulation model. The large data set of ships is used as a test set for the validation of the models. Table 7.2 lists the specific tests that are performed.

Table 7.2: Model tests.

Test	Check
General	
If the cargo volume capacity of the ship is smaller than the volume of the transported cargo during the trip, the transported cargo is reduced to fit the cargo volume capacity.	✓
If the cargo weight capacity of the ship is smaller than the volume of the transported cargo during the trip, the transported cargo is reduced to fit the cargo weight capacity.	✓
If the ship cannot complete the total route with the current fuel tank volume, the fuel tank volume is not considered as an optimal solution.	✓
If the trip speed of the ship according to the AIS data is smaller than 50% of the ship's design speed, the trip speed is corrected to 50% of the ship's design speed.	✓
If the trip speed of the ship according to the AIS data is larger than 110% of the ship's design speed, the trip speed is corrected to 110% of the ship's design speed.	✓
Rerouting	
If the fuel tank volume is smaller than the required fuel for the trip, the reroute model is activated, and an alternative route is provided.	✓
If the reroute model does not provide an alternative route for the ship, the trip is defined as not feasible, and the ship will not complete the total route.	✓
The number of trips in the ship's route after rerouting is larger or equal to the number of trips in the original route of the ship.	✓
Forward bunker strategy	
If the ammonia bunker price in port k of the ship's route is lower than the ammonia bunker price in the current port and port k is within the ship's sailing range, the ship only bunkers the amount of ammonia required to reach port k.	✓
In the forward bunker strategy, the total amount of ammonia bunkered is equal to the minimal required amount of ammonia to complete the route.	✓
The total bunker ammonia in one port is smaller or equal to the ship's maximum fuel tank capacity.	✓
If the ammonia bunker price in the current port is lower than the ammonia bunker price of the ports within the ship's sailing range, the ship bunkers the amount of ammonia to fill up the ship's maximum fuel tank capacity.	✓
The amount of ammonia bunkered in the port is equal to or larger than zero.	✓

8 Results

In this chapter, the results of the model are presented according to the scenarios that were performed. First, the baseline scenarios S0A and S0B are discussed in section 8.1. These results are used as reference data for the other scenarios to indicate the operational impact of ammonia. Section 8.2 elaborates on the results of the speed scenarios (S1) and fuel tank (S2) scenarios. The results are explained in section 8.3. The results of the bunker strategy optimisation scenarios (S3) are divided into sections 8.4 for the trip bunkering optimisation (S3A) and 8.5 for the forward bunkering optimization (S3B). Besides, section 8.5 includes an additional review of the result for the EU port in the context of the MAGPIE project. The description of the specific considerations for each scenario can be found in Chapter 6. Finally, the results are summarized in conclusion 8.6. In this chapter, the results regarding the impact on the ship are presented as the average per fleet type.

8.1. Baseline S0A and S0B

The first set of scenarios is applied to get a general overview of the impact of the transition to ammonia. Whereas Scenario S0A is considered a shipping network powered by fuel oil, and Scenario S0B is based on an ammonia-powered shipping network.

Scenario S0A represents the performance of the ships in the current situation, powered by fuel oil and based on the AIS data. This scenario is used as the baseline scenario. The results for the fuel consumption, fuel costs, cargo income and annual revenue for this scenario are summarized in the table 8.1. Comparing these results with the results of scenario S0B in table 8.2 provides a general overview of the impact of the transition to ammonia on fuel consumption and the feasibility of the original operational pattern.

Table 8.1: The results of the fuel consumption, fuel costs, cargo income and the annual revenue for scenario S0A for each fleet type.

Fleet Type	FC_M [t]	C^B [mUSD]	I^C [mUSD]	R [mUSD]
Bulkers	6831	5.48	24.16	18.68
Containerships	28377	22.77	493.63	470.85
Crude Tankers	6431	5.04	12.45	7.41
Product Tankers	6297	4.98	17.43	12.45
LNG Carriers Carriers	21056	16.63	25.32	8.68
Total Fleet	15393	12.26	157.38	145.12

In table 8.2, the results for the same routes are simulated based on the transition to ammonia. This table shows the increase in fuel costs and the loss of revenue related to this. In this scenario, the fuel tank volume is not changed. Therefore, the fleet has the same potential cargo capacity. However, due to the higher fuel consumption, a large part of the ships are not able to fulfil all the trips in their route due to a fuel tank volume that is too small. Table 8.3 summarizes the number of ships with unfeasible trips for S0B and the other scenarios. These ships required changes in the fuel tank volume, sailing speed, or route. In extinction, table 8.4 shows the average percentage of trips that are not feasible for the ship; on the left side is the fleet average, and on the right side is the average for the ships that require change. This quantifies the size of the problem that needs attention in further scenarios.

Table 8.2: Scenario S0B: The annual change of fuel consumption, cargo loss, fuel costs, cargo income and revenue in percentage for scenario S0B compared to the baseline scenario S0A.

Fleet Type	ΔFC_M [t]	ΔV^C [m^3]	ΔC^B [mUSD]	ΔI^C [mUSD]	ΔR [mUSD]
Bulkers	+86.23%	0.0%	+191.01%	0.0%	-50.94%
Containerships	+85.15%	0.0%	+59.63%	0.0%	-3.44%
Crude Tankers	+85.6%	0.0%	+133.86%	0.0%	-141.85%
Product Tankers	+85.78%	0.0%	+141.7%	0.0%	-62.8%
LNG Carriers	+85.7%	0.0%	+80.57%	0.0%	-271.04%
Total Fleet	+85.57%	0.0%	+110.19%	0.0%	-103.95%

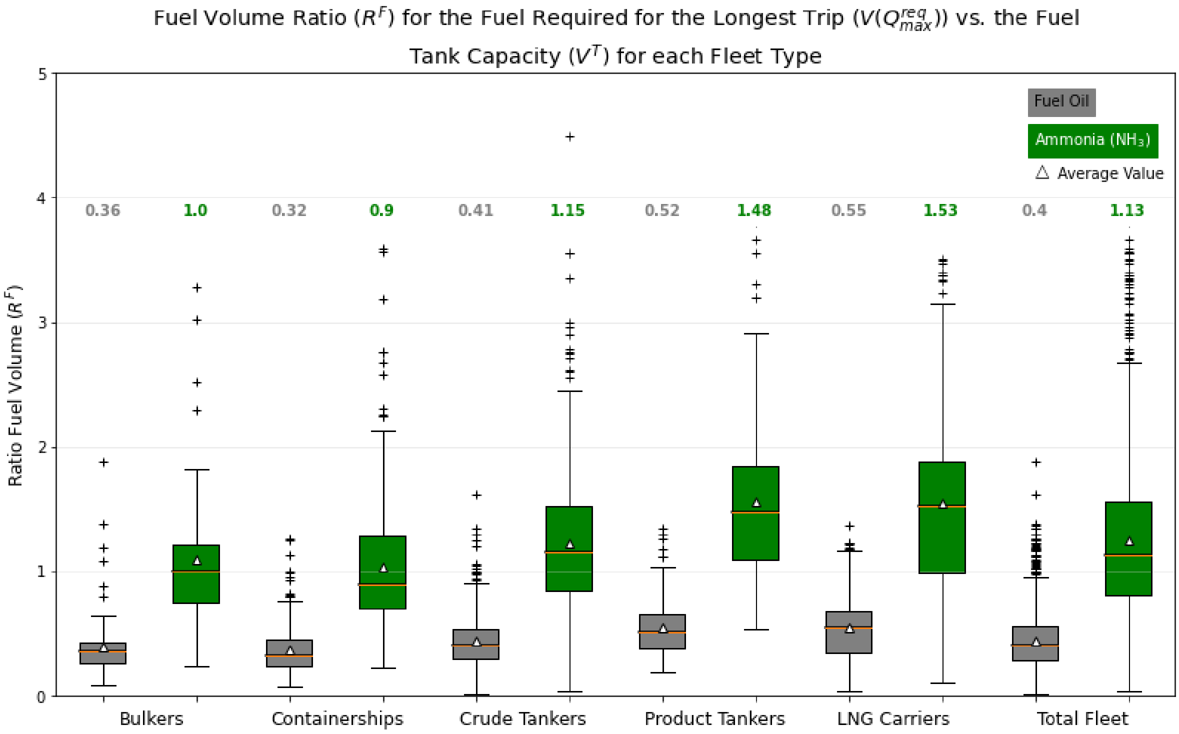

Figure 8.1: Fuel Volume Ratio (R^F) for fuel oil (grey) and ammonia (green) for all ships presented per fleet type.

To further visualize the difference in fuel consumption, figure 8.1 shows in a box plot per fleet type the fuel volume ratio (R^F). The fuel volume ratio is defined as the volume of fuel required for the longest trip ($V(Q^{req}_{max})$) divided by the volume of the original fuel tank of the ship (V^T), as denoted in equation 8.1. If the fuel volume ratio is more than one, the fuel tank of the ship should increase to complete all the assigned trips. The fuel volume ratio for fuel oil confirms that the fuel tanks of the ships are overdesigned for their current operational patterns and, therefore, provide more freedom regarding the bunker strategy. Comparing the fuel volume ratio for both fuels, the increase in the fuel volume ratio is equal to the increase in fuel consumption in table 8.2. The fuel volume ratio of ammonia is around 182 % higher and illustrates the impact of ammonia on fuel consumption. Besides, figure 8.1 suggests the fuel volume ratio is more than one for half of the LNG carriers and product tankers and thus, the impact of ammonia is more critical for these fleet types than the other ships.

$$R^F = \frac{V(Q^{req}_{max})}{V^T} \tag{8.1}$$

It should be noted that for scenario S0A, powered by fuel oil, some of the ships have a fuel volume ratio that is larger than one and would not be able to complete their longest trip. This applies to less than 5% of the total fleet and is caused by the generalized power assumption made in Chapter 5. This margin is considered an acceptable error margin.

The number of ships that are not able to complete all their assigned trips in scenario S0B are summarized in table 8.3. In this scenario, around 65% of the ships have not completed their route. In addition, table 8.4 lists the average part of the trips that are not accomplished in the scenario for each fleet type. The numbers on the left side of the columns represent the average of all ships in the fleet, and the numbers on the right side represent the average of the ships with unfeasible trips. Comparing these two numbers indicates the number of ships affected by the transition to ammonia. The tables also include the scenarios analysed in the next two sections.

The tables show the number of ships per fleet type that require a resizing of the fuel tank volume to maintain their operational deployability. Alternatively, these ships could lower their speed to reduce their fuel consumption or change their routes by splitting long trips into smaller trips. In these ways, the increase in the fuel tank volume can be reduced. The impact of ammonia on the feasibility of the trips is the strongest for LNG carriers, and containerships experience the smallest impact of the five fleet types.

Table 8.3: Number of ships that cannot complete their current route with the original fuel tank volume and sailing speed.

	Number of ships that require change							Total ships
Fleet	S0B	S1A	S1B	S1C	S2A	S2B	S2C	in fleet
Bulkers	64	110	13	64	3	0	112	112
Containerships	148	298	45	148	3	0	300	300
Crude tankers	216	300	96	216	5	0	312	312
Product tankers	106	125	44	106	6	0	125	125
LNG carriers	142	171	94	142	10	0	176	176
Total fleet	676	1004	292	676	27	0	1025	1025

Table 8.4: Percentage of unfeasible trips of the total number of trips, without considering rerouting, presented per fleet type. The numbers on the left side of the columns represent the average of all ships in the fleet, and the numbers on the right side represent the average of the ships with unfeasible trips.

Fleet	S0B	S1A	S1B	S1C	S2A	S2B	S2C
Bulkers	10.5%	52.9%	2.0%	10.5%	0.43%	0%	17.9%
	18.1%	53.9%	12.3%	18.1%	16.2%	0%	17.9%
Containerships	4.8%	22.7%	0.54%	4.8%	0.03%	0%	10.2%
	9.7%	22.8%	3.6%	9.7%	3.6%	0%	10.2%
Crude tankers	14.6%	52.1%	4.3%	14.6%	0.20%	0%	16.9%
	21.1%	54.2%	13.8%	21.1%	12.5%	0%	16.9%
Product tankers	18.7%	50.0%	3.1%	18.7%	0.26%	0%	14.2%
	22.1%	50.0%	8.8%	22.1%	5.6%	0 %	14.2%
LNG carriers	24.4%	75.3%	8.5%	24.4%	0.38%	0%	22.6%
	30.3%	77.5%	15.9%	30.3%	6.6%	0%	22.6%
Total fleet	13.5%	47.3%	3.5%	13.5%	0.22%	0%	15.7%
	20.4%	48.3%	12.3%	20.4%	8.2%	0%	15.7%

The scenarios in S0 compare the conventional fueled and ammonia-powered fleets and show the need for a larger fuel tank volume for the ammonia-powered ships. In order to have a baseline for the APSN model that is used later, table 8.5 shows the ports that are currently visited by the ships in the AIS data and the amount of fuel that is bunkered in the ports. The table includes the 20 ports with the highest demand and the ten ports with the smallest demand. For future use, the fuel oil is recalculated based on the ammonia-to-fuel oil mass ratio of 1.85. The last column of the table shows the estimated ammonia bunker price in the ports based on the demand following scenario S0B. These bunker prices are used for the S1 and S2 scenarios and the initial starting point for the APSN model in the simulations of scenario S3 simulations. Besides, it is used as a baseline to see the effect of ammonia on the shipping network.

Table 8.5: The top 20 ports with the highest demand and the bottom 10 with the lowest demand in scenarios S0A and S0B before including the forward bunker strategy. The ports with a demand of zero tons are excluded from the table.

	Ports (country)		Fuel Oil Demand t	Ammonia Demand t	Number of Visits -	Ammonia Bunker Price USD/t
1	SINGAPORE	SG	1976200	3675400	1231	546.78
2	ROTTERDAM MAASVLAKTE	NL	847300	1575100	926	654.56
3	YANTIAN	CN	706500	1312400	581	796.00
4	TANJUNG PELEPAS	MY	553300	1030300	246	539.23
5	SABINE PASS	US	439300	815100	242	735.14
6	INGLESIDE	US	418000	777600	260	709.31
7	SHANGHAI	CN	393500	732200	799	820.45
8	NINGBO	CN	392400	731000	754	820.60
9	ANTWERP	BE	364100	678300	459	623.74
10	PIRAEUS	GR	346200	644400	302	695.30
11	SABETTA	RU	312200	589800	248	1321.20
12	ZEEBRUGGE	BE	294400	549300	204	674.22
13	TANGER MED II	MA	272500	506000	178	530.47
14	JEDDAH	SA	271100	503200	254	547.98
15	BUSAN NEW PORT	KR	254900	473300	362	696.24
16	JEBEL ALI	AE	251200	467200	211	635.12
17	SINES	PT	245400	455300	220	589.72
18	LAKE CHARLES	US	218100	405100	117	764.41
19	LONG BEACH	US	214900	398300	106	766.36
20	COLOMBO	LK	211500	392900	119	597.59
	...	...	...	...	...	...
627	KAMAISHI	JP	88	164	1	29907.08
628	ST PETERSBURG	RU	73	135	4	33236.50
629	VOLVE	IIW*	69	129	1	33104.85
630	NAKHODKA	RU	61	114	1	35375.76
631	ANCONA	IT	58	108	1	35359.56
632	LIVERPOOL BAY OSI	GB	55	103	1	36111.86
633	ARICA	CL	46	86	1	38016.80
634	HUASCO	CL	26	49	1	43584.25
635	PORTO TORRES	IT	23	42	1	44961.46
636	ATRECO	US	16	30	1	47245.31

8.2. Sailing Speed Scenario S1

The S1 scenarios simulate the impact of speed on fuel consumption, related costs and revenue. The scenarios S1A (table 8.6), S1B (table 8.7), and S1C (table 8.8) are respectively run with the design speed of the ship, the sailing speed related to 60%MCR and the trip speeds based on the AIS-data. The tables give a quantification of the impact of speed on fuel consumption (FC_M). In these scenarios, the fuel tank volume is not changed, and thus, the cargo capacity is not reduced. Besides the costs, this also affects the range that ships can sail, as is clearly shown in table 8.3 and 8.4. Due to the relation between the speed and the fuel consumption, see equation 4.5, the change in speed have a significant impact on the fuel consumption. Therefore, scenario S1A results in a fuel consumption eight times higher than S0A and nearly three times higher than scenario S1C, even though the average speed difference is 30%. Next to that, 27% of the ships cannot complete their route in S1A, even with rerouting.

The significant increase in fuel consumption results in extremely high fuel costs and substantially negative revenues. Therefore, a fuel transition to ammonia would involve a reduction in the design speed or a fuel tank volume increase of over 1000%. This suggestion is supported by the results for scenario S1B, which shows a smaller fuel consumption that is the same as scenario S0A. It should be noted that these results show the fuel consumption mass, not the volume. Therefore, the fuel volume still increases by nearly 100%. However, considering the results for S0A in figure 8.1, most ships have overcapacity and can handle this volume increase. This shows opportunities for the transition to ammonia in scenario S1B.

The consideration of the last speed scenario, S1C, is nearly the same as scenario S0B. However, this scenario considers rerouting. Comparing these scenarios, the results of S1C show a minimal difference compared to S0B. For the containerships, crude tankers and LNG carriers, the fuel consumption, and thus costs, decrease by 0.5%. On the other hand, the opposite happens for the bulkers and product carriers. Considering the large set of ships and the generalized equation, it concludes that rerouting has no significant impact on the results.

Table 8.6: Scenario S1A: Fuel consumption, fuel costs, change of fuel costs and revenue.

Fleet Type	FC_M [t]	C^B [mUSD]	ΔC^B [mUSD]	ΔR [mUSD]
Bulkers	38061	32.91	27.43	-27.43
Containerships	168000	107.93	85.16	-85.16
Crude Tankers	36372	28.39	23.34	-23.34
Product Tankers	29689	24.91	19.94	-19.94
LNG Carriers	80483	61.19	44.55	-44.55
Total Fleet	81841	57.37	45.11	-45.11

Table 8.7: Scenario S1B: Fuel consumption, fuel costs, change of fuel costs and revenue.

Fleet Type	FC_M [t]	C^B [mUSD]	ΔC^B [mUSD]	ΔR [mUSD]
Bulkers	6840	14.9	9.42	-9.42
Containerships	28367	22.2	-0.57	0.57
Crude Tankers	6930	9.74	4.7	-4.7
Product Tankers	5550	10.31	5.33	-5.33
LNG Carriers	19434	18.03	1.39	-1.39
Total Fleet	15173	15.44	3.18	-3.18

Table 8.8: Scenario S1C: Fuel consumption, fuel costs, change of fuel costs and revenue.

Fleet Type	FC_M [t]	C^B [mUSD]	ΔC^B [mUSD]	ΔR [mUSD]
Bulkers	12977	18.66	13.19	-13.19
Containerships	53432	37.27	14.49	-14.49
Crude Tankers	11837	12.92	7.87	-7.87
Product Tankers	11730.	14.16	9.18	-9.18
LNG Carriers	39618	31.9	15.27	-15.27
Total Fleet	28893	24.08	11.82	-11.82

8.3. Fuel Tank Volume S2

The S2 scenarios simulate the impact of fuel tank capacity on the costs and revenue. The three scenarios, S2A (table 8.9), S2B (table 8.10), and S2C (table 8.11), respectively, use a fuel tank volume that is scaled from fuel oil to ammonia, a fuel capacity that is optimized to the longest trip in the route of each ship and a third scenario with the approach of elimination of the longest route as explained in section 6.3. These scenarios are used to narrow the scope of the optimization in the scenarios of S3 and find the boundaries for the increase in fuel tank volume. Above this, these simulations show to what extent the rerouting of S2C has an effect on the necessary tank volume compared to the other scenarios.

The column E_t shows the number of ships that could not complete all the trips on the route, and ΔV^T shows the average change of the fuel tank volume. In the S2A scenario, all fuel tanks increase with the same ratio, the volumetric energy density ratio from ammonia to fuel oil, which is a substantial increase in volume. However, there are 27 ships, so not all trips are feasible. For scenario S2B, the longest trip is used to determine the new fuel tank volume, so all trips should be feasible as supported by the results of E_t are all zero. As shown by scenario S0B, 35% of the ships can fulfil their route without increasing the fuel tank volume. Therefore, the average increase of the fuel tank volume is smaller than in scenario S2A.

The same remark applies to the results of scenario S2C; the fuel tank volume is changed to 75% of the required fuel volume for the longest route or the second longest route. Referring to figure 8.1, the fuel volume ratio for ammonia is smaller or around one for some ships. Following the approach for scenario S2C, this results in fuel tank volume smaller than the original fuel tank volume. This applies to the bulkers and containerships. However, a decrease in the fuel tank volume is not plausible for two reasons. There is no advantage regarding extra cargo capacity or income due to the model constraints and a smaller fuel tank results in less freedom regarding the bunker strategies.

In order to define the boundaries of the fuel tank volume range for the optimization, the results of scenarios S2A, S2B and S2C are reviewed, and the range is set from 100% to 400% of the fuel tank volume. This is done to ensure plausible results and include the possibility for each ship to complete its longest route without rerouting.

Finally, the scenarios of S2 suggest that the revenues of scenario S2b, compared to scenario S2C, show minimal difference. Therefore, it confirms the minimal effect of rerouting on the annual costs and revenues of the trip bunkering strategy.

Table 8.9: S2A Scenario: Fuel tank capacity, increase of the fuel tank, number of ships that require rerouting, cargo loss, change in cargo income and revenue.

Fleet Type	V^T [m^3]	ΔV^T	E_t [-]	ΔV^C [m^3]	ΔI^C [mUSD]	ΔR [mUSD]
Bulkers	9473	351%	3	-2436	-0.08	-10.31
Containerships	20596	351%	3	-1614*	-3.8	-18.09
Crude Tankers	7409	351%	5	-609	0	-7.06
Product Tankers	5236	351%	6	-913	-0.02	-7.49
LNG Carriers	11683	351%	10	-30551	-0.33	-15.78
Total Fleet	11963	351%	27	-6281	-1.18	-12.2

* The volume cargo loss of constainerships is measures in TEU.

Table 8.10: S2B Scenario: Fuel tank capacity, increase of the fuel tank, number of ships that require rerouting, cargo loss, change in cargo income and revenue.

Fleet Type	V^T [m^3]	ΔV^T	E_t [-]	ΔV^C [m^3]	ΔI^C [mUSD]	ΔR [mUSD]
Bulkers	5646	209%	0	-1359	-0.05	-13.38
Containerships	10336	176%	0	-128*	-0.24	-14.36
Crude Tankers	4947	234%	0	-439	0	-8.55
Product Tankers	4232	283%	0	-465	-0.01	-9.71
LNG Carriers	9872	296%	0	-42669	-0.45	-15.93
Total Fleet	7359	216%	0	-7703	-0.16	-12.19

* The volume cargo loss of constainerships is measures in TEU.

Table 8.11: S2C Scenario: Fuel tank capacity, increase of the fuel tank, number of ships that require rerouting, cargo loss, change in cargo income and revenue.

Fleet Type	V^T [m^3]	ΔV^T	E_t [-]	ΔV^C [m^3]	ΔI^C [mUSD]	ΔR [mUSD]
Bulkers	2430	90%	112	-129	0	-13.17
Containerships	4475	76%	300	-1*	0	-14.39
Crude Tankers	2142	101%	312	-10	0	-8.17
Product Tankers	1829	122%	125	-10	0	-9.43
LNG Carriers	4273	128%	176	-3090	-0.03	-14.75
Total Fleet	3184	93%	1025	-549	-0.01	-11.82

* The volume cargo loss of constainerships is measures in TEU.

8.4. Trip Bunker Strategy Optimization S3A

In scenario S3A, the simulation is performed for a range of different ammonia fuel tank volumes starting at 100% compared to the original fuel tank volume until 400% in steps of 25%. In this scenario, the model determines the fuel tank increase that results in minimal loss of revenue for the ship. The ship bunkers the ammonia fuel required for the upcoming trip in each departure port, according to the trip bunkering approach. Firstly, the impact of the fuel tank volume increase on the cargo is explained. This impact is the same for scenarios S3A and S3B. Subsequently, the impact on the fuel costs and revenues are described for scenario S3A, resulting in the optimal increase of the fuel tank volume. Finally, the impact of ammonia-powered ships on the bunker port network is presented, considering all ships are operating with their optimal increase of fuel tank volume and a homogeneous shipping market.

8.4.1. Cargo Losses

The diagrams of figure 8.2 show the impact of fuel tank volume related to the cargo capacity. Initially, the increase in fuel tank volume results directly in a decrease in the cargo capacity. However, the ships are not fully loaded during most of their trips, according to the results for the average cargo capacity (V^C) and the average transported cargo volume ($V^C_{k,avg}$) in tables5.4 and 5.9. Figure 8.2a shows the result of the calculated average number of trips per ship that experience effective cargo loss. This was calculated using the current draught data of the ship in the AIS data. Figure 8.2b[1] shows the average relative cargo loss regarding the original cargo capacity for each fleet type. The related loss in cargo income is depicted in figure 8.2c in a million USD, and figure 8.2d shows the relative loss of income compared to the baseline scenario S0A.

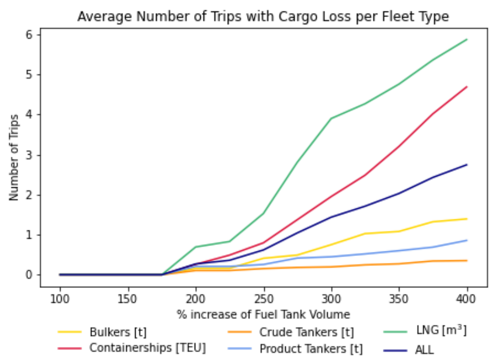

(a) Average number of trips with cargo loss per ship as a result of the fuel tank volume increase.

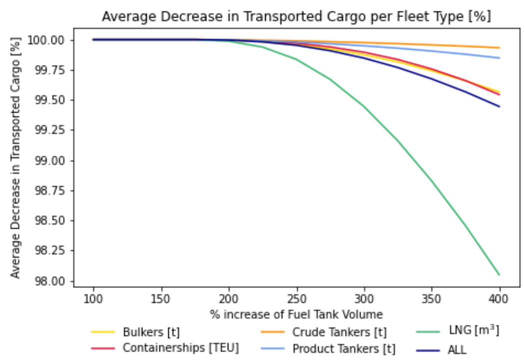

(b) Average decrease in transported cargo as a result of the fuel tank volume increase.[1]

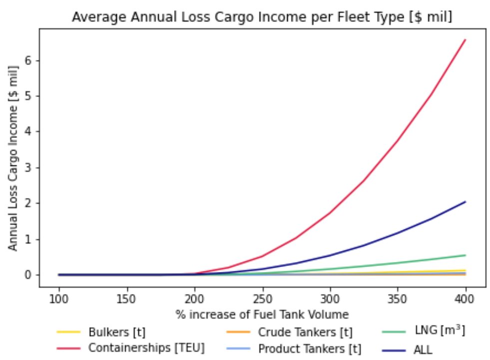

(c) Average loss in cargo income as a result of the fuel tank volume increase.

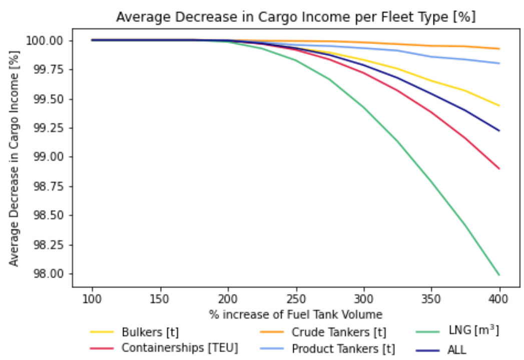

(d) Average relative loss in cargo income as a result of the fuel tank volume increase.

Figure 8.2: Cargo and income losses as a result of increasing the fuel tank of the ships, representing each fleet type in scenarios S3A and S3B.

For a fuel tank volume increase up to 200%, the figures depict no significant impact. However, when the increase builds up, the results of the cargo loss show some remarkable differences between the fleet types. First of all, the figures reveal a minimal impact on the cargo losses for bulkers, crude tankers and product tankers by increasing the fuel tank volume. Most crude and product tankers experience effective cargo loss for less than one trip a year. This results in a reduction of cargo capacity and

[1]The decrease in transported cargo is almost the same. Therefore, the yellow line representing the bulkers is not clearly visible.

income of less than 0.25%, which is neglectable considering the general approach of this research. The impact on the bulkers is a little higher, but still, only one trip a year is affected by the increase of the fuel tank, and the average relative losses are not larger than 0.5%. On the contrary, the results for containerships and LNG carriers show more impact.

For the LNG carriers, the diagrams in figure 8.2 show the highest impact, as these ships experience the most trips with effective cargo loss, and this reflects on the loss in cargo income. A reason for this can be related to the density of LNG compared to ammonia. The density of LNG is smaller than the density of ammonia; therefore, an increase in the fuel tank volume encounters not only the volume limitations but also the mass limitations. For the other fleet type, the mass limitations are not dominant because the density of the cargo is larger than the density of ammonia. Besides, the difference between the average cargo capacity and the actual volume of cargo transported is smaller compared to the other fleet types.

Besides the LNG carriers, the containerships show a higher impact compared to the total fleet, especially in figure 8.2c. In general, containerships perform substantially more trips than the other fleet types (table 5.9), and the applied freight rate for containerships is higher (table 5.8). As a result, the annual cargo income of the containerships is significantly higher than that of the other ships, see table 8.1, and therefore, the loss of cargo results in a large sum of cargo income loss. However, the relative loss in cargo income is more balanced, as shown in figure 8.2d.

The diagrams in figure 8.2 show the impact of ammonia on the cargo capacity of the ships, considering a fuel tank volume increase as a result of the lower energy density of the renewable fuel. The results of the parameters related to the cargo do not depend on the bunker strategy approach. Therefore, the effects for the cargo suggested in this subsection are considered for both scenarios S3A and S3B. However, the results for the fuel costs and revenue strongly depend on the bunker strategy. Therefore, the results for these parameters are discussed separately.

8.4.2. Fuel Costs and Revenue

This subsection includes the results for the fuel consumption and the revenue for scenario S3A, considering the trip bunker strategy. The total simulation of this scenario contains five iterations to obtain a balance in the results. The iterations are referred to as run 0 to run 5. Whereas run 0 is based on the port results from S0A and SOB, and run 5 shows the results after five complete simulations of the BS model and the Port model. However, after run 3, no notable change in the results is observed, and thus, the results for run 0 and run 3 are used to illustrate the development of the results during the iterations. In figure 8.3, the results for the fuel costs are illustrated, and figure 8.4 shows the results for the loss in revenue.

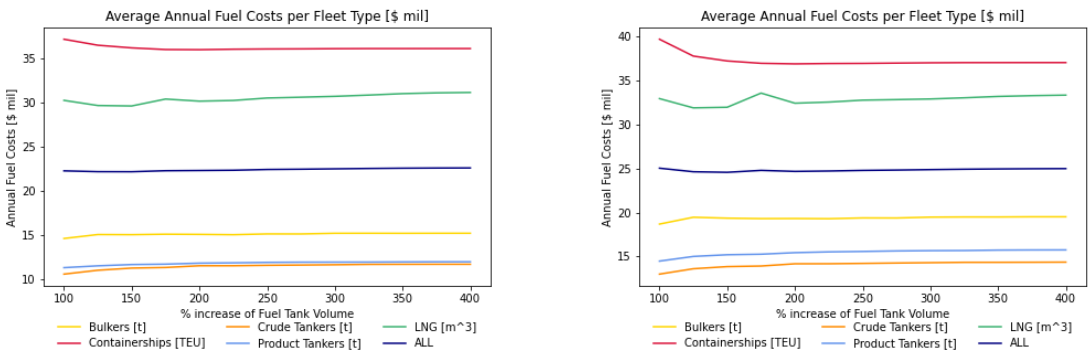

(a) run 0 **(b)** run 3

Figure 8.3: Annual fuel costs as a result of increasing the fuel tank of the ships. Presented per Fleet Type in Scenario S3A.

The results of the fuel costs show a small increase between run 0 and run 3. This is due to the recalculation of the ammonia bunker prices in the Port model. Next to that, the slopes of the fuel costs are balanced after an increase of 200% and show no extra advantage for increasing the fuel tank volume further. This is the result of the bunker strategy approach to bunker the amount of ammonia required for the upcoming trip in the departure port of the trip. Therefore, the ships only required enough volume to cover the trip.

Except for the containerships, the slopes for the fuel costs show a small increase for larger fuel tank volumes. This is the result of the assumption regarding the fuel reserve (Q^{res}) for unpredicted events. The fuel reserve has to be 10% of the fuel tank capacity; therefore, Q^{res} increases by the same proportion as the fuel tank volume. At the first port on the route, the ship is required to bunker the amount of the fuel reserve added to the required amount of ammonia for the trip. Therefore, the ship has to bunker more fuel when it has a larger fuel tank, and thus, the fuel costs are higher. If the start port of the ship is a low-demand port, the bunker prices are significantly higher; see table 8.13. This results in extremely high extra costs for the ship, and therefore, the annual fuel cost increases for larger fuel tank volumes.

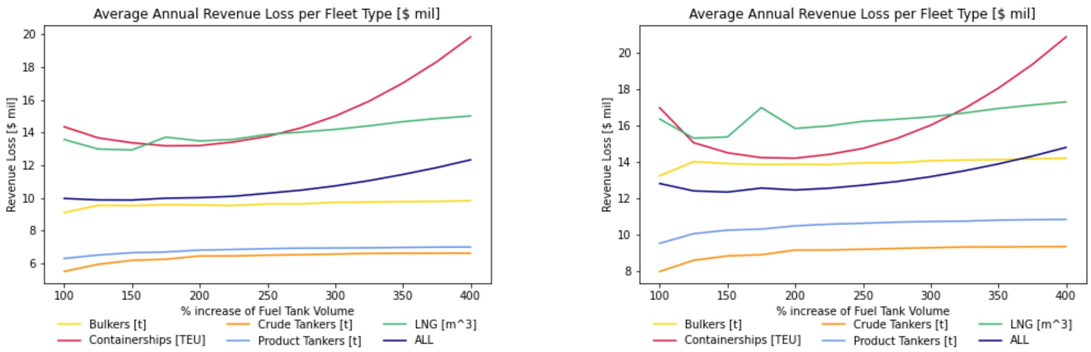

(a) run 0

(b) run 3

Figure 8.4: Annual loss of revenue as a result of increasing the fuel tank of the ships. Presented per Fleet Type in Scenario S3A.

The results of the loss in revenue in figure 8.4 show a similar slope as the fuel costs result for the bulkers, crude tankers and product tankers, as these ships have no substantial cargo losses. Therefore, the loss in revenue is similar to the increase in fuel costs. However, containerships and LNG carriers are more affected by the loss of cargo capacity, which results in additional revenue loss. In these slopes, the impact of the decrease in cargo income is displayed as more revenue loss for larger fuel tanks.

8.4.3. Increase of Fuel Tank Volume

In order to optimize the bunker strategy of the ship, the BS model selects the fuel tank volume increase that results in a minimal loss in revenue. In figure 8.5, the optimal fuel tank volume is displayed and shows the number of ships for each fuel tank volume increase. Table 8.12 summarizes the average increase in fuel tank volume and the related monetary results compared to scenario S0A.

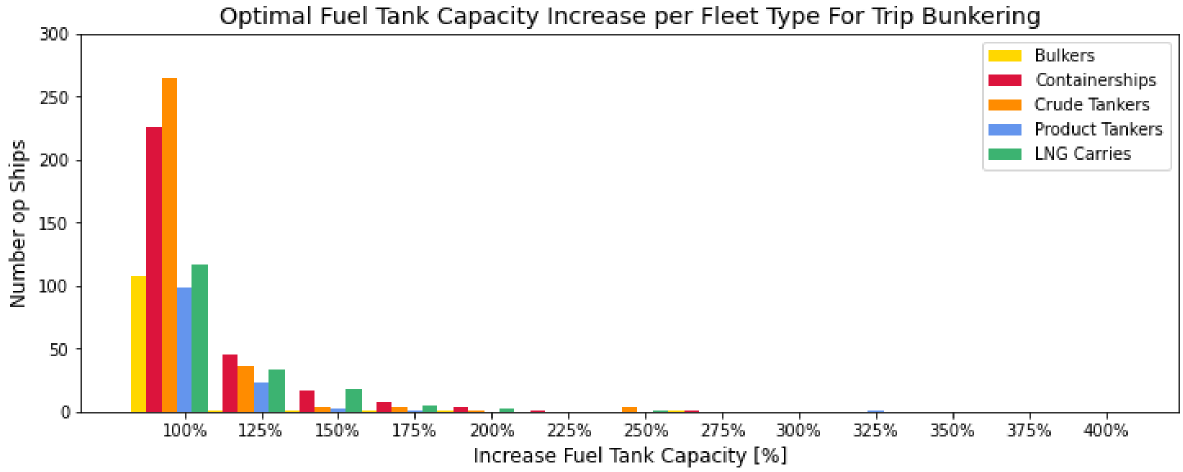

Figure 8.5: The optimal fuel tank volume increase divided per fleet type, considering trip bunkering.

Table 8.12: S3A Scenario: Change of fuel tank volume, fuel consumption, cargo loss, fuel costs, cargo income and revenue.

Fleet Type	ΔV^T [m^3]	ΔFC_M [t]	ΔV^C [m^3]	ΔC^B [mUSD]	ΔI^C [mUSD]	ΔR [mUSD]
Bulkers	104.8%	+86.98%	0.0%	+180.75%	0.0%	-49.12%
Containerships	110.5%	+85.62%	0.0%	+56.96%	0.0%	-3.26%
Crude Tankers	106.0%	+85.79%	0.0%	+117.68%	0.0%	-181.47%
Product Tankers	107.8%	+87.07%	0.0%	+122.74%	0.0%	-53.61%
LNG Carriers	114.1%	+87.7%	0.0%	+70.72%	0.0%	-221.79%
Total Fleet	108.7%	+86.35%	0.0%	+99.35%	0.0%	-106.18%

Due to the bunker strategy approach for scenario S3A, trip bunkering, the cargo losses are more determinative for the loss in revenue than the fuel costs. Therefore, the optimal increase in fuel tank volume is small for the total fleet.

8.4.4. Bunker Ports

The Port model determines the total demand in each port and the related ammonia bunker price. The results after three runs, related to the results for the bunker strategy, are listed in table 8.13. This table shows the 20 ports with the highest demand and the ten ports with the lowest demand in the shipping network. In general, the number of active ports in the shipping network reduces from 636 to 625, and the results show a little reduction in the average bunker price for ammonia.

The bunker strategy approach in this scenario applies in that the ships have a bunker in each port on their route. Therefore, most ports do not show significant shifts in ammonia demand. However, the optimal fuel tank volume results in figure 8.5 reveal a minimal increase in the fuel tanks. Therefore, it is assumed that rerouting is applied for most ships. This defines the results for the larger ports in the network. For these ports, the demand decreases, and the number of visits increases. Considering that the larger ports are located on the main sailing routes and are visited by ships with longer trips, these trips had to be divided into smaller routes. As a result, the ships have to bunker less ammonia in these ports.

However, comparing the results of the five runs, around 10% of the ports have fluctuations in the ammonia demand and number of port visits. For the ports in the APSN model, only 4% has a demand difference from more than 10 visits a year, which is expected considering the bunker strategy in this scenario. During the five runs simulated for this scenario, around 5% of the ports switch up and down with the same demand changes. An explanation for this is that the original demand of the port is close to the maximum storage capacity of the port; therefore, higher demand results in an extra ammonia terminal and significantly higher CAPEX. As a result, the ammonia price of the port increases, and bunkering in this port becomes less profitable. These fluctuations are not considered to have a significant impact on the ports.

Table 8.13: Top 20 ports with the highest demand and the bottom 10 with the lowest demand in scenario S3A after run 3. The ports with a demand of zero tons are excluded from the table.

	Ports		Ammonia Demand in tonnes	Number of visits	Ammonia Bunker in USD/t
1	SINGAPORE	SG	2944700	1346	530.07
2	ROTTERDAM MAASVLAKTE	NL	1001700	928	634.93
3	YANTIAN	CN	921100	582	785.70
4	TANJUNG PELEPAS	MY	868300	245	535.79
5	TANGER MED	MA	724700	374	493.05
6	KOCHI	IN	674800	416	462.92
7	SABINE PASS	US	572200	242	718.61
8	INGLESIDE	US	491600	260	696.79
9	SABETTA	RU	480800	248	1324.57
10	KING ABDULLAH	SA	477000	323	518.42
11	PIRAEUS	GR	455200	303	710.00
12	ANTWERP	BE	447800	459	641.42
13	ZEEBRUGGE	BE	406400	205	686.84
14	JEDDAH	SA	391000	256	536.68
15	JEBEL ALI	AE	387200	211	637.68
16	TANGER MED II	MA	368600	178	525.84
17	SINES	PT	361300	250	573.80
18	NINGBO	CN	358700	760	788.02
19	RODEO	US	300700	121	712.92
20	SHANGHAI	CN	297700	801	805.85
	...	...	...	...	
616	GIBRALTAR	GI	100	1	36400.73
617	PERAMA	GR	100	1	36349.13
618	ANCONA	IT	100	1	36287.33
619	SLOVAG	NO	100	2	36375.33
620	NAKHODKA	RU	100	1	36968.33
621	KO SICHANG	TH	100	1	36144.33
622	SUNSHINE	US	100	1	36374.33
623	BEAUMONT	US	100	1	23950.35
624	TACOMA	US	100	2	36505.13
625	VOLVE	IIW*	100	1	36253.33

8.5. Forward Bunker Strategy Optimization S3B

In scenario S3A, the simulation is performed for a range of different ammonia fuel tank volumes starting at 100% compared to the original fuel tank volume until 400% in steps of 25%. In this scenario, the model determines the fuel tank increase that results in minimal loss of revenue for the ship, according to the forward bunker strategy. In each port on the route, the ship considers how much ammonia it should bunker to minimize the fuel costs. This consideration depends on the ammonia bunker price in the port and the fuel tank capacity of the ship. The results of the impact of the fuel tank volume increase on the cargo are explained in subsection 8.4.1. This impact is the same for scenarios S3A and S3B. This section describes the impact on the fuel costs and revenues for scenario S3B, resulting in the optimal increase of the fuel tank volume. Subsequently, the impact of ammonia-powered ships on the bunker port network is presented, considering that all ships operate with their optimal increase of fuel tank volume and a homogeneous shipping market, more specifically, the ports in the EU territory.

The total simulation of this scenario contains ten iterations to obtain a balance in the results. The iterations are referred to as run 0 to run 10. Whereas run 0 is based on the port results from SOB, and run 10 shows the results after ten complete simulations of the BS model and the Port model.

8.5.1. Fuel Costs and Revenue

The diagrams in figure 8.6 show the fuel cost results for scenario S3B. Comparing the results of runs 0 and 3 with the results of runs 5 and 10, the effect of the bunker strategy is visualized. In appendix A, the diagrams for all the ten runs are shown. The costs after the implementation of the forward bunker strategy are higher than for run 0. In this scenario, the ships can avoid the ports with high ammonia bunker prices, and this results in lower fuel costs for the ships and smaller demands in the expensive ports. This last result is elaborated further in subsection 8.5.4. Ships with a larger fuel tank volume have more flexibility in the bunker strategy and, therefore, have lower fuel costs.

However, not all expensive bunker ports can be avoided. There are two main reasons why ships cannot skip an expensive port. Firstly, if the ship's route starts in an expensive bunker port, the ship has to tank at least the amount of ammonia required for the first trip before cheaper options are available for bunkering. Secondly, the forward bunker strategy is applied after the final route is defined by the rerouting sub-model, and therefore, the ship depends on this fixed route. When there are expensive ports on the route, the ship can be forced to bunker at an expensive port due to the limitations regarding the maximum range of the ship. This second observation applies especially to the ships with smaller bunker tanks.

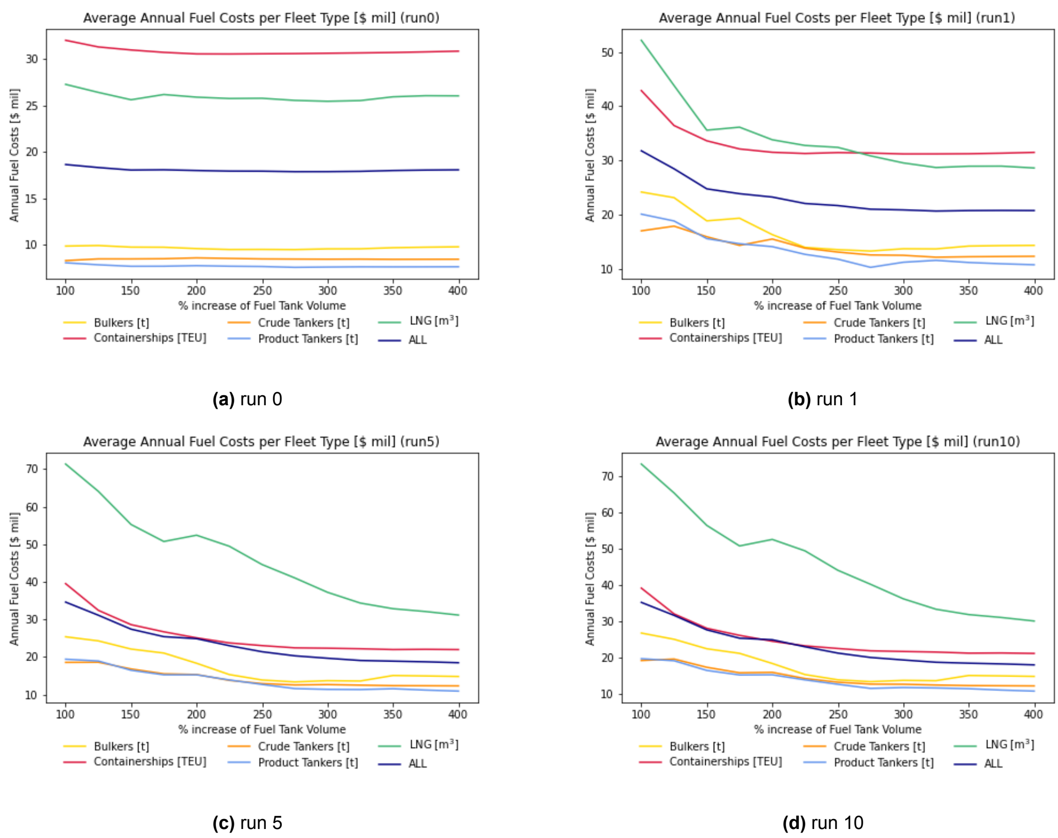

(a) run 0

(b) run 1

(c) run 5

(d) run 10

Figure 8.6: Evaluation of the Annual Fuel Costs per Fleet Type in Scenario S3B.

The results for the revenues are shown in figure 8.7. This figure contains the results of runs 0, 1, 5 and 10 of the simulation. The general trend is a decreasing loss of revenue compared to the baseline S0A scenario, and the decisive factor in this is the lower fuel costs for larger fuel tank volumes. For this scenario, the results of the fuel costs show similarities with the results of the revenue losses. Especially for the LNG carriers, for which the slopes are nearly equal.

However, the results of the containerships show a different pattern. For containerships, the loss in revenue increases when the fuel tank volume is more than 250% of the original fuel tank volume. This is the result of the reduction of the cargo capacity as shown in figure 8.2. Therefore, the optimal increase in fuel tank volume will be between 200% and 300%. Besides the containerships, the bulkers show a small increase in revenue loss when the fuel tank volume increases by more than 300%.

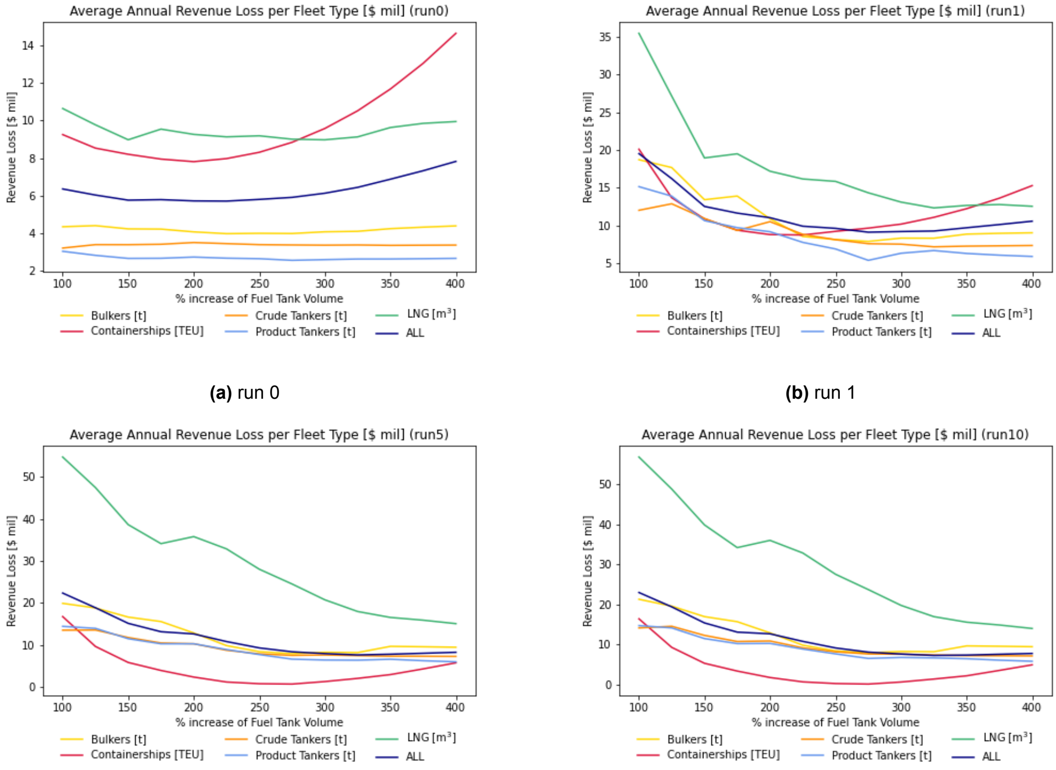

(a) run 0

(b) run 1

(c) run 5

(d) run 10

Figure 8.7: Evaluation of the annual loss of revenue per Fleet Type in Scenario S3B.

8.5.2. Increase of Fuel Tank Volume

The results in the prior subsection show the average results of each fleet type. However, the BS model is developed to generate the optimal increase of fuel tank volume for each ship based on its characteristics and individual route. Figure 8.8 shows the optimal increase of the fuel tank volume presented in a number of ships per fleet type. This figure supports the optimum for the containership, shown in figure 8.7c and 8.7d. Table 8.14 lists the average increase in the fuel tank volume and the related financial results for each fleet type. The result for revenue loss of containerships is 0.25% at an increase of fuel tank volume of 250%, and thus, the revenue is nearly the same as in the baseline scenario S0A. In contrast, the revenue loss of LNG carriers is more than 220%, which could explain the peak at an increase of 400%. This is because of the significant difference between the fuel income and the cargo income.

Comparing figure 8.8 and 8.5 from scenario S3A, the ships are divided over the whole range of the fuel tank volume increase options instead of clustered at the small increases. This shows the impact of the bunker strategy on the optimal increase of the fuel tank volume. Scenario S3B depicted a peak at 400% increase, which suggests that these ships prefer an extensive sailing range over the reduction of cargo loss. As explained, this is due to the flexibility in ammonia fuel purchasing, which comes with the larger available fuel tank volume. For these ships, it could be possible that an increase of more than 400% would result in a more optimal result.

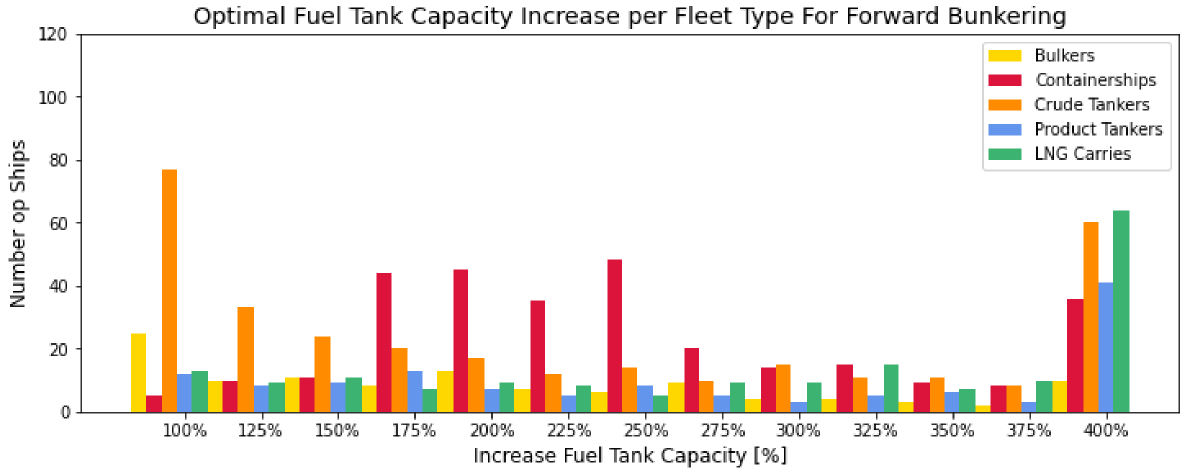

Figure 8.8: The optimal fuel tank capacity increase divide per fleet type, considering forward bunkering.

Table 8.14: Scenario S3B: Change of fuel tank volume, fuel consumption, cargo loss, fuel costs, cargo income and revenue for scenario S3B

Fleet Type	ΔV^T [m^3]	ΔFC_M [t]	ΔV^C [m^3]	ΔC^B [mUSD]	ΔI^C [mUSD]	ΔR [mUSD]
Bulkers	207.6%	+95.48%	-0.06%	+124.62%	-0.06%	-39.5%
Containerships	250.3%	+90.12%	-0.04%	-6.91%	-0.08%	-0.25%
Crude Tankers	225.0%	+94.67%	-0.02%	+111.92%	-0.02%	-88.21%
Product Tankers	271.0%	+92.87%	-0.06%	+78.12%	-0.07%	-22.87%
LNG Carriers	295.5%	+91.99%	-0.91%	+64.76%	-0.92%	-220.66%
Total Fleet	248.2%	+92.75%	-0.19%	+66.31%	-0.2%	-71.92%

8.5.3. Ports

The results from the Port model show that the effect of the forward bunkering approach reflects the ammonia bunker ports. This bunker strategy enables ships to avoid ports with high ammonia bunker prices. This results in lower demand in the ports and, in sequence, increases the ammonia bunker prices. Therefore, more ships will avoid these ports and the demand decrease even more. On the contrary, ports with relatively low ammonia bunker prices attract more demand, and thus, bunker prices get lower, like the ports of Singapore and Rotterdam Maasvlakte. As a result, the demand converges to a smaller set of ports. This results in higher ammonia bunker prices in the other ports. The number of ports participating in the ammonia bunker network reduces by almost 50%, from 644 to 336, as shown in table 8.12. This map presents the division of ammonia bunker ports all over the world, and the top 10 bunker ports, based on their demand, are marked with a blue star. The top 50 ammonia bunker ports are marked in blue. These ports are predicted to show high potential for becoming ammonia bunker ports. The set of high-potential ports for ammonia bunkering is strongly dependent on the main routes of the applied ships.

Table 8.15 lists the ammonia demand, port visits and related ammonia bunker price for the twenty ports with the highest demands and the ten ports with the smallest demand after the fifth run. In this selection, the inactive ports, ports with zero demand, are not included. The results in this table propose an average reduction of the ammonia bunker price in the active ports and an increase in the demand of the top five of the ports. The ports of Singapore and Rotterdam Maasvlakte experience an extensive growth in their demand of around 500%. Due to the assumption that unlimited growth of the ammonia facilities is possible, the demand increases and bunker price decreases further. The number of port visits represents only the port visits for bunkering and does not show the same level of increase. This suggests that the amount of ammonia bunkered per visit is larger as a result of the bunker strategy.

However, a remark should appointed that the ships are operating by a fixed route after the rerouting and, therefore, cannot bunker in a port other than the ports in their route.

The Port model includes no limits for the bunker price or demand in the ports, and therefore, the ammonia bunker price decreases when the demand grows, as illustrated in figure 4.7 in chapter 4. The diagrams in figures 8.9 and 8.10 depict the development during the ten iterations for, respectively, the demand and the ammonia bunker price of the top 10 bunker ports. The diagrams suggest that after run 5, the results are balanced, and the demand and bunker prices do not show substantial transformations. In order to illustrate the effect on the bunker ports with a small demand, figure 8.11 shows the demand fluctuation of the bottom ten ammonia bunker ports. This diagram demonstrates that the opposite effect applies to small bunker ports.

Table 8.15: Top 20 ports with the highest demand and the bottom 10 with the lowest demand in scenario S3B after run 5. The ports with a demand of zero tons are excluded from the table.

	Ports		**Ammonia Demand in tonnes**	**Number of visits**	**Ammonia Bunker in USD/t**
1	SINGAPORE	SG	10520200	1470	182.21
2	ROTTERDAM MAASVLAKTE	NL	4490800	814	413.49
3	TANGER MED II	MA	796600	202	573.35
4	INGLESIDE	US	635700	206	738.03
5	SINES	PT	544000	146	647.69
6	TANJUNG PELEPAS	MY	473000	168	647.24
7	CALLAO	PE	447000	151	596.29
8	SABINE PASS	US	396900	148	879.88
9	MONTOIR	FR	324100	91	816.41
10	AIN SUKHNA	EG	292400	119	596.19
11	DUNKIRK	FR	275400	63	799.53
12	LE HAVRE	FR	272700	157	712.9
13	LAZARO CARDENAS	MX	269500	79	836
14	CARTAGENA	ES	263300	85	733.75
15	ROTTERDAM	NL	260000	241	848.89
16	FREEPORT	US	254600	67	833.95
17	DAMPIER	AU	249800	56	652.91
18	ZEEBRUGGE	BE	244700	89	867.53
19	KOCHI	IN	244700	74	589.37
20	HUELVA	ES	233000	61	555.3
	...	...	...	...	...
327	YUEDONG	CN	200	1	35726.36
328	FLOTTA	GR	200	2	35640.94
329	PERAMA	GR	200	2	35649.41
330	GALVESTON	US	200	2	35678.06
331	PORT ALLEN	US	200	2	35678.06
332	PRINCE RUPERT	CA	100	1	24428.51
333	MORMUGAO	IN	100	2	23750.46
334	ANJEONG	KR	100	1	23962.78
335	SKHIRA	TN	100	1	23813.46
336	DORTYOL	TR	100	1	23907.95

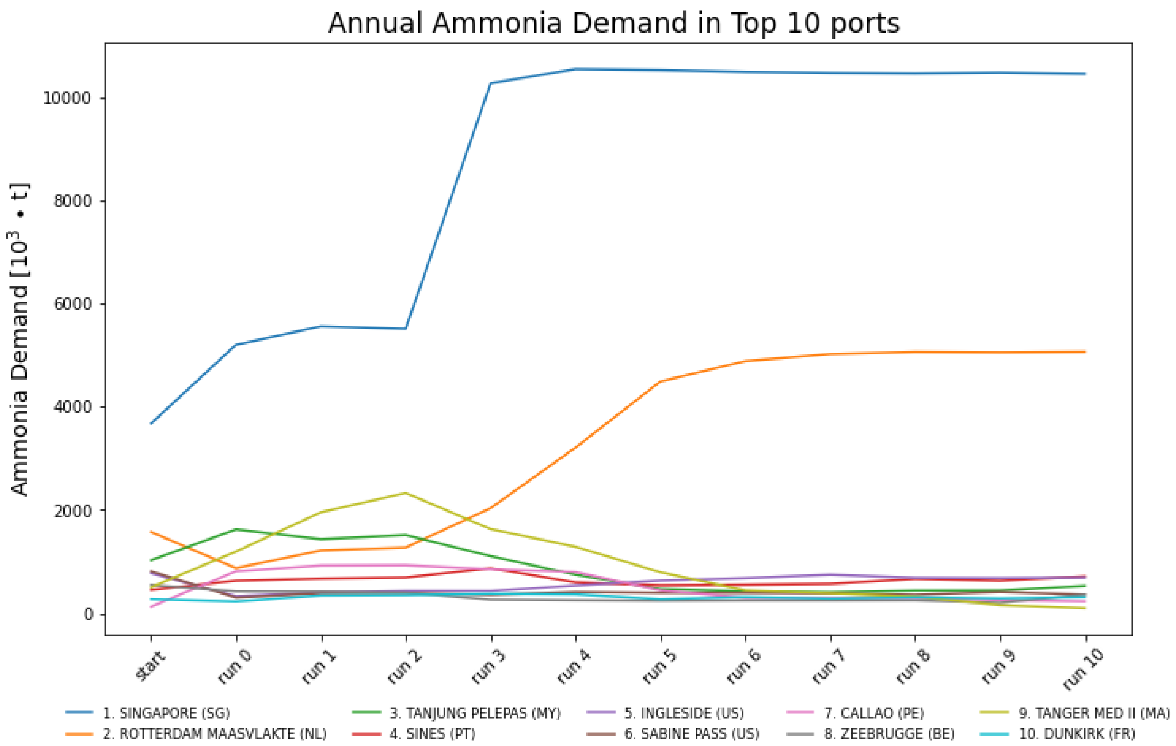

Figure 8.9: The trend on the ammonia demand in the top 10 bunker ports per run.

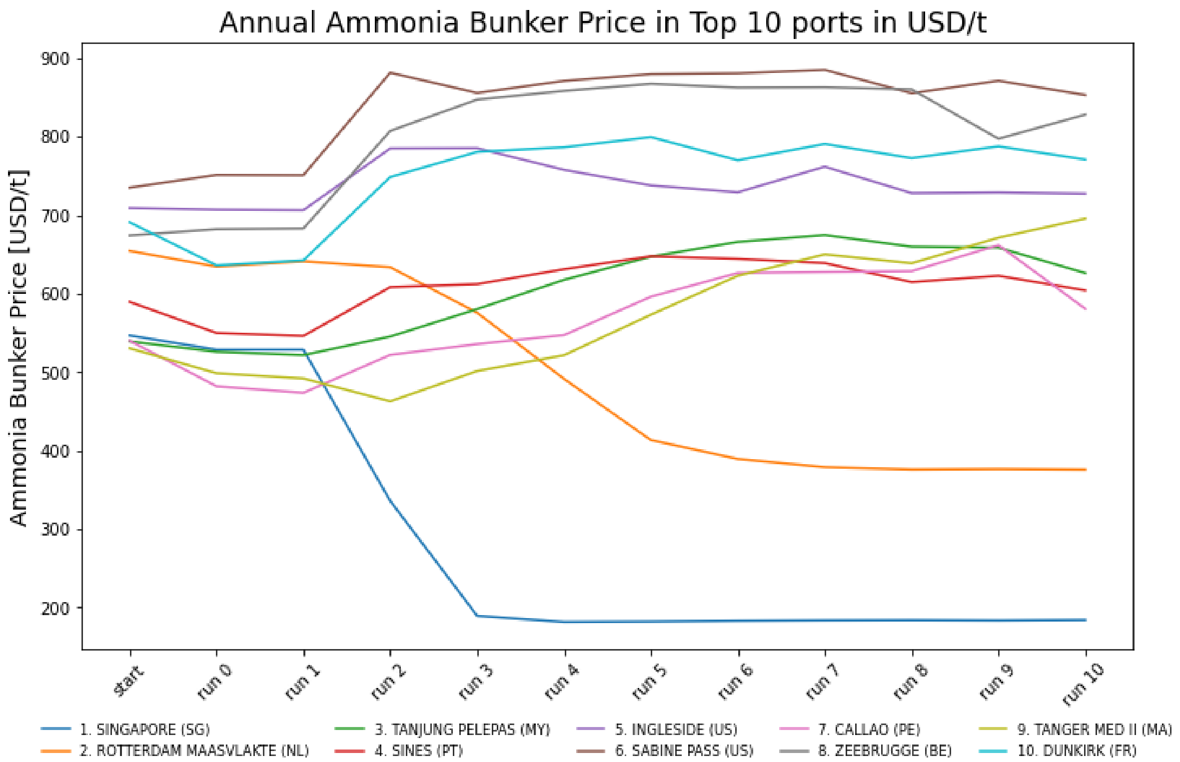

Figure 8.10: The trend on the ammonia bunker price in the top 10 bunker ports per run.

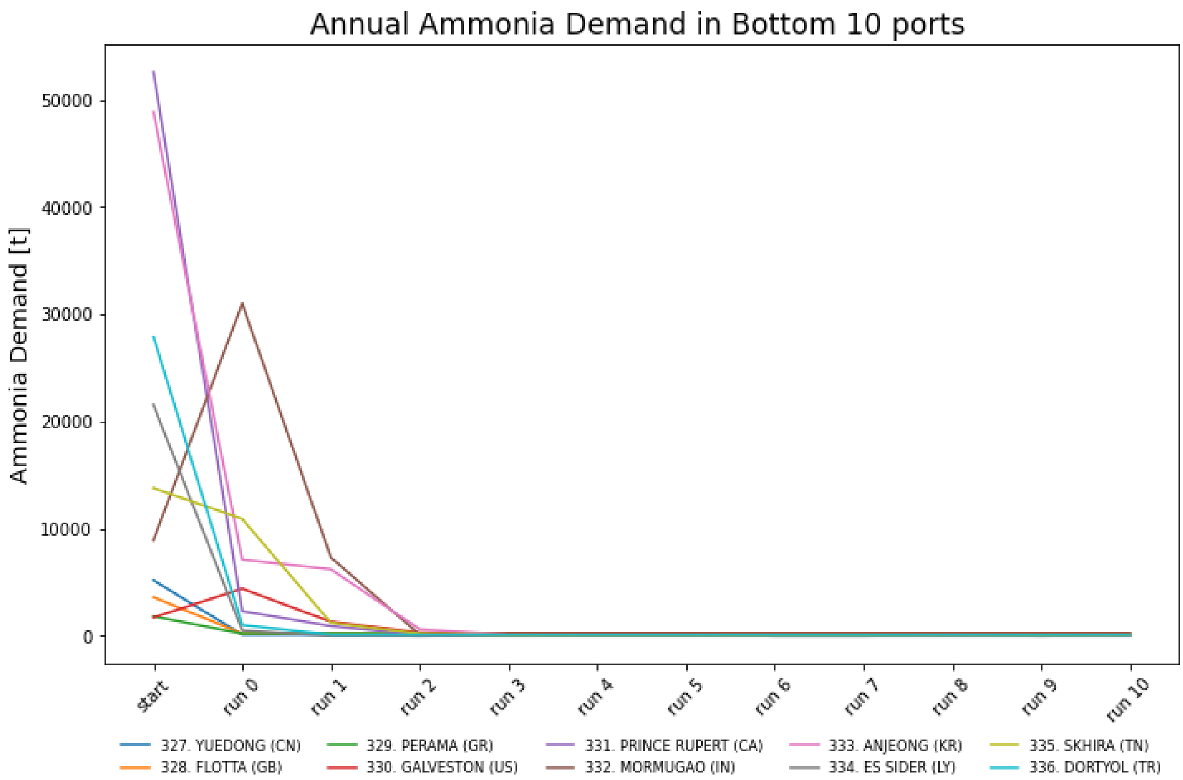

Figure 8.11: The trend on the ammonia demand in the bottom 10 bunker ports per run.

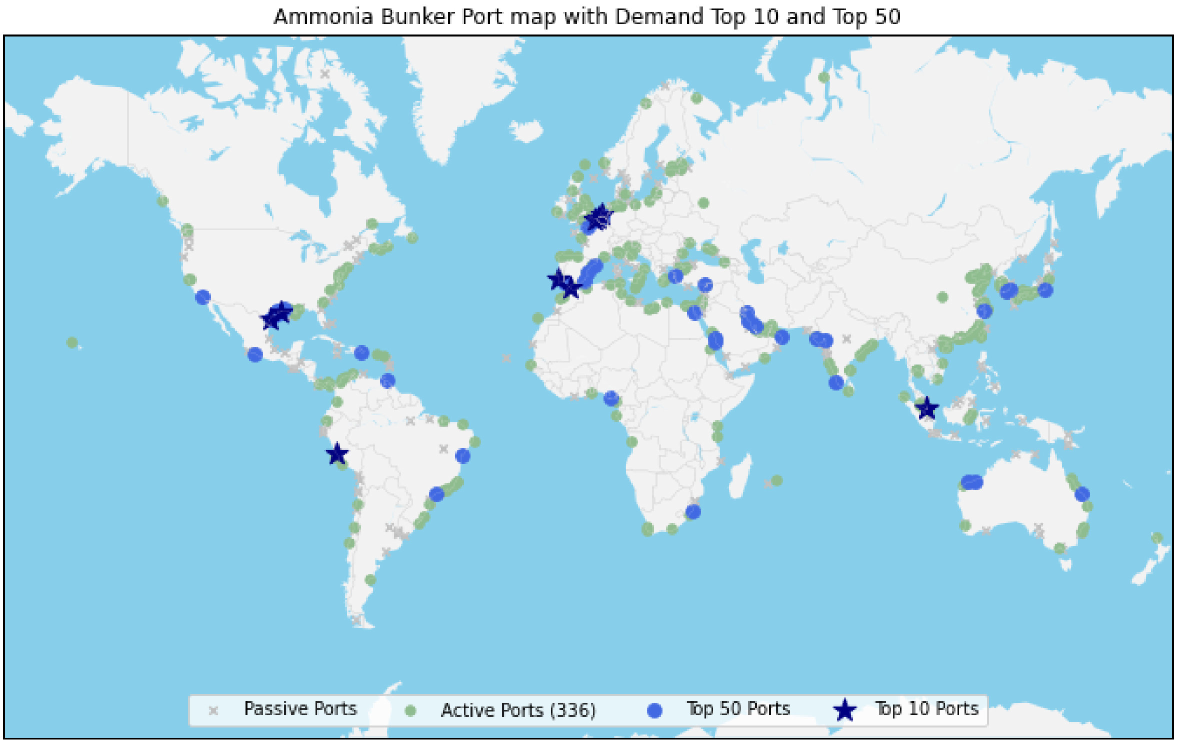

Figure 8.12: Ammonia demand in bunker ports represented in the world.

8.5.4. EU Ports

Since this research is related to the MAGPIE project, which is an European Union (EU)-oriented project, this section contains an extension of the results regarding bunker ports in Europe. Table 8.16 summarizes the results for the demand, port visits and ammonia bunker price for the top ten ports in the EU and figure 8.13 shows the ports deviation of the ammonia bunker ports in the EU. The table also lists the position of the ports on the global ranking between the breaks. These results are promising for the position of Europe in the ammonia-powered shipping network, as nine ports out of the EU top ten are also represented in the global top 20.

Table 8.16: Top 10 EU ports with the highest ammonia demand in scenario S4B after run 5.

	Ports		Ammonia Demand in tonnes	Number of visits	Ammonia Bunker in USD/t
1 (2)	ROTTERDAM MAASVLAKTE	NL	4490800	814	413.49
2 (5)	SINES	PT	544000	146	647.69
3 (9)	MONTOIR	FR	324100	91	816.41
4 (11)	DUNKIRK	FR	275400	63	799.53
5 (12)	LE HAVRE	FR	272700	157	712.9
6 (14)	CARTAGENA	ES	263300	85	733.75
7 (15)	ROTTERDAM	NL	260000	241	848.89
8 (18)	ZEEBRUGGE	BE	244700	89	867.53
9 (20)	HUELVA	ES	233000	61	555.3
10 (23)	SAGUNTO	ES	221000	35	563.77

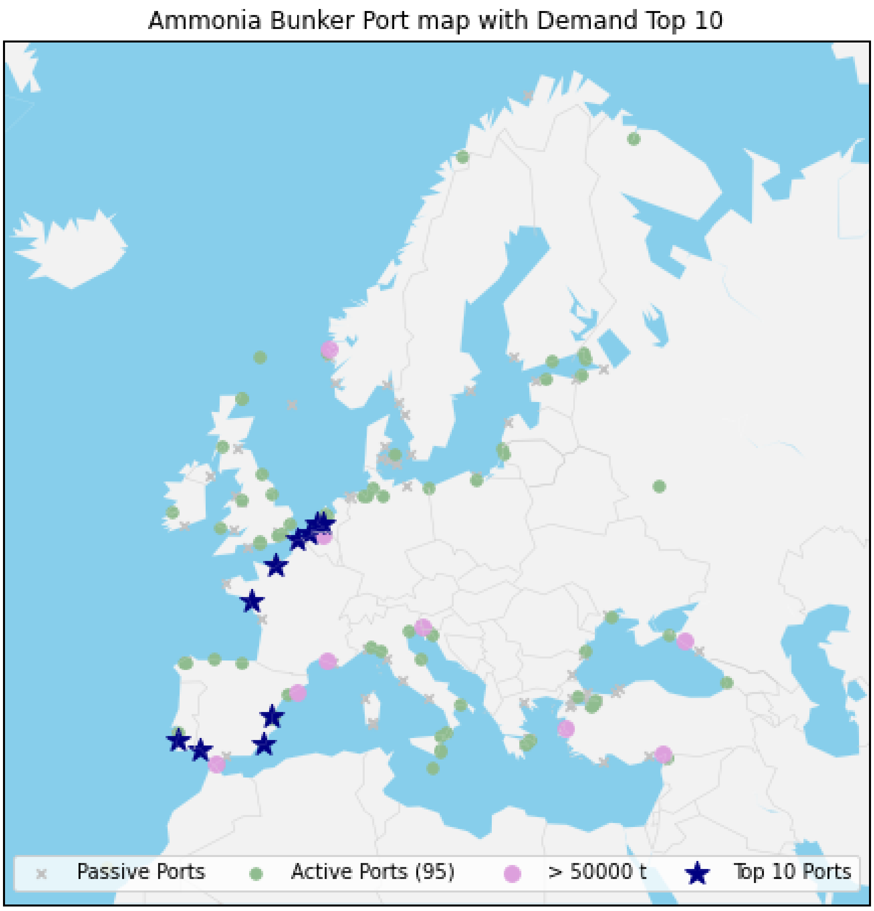

Figure 8.13: The ammonia demand of bunker port in the EU.

9 Discussion and Recommondations

This research presents a model for an ammonia-powered shipping network to simulate the operational impact of ammonia. In order to develop this model, assumptions are made to narrow the scope and complexity of the model and maintain a relevant reflection of the shipping network. These assumptions affect the results of the research. Besides, the developed model is generalized to process a large number of ships and highly depends on the input data. In this chapter, the assumptions, limitations and overall interpretation of the research results are discussed. Furthermore, the set of recommendations is presented for further research and suggestions for improvements on the APSN model.

9.1. Discussion

The model developed in this research should be interpreted as a general simulation of a shipping network powered by ammonia. The model is based on an existing bunker strategy optimization model for the shipping industry. Current research shows bunker strategy models for a small set of ships that perform a fixed route, and the bunker prices considered are independent of the ship's behaviour. The APSN model offers novelty in the simulation of the bunker strategy for 1025 ships and integrates the ammonia demand into the Port model to determine the bunker price for each port. In addition, the shipping network is implemented in the context of ammonia.

The final APSN model is based on assumptions to facilitate the performance for 1025 ships and the implementation of ammonia. In order to develop a model applicable to all ships, the equations used in the data processing and final model are generalized. This is done to narrow the complexity of the model to maintain a feasible research objective within the scope of the master thesis. Therefore, the findings in this research should be interpreted as an indication of the impact of ammonia on the operational feasibility of the ships and bunker ports.

In this section, the remarks regarding the assumptions, data limitations and model implementations are discussed.

9.1.1. Assumptions

The assumptions made in this research that reflect the results and the interpretation of the model are listed and briefly explained in this subsection.

Green Ammonia

This research is focused on the operational feasibility of ammonia as a marine fuel, following the promising research regarding the environmental impact, the carbon-free character, and technological developments. In order to test the operational feasibility, the research assumes the technological challenges are solved and do not result in operational complexities. Besides, the assumption is made that ammonia safety restrictions are developed, and the effects of toxicity and corrosiveness are not considered in this research.

Homogenuous Shipping Market
The research is based on a homogeneous market for green ammonia. This assumes that there is no competition from other marine fuels, and each port supplies the same quality of green ammonia. In reality, the energy demand of the shipping industry will be supplied by several energy carriers, see figure 1.3, and not all ships will make the transition to ammonia. This will impact the demand in the ports and the market position of ammonia. Besides, the homogeneous shipping market assumes an immediate transition of ammonia. However, the 1.5°C pathway for IRENA shows a gradual transition to ammonia. This will increase the impact on the operational feasibility of the first movers.

EU
This research is dedicated to the MAGPIE project, which is EU-oriented. As a result, the ships are selected for their operations in the EU territory, and all ships have to visit at least one EU port during 2022. This provides an advantage for the EU ports compared to the ports located in other regions.

Availability of Ammonia
In order to ensure a homogeneous shipping market, it is assumed that the green ammonia is available in all ports in the shipping network. In reality, many ports do not have ammonia bunker facilities.

Subsidies and Emission Taxes
In order to stimulate the GHG reduction, governments or other organizations will likely use subsidies and taxation, like the EU ETS. Regulations for bunker levy on marine fuels and emission trading systems will speed up the transition to alternative fuels and will play a significant role of Market-based Measures (MBM) (Lagouvardou et al., 2022; Psaraftis et al., 2021; Y. Wang and Wright, 2021). This will reduce the loss of revenue that is found in the results. However, regulations like these are not considered in this research.

Ship Design
In this research, the size of the ships is considered a fixed parameter, and the total volume of the cargo capacity, fuel tank, and energy system is constant, as is the related total weight. The ammonia fuel energy systems replace the existing energy systems, which will extend the required volume. This results in a reduction of the cargo capacity. However, it could also be considered to enlarge the total ship according to the increase of the energy system and fuel tank if this results in smaller revenue losses.

9.2. Model and Data Limitations

9.2.1. Ammonia Bunker Strategy Model

Fleet selection
Due to the size requirement, there are no Ro-Ro ships included in this research;. These can also play an interesting part in the transition to ammonia, as the ships are mostly sailing a fixed route on frequent rotation. This would ensure a certain demand in the ports and it secures a base fuel sale for ports to start with the bunker supply for ammonia. Besides, the conditions of the route of the Ro-Ro ships also raise the question of what their bunker strategy will be.

Freight rates
The available information on container freight rates and tanker earnings is not completely comparable and could explain the significant difference in the results. Therefore, the results of fleet revenues should not be compared to other fleet types. This could be improved by more specific freight rates data and more accurate data on the cargo transported during each trip.

Sailing speed optimization
One of the initial goals was to optimize the sailing speed in order to extend the range. A clear result was difficult to reach with the available AIS data. This data contains time stamps for departure and arrival in ports, but the exact trip distance and sailing speed need to be estimated. In many cases, the average trip speed was below the 60% MCR, and it is not likely that ships were sailing at this speed. In those cases, the assumed sailing speed was corrected. More detailed trip and fuel consumption data is necessary to conclude the sailing speed optimization. In addition to this, multiple previous studies

have been done on this matter. Lowering the speed of the ships and even more to decrease fuel consumption regarding ammonia may not be very realistic.

Distance Calculation

The AIS data used for the port calls is very gross. This only provides a start and an endpoint for each trip, but not specific routing. For smaller trips and trips closer to land, there is no significant difference in the actual sailed distance. However, considering the longer trips and the trips crossing the oceans or other wide waters, the determination of the exact route and sailed distance is much harder and, therefore, less accurate. The python toolkit `searoute` only calculates the shortest route between two points, avoiding crossing land, but does not consider less preferable areas to avoid because of weather or environmental conditions that can slow down the sailing speed or expand the sailed distance. It is plausible to consider this to be the reason for the low speeds for a significant number of trips. It is important to consider this when looking at the results of the impact of ammonia on sailing speed.

Bunker Strategies

The model applies two bunker strategies. It would be interesting to know from shipowners what their approach is. Do they use contracts with ports and what are their ways to avoid or compensate the higher fuel prices. This information is known to be of strategic importance to shipowners and is kept as company confidential information. However, knowing the actual bunker ports on the route of each ship would help to generate a sufficient baseline scenario.

9.2.2. Port Model

Linear Bunker Price Elasticity

The price elasticity for ammonia is considered to decrease linearly with the increasing demand. When limits of the ammonia bunker facility capacity are reached, the CAPEX increases by the fixed costs of the ammonia bunker facilities to supply the extra capacity. The Port model does not consider bunker price and demand limits. Therefore, the ammonia bunker price for ports with substantially high or low demands results in extra values. This occurs especially for the ports with low demand, which will supply ammonia for 30000 USD/t. In reality, it is not likely that this will be the case, and the bunker price elasticity will have limitations due to all kinds of circumstances.

Time Integration

The current APSN model does not vary with the time to limit the computational time of the simulations. Therefore, the ammonia demand in each port is estimated for the whole year, and the ammonia bunker price is based on the required capacity to supply this demand. However, the ammonia demand in the ports fluctuates during the year and could result in peak demand at certain moments. This could affect bunker prices and the availability of ammonia in the ports.

Initial port parameters

The initial port parameters determine the attractiveness of the port to be used as a bunker port in the first runs. This affects the number of visits and bunker demand in the following runs. It would be interesting to investigate the sensitivity of the results to the parameters that determine the initial attractiveness.

Start port is first bunker port

The assumption is that the ships always have to bunker at the first port of the route. Otherwise, the ship cannot complete the first trip. However, a significantly high ammonia bunker price in the first port has a high impact on the total annual fuel costs of the ship. For example, the ports with higher prices vary from 1500 to >38000 USD/t. This can be the reason for the small increase in fuel costs for larger fuel tanks. Besides, ships are always required to have a fuel reserve in case of unpredictable circumstances. This fuel margin is 10% of the fuel tank capacity and will also be bunkered at the start port. If the fuel tank increases, the amount of ammonia bunkered for the fuel margin increases as well. This results in extra bunker costs in the first port.

Shared ammonia facilities

The ports in the model are identified based on their UN/LOCODEs. However, the locations related to the UN/LOCODEs suggest that some larger ports have multiple UN/LOCODEs referring to different areas in the port. These areas are approached as different ports, and their demands are calculated separately. In reality, these ports could cooperate and arrange one ammonia bunker facility for the total port instead of each area. In this case, the demand for the ammonia bunker facility increases, and this could reduce the bunker price of the port.

9.3. Recommendations

The APSN model as applied in scenario S3B should be interpreted as a first draft. The results of the model show a well-performed structure between the different segments of the model. In this section, four recommendations are discussed to refine the simulation of an ammonia-powered shipping network:

1. Speed Optimization

Due to the inaccurate time and speed data obtained from the AIS data, the speed optimization needs further research. For this, it would be necessary to have more accurate speed data recorded during the trips. The optimization in the APSN model assumes a constant speed of 60% MCR; this is a theoretical optimization, and more detailed data could give insight into the realistic improvement of fuel consumption.

2. Extension of the Port model

The port model calculates the ammonia fuel price based on demand in a homogeneous market. There might be influences like taxes and subsidies or limitations to the growth of the production facilities that would affect the market position of the ports. The sensitivity to the initial pricing and attractiveness of ports could be further investigated by simulating the effect of strong national policy to stimulate the development of ammonia production facilities. A separate study of the port model could include a stepwise transition of ammonia by increasing the market share of ammonia over a certain period. This would give an additional quantitative overview of the transition phase.

3. Input data

The APSN model could be improved to be more accurate for the ammonia impact on the ships by collecting more input data. For example, more specific data on the bunker strategy, accurate cargo data, the CAPEX for retrofit and newly built ammonia-powered ships and an indication of the subsidies can improve the results of the model.

4. Smaller Ships

The current APSN model is applied to a set of ships with a DWT larger than 50000 tonnes. This represents the largest group of ships in the global fleet. *Deliverable 3.1* suggests that ships with a DWT over 25000 tonnes are feasible for a transition to ammonia (Pruyn et al., 2022). Therefore, it would be interesting to investigate the impact of ammonia on these ships in further research. An increase in the fuel tank volume could have more impact on these ships due to their smaller size.

10
Conclusion

Last year, IMO expanded their goal to reduce the GHG emissions from international shipping to 80% by 2050 to prevent global warming by 1.5°C. Regulations, like the ETS, are introduced to stimulate the energy transition in the maritime industry and discourage the use of conservative fuels. Recent research, both academic and from the industry, suggests ammonia as a high-potential alternative fuel due to its carbon-free character. Despite the technical developments in ammonia, its energy density is almost three times lower than that of fuel oil. This results in a challenge for the ship's design and performance, considering larger fuel volumes. Besides, ammonia bunker ports do not exist at this moment, and therefore, the bunker opportunities for ammonia are uncertain. These two challenges result in the main research question of this research, as formulated in Chapter 2:

What is the operational impact on the ship design, performance and bunker port network when switching to ammonia as a marine fuel, considering a homogeneous shipping market?

In order to substantiate the answer to the main research question, the following sub-questions are investigated:

1. What parameters have a significant influence on the operational performance of seagoing vessels, like the fuel consumption and bunkering pattern?
2. What are the model requirements to simulate the operational impact of ammonia on the ship design and performance and the bunker port network?
3. What is the impact on the **fuel tank volume** of seagoing vessels with an economical and operational feasible ammonia bunker strategy?
4. What is the impact on the **sailing speed** of seagoing vessels with an economical and operational feasible ammonia bunker strategy?
5. What is the impact on the **sailing range** of seagoing vessels with an economical and operational feasible ammonia bunker strategy?
6. Which **ports** are suitable to be part of an ammonia bunker port network, which is economical and operationally feasible?

In the first part of this research, a MILP optimization model is developed to simulate an ammonia-powered shipping network. This model demonstrates the relationship between the fuel tank volume, the sailing speed, and the range of the ship and simulates, based on AIS data, the optimal balance between the increase of the fuel tank volume and the reduction of the sailing range. In order to quantify the impact of ammonia on these parameters, the optimization is monetized by calculating the fuel costs and cargo income and minimizing the loss in revenue. The APSN model includes a rerouting model to provide alternative routes when the range limits the feasibility of the trips and considers two bunker strategies: trip bunkering and forward bunkering. The large set of ships of five fleet types facilitates the ammonia demand to the bunker port network. Based on this demand, the ammonia bunker price is determined in the enclosed port model.

The scenarios in S0, S1 and S2 develop the base for the final simulation in scenarios S3A and S3B. Scenario S0 define the baseline for the APSN model and is the reference data for the following scenarios. The scenarios in S1 are directed to the impact of the sailing speed. The results of this scenario show a substantial impact of the sailing speed on fuel consumption and, with that, in the loss in revenue. This suggests that the ships have to reduce their sailing speed to realize the transition to ammonia. However, due to inaccurate AIS data for sailing speeds, it is not possible to include a plausible speed optimization in the model. The scenarios in S2 determine the range for the fuel tank volume increase considered in the optimization scenarios of S3. For a fuel tank volume of 350%, there are still ships that cannot complete all the trips in their route. There, the maximum increase is set to 400%. The minimum increase is assumed to be equal to the original volume of the fuel tank.

The simulations in scenarios S3A and S3B show the impact of ammonia on the fuel tank volume and sailing range of the ships. The optimal increase of the fuel tank volume strongly depends on the bunker strategy of the shipowner. The trip bunkering strategy (S3A) results in a preference for smaller fuel tank volume and thus accepts a shorter sailing range. Due to the strategy to bunker in each port on the route, this creates no benefits for extensive ranges. This results in an average increase of the fuel tank volume to 109% for the total fleet. On the other side, the forward bunker strategy results in significant benefits for the ships with larger fuel tank volumes, especially for the LNG carriers and product tankers, as shown in figure 8.8. The results of the crude tankers are divided over the whole range, but they also show a peak for high tank volumes and an increased range. The results show no evident preference for a specific increase for the bulkers; besides, their average increase is smaller than that of the rest of the fleet. Finally, the containerships have the lowest loss of revenue between 175% and 275% increase in the fuel tank volume.

The approach of the bunker strategy strongly reflects the impact of the switch to ammonia on the bunker port network. For the trip bunkering strategy, nearly all ports in the model remain active, and the deviation of the ammonia demand in the ports resembles the initial deviation. The forward bunker strategy shows the impact of the new bunker port choice on the ammonia demand in ports in the bunker network. The forward bunker strategy searches for the ports with the lowest bunker price, making the model converge the general demand to a smaller set of ports. This implies that the larger ports continue to attract more demand as their ammonia bunker price gets lower. The two largest ports especially show a significant increase in demand. Considering the MAGPIE project, the results for the EU ports emphasize the promising position of Europe in the transition to ammonia.

To conclude, the technological and environmental opportunities for ammonia as a marine fuel nominate the fuel as a solution for a carbon-free shipping industry. In this research, the APSN model shows that the operational impact of ammonia on the ship design and performance is manageable for containerships, bulkers and product tankers. For crude tankers and LNG carriers, the operational feasibility of switching to ammonia requires more research. Further research into speed optimization is recommended. Although the simulations of sailing speed scenarios demonstrate that the sailing speed affects the fuel consumption and revenue of the ships significantly, more accurate speed and time data will improve the credibility of the APSN model with an optimization including the sailing speed.

References

Aardal, K., van Iersel, L., & Janssen, R. (2020). *Optimization - lecture notes am2020*. Faculty of Engineering, Mathematics; Computer Science, Delft University of Technology.

ABS. (2020). *Sustainable whitepaper - ammonia as marine fuel*. www.eagle.org

Al-Aboosi, F. Y., El-Halwagi, M. M., Moore, M., & Nielsen, R. B. (2021). Renewable ammonia as an alternative fuel for the shipping industry. *Current Opinion in Chemical Engineering*. https://doi.org/10.1016/j.coche.2021.100670

Al-Enazi, A., Bicer, Y., Okonkwo, E. C., & Al-Ansari, T. (2022). Evaluating the utilisation of clean fuels in maritime applications: A techno-economic supply chain optimization. *Fuel*, *322*. https://doi.org/10.1016/j.fuel.2022.124195

ALFA LAVAL, HAFNIA, HALDOR TOPSØE, VESTAS, & SIEMENS GAMESA. (2020). *Ammonfuel - an industrial view of ammonia as a marine fuel*.

Armijo, J., & Philibert, C. (2020). Flexible production of green hydrogen and ammonia from variable solar and wind energy: Case study of chile and argentina. *International Journal of Hydrogen Energy*, *45*, 1541–1558. https://doi.org/10.1016/j.ijhydene.2019.11.028

Butler, T., Kopp, J., Moritz, M., Stoelinga, M., van Dijk, K., & Pruyn, J. (2023). *Deliverable d3.6: Gaps and developments ammonia supply chain for future demand*. Zero Carbon Shipping.

Cepsa & Fertiberia. (2023). *Fertiberia and cepsa form a strategic alliance to boost green hydrogen production and decarbonize industry in huelva*. https://www.cepsa.com/stfls/corporativo/FICHEROS/np-fertiberia-y-cepsa-se-alian-para-producir-hidrogeno-verde_english.pdf

Christodoulou, A., & Cullinane, K. (2022). Potential alternative fuel pathways for compliance with the 'fueleu maritime initiative'. *Transportation Research Part D: Transport and Environment*, *112*. https://doi.org/10.1016/j.trd.2022.103492

Clarkosn Research. (2023a). *Shipping intelligence network (sin)*. https://www.clarksons.net/SIN

Clarkosn Research. (2023b). *World fleet register (wfr)*. https://www.clarksons.net/WFR

DNV. (2021). *External safety study-bunkering of alternative marine fuel for seagoing vessels port of amsterdam*. www.dnvgl.com

DNV.com. (2023). *Mrv – monitoring, reporting and verification (eu and uk)*. https://www.dnv.com/maritime/insights/topics/mrv/FAQs-EU-MRV.html

EMSA. (2023). *Thetis-mrv - co_2 emission report 2022*. https://mrv.emsa.europa.eu/#public/emission-report

ETC. (2020). *The first wave - a blueprint for commercial-scale zero emission shipping*. https://www.energy-transitions.org/wp-content/uploads/2020/11/The-first-wave.pdf

European Commission. (2021). *Regulation of the european parliament and of the council on the use of renewable and low-carbon fuels in maritime transport and amending directive 2009/16/ec* [Accessed 10 May 2023]. https://eur-lex.europa.eu/legal-content/EN/TXT/HTML/?uri=CELEX:52021PC0562

European Maritime Safety Agency. (2022). *Potential of ammonia as fuel in shipping*. EMSA, Lisbon.

familyDNV. (2023). *Energy transition outlook 2023 – maritime forecast to 2050*.

FLUOR. (2023). *Large-scale industrial ammonia cracking plant - executive summary of pre-feasibility study* [Commissioned by Port of Rotterdam Authority (PoR),EON/Essent,ExxonMobil,Gasunie,Global Energy Storage (GES),HES International,Koole Terminals,Linde Gas,RWE,Sasol,Shell,Uniper,Vopak and VTTI,bp].

Foretich, A., Zaimes, G. G., Hawkins, T. R., & Newes, E. (2021). Challenges and opportunities for alternative fuels in the maritime sector. *Maritime Transport Research*, *2*. https://doi.org/10.1016/j.martra.2021.100033

Ghane-Ezabadi, M., & Vergara, H. A. (2016). Decomposition approach for integrated intermodal logistics network design. *Transportation Research Part E: Logistics and Transportation Review*, *89*, 53–69. https://doi.org/10.1016/j.tre.2016.02.009

IMO. (2021). *Fourth imo greenhouse gas study 2020 - full report and annexes*.

Gore, K., Rigot-Müller, P., & Coughlan, J. (2022). Cost assessment of alternative fuels for maritime transportation in ireland. *Transportation Research Part D: Transport and Environment*, *110*. https://doi.org/10.1016/j.trd.2022.103416

Halili, G. (2023). *Searoute 1.2.2*. https://pypi.org/project/searoute/

Hansson, J., Brynolf, S., Fridell, E., & Lehtveer, M. (2020). The potential role of ammonia as marine fuel-based on energy systems modeling and multi-criteria decision analysis. *Sustainability (Switzerland)*, *12*. https://doi.org/10.3390/SU12083265

HES International, Vopak, & Gasunie. (2022). *Gasunie, hes international and vopak join forces to develop an import terminal for a hydrogen carrier in the port of rotterdam*. www.hesinternational.eu

IEA. (2021). *Net zero by 2050 - a roadmap for the global energy sector*. International Energy Agency. https://www.iea.org/reports/net-zero-by-2050

IEA. (2022). *Internatioanl shipping*. https://www.iea.org/reports/international-shipping

International Maritime Organization. (2018). *Initial imo strategy on reduction of greenhouse gas emissions from ships*.

IRENA. (2021). *A pathway to decarbonise the shipping sector by 2050*. International Renewable Energy Agency. www.irena.org

Işıklı, E., Aydın, N., Bilgili, L., & Toprak, A. (2020). Estimating fuel consumption in maritime transport. *Journal of Cleaner Production*, *275*. https://doi.org/10.1016/j.jclepro.2020.124142

Jensen, R. M., & Ajspur, M. L. (2022). Revenue management in liner shipping: Addressing the vessel capacity challenge. *Maritime Transport Research*, *3*. https://doi.org/10.1016/j.martra.2022.100069

Ji, C., Jiao, Z., Yuan, S., El-Halwagi, M. M., & Wang, Q. (2021). Development of novel combustion risk index for flammable liquids based on unsupervised clustering algorithms. *Journal of Loss Prevention in the Process Industries*, *70*. https://doi.org/10.1016/j.jlp.2021.104422

JRC. (2019). *Policy oriented tool for energy and climate change impact assessment*. https://ec.europa.eu/jrc/en/potencia

Klein-Woud, H., & Stapersma, D. (2002). *Design of propulsion and electric power generation systems*. IMarEST.

Klerke, A., Christensen, C. H., Nørskov, J. K., & Vegge, T. (2008). Ammonia for hydrogen storage: Challenges and opportunities. *Journal of Materials Chemistry*, *18*.

Kouzelis, K., Frouws, K., & van Hassel, E. (2022). Maritime fuels of the future: What is the impact of alternative fuels on the optimal economic speed of large container vessels. *Journal of Shipping and Trade*, *7*. https://doi.org/10.1186/s41072-022-00124-7

Lagemann, B., Lagouvardou, S., Lindstad, E., Fagerholt, K., Psaraftis, H. N., & Erikstad, S. O. (2023). Optimal ship lifetime fuel and power system selection under uncertainty. *Transportation Research Part D: Transport and Environment*, *119*, 103748. https://doi.org/10.1016/j.trd.2023.103748

Lagemann, B., Lindstad, E., Fagerholt, K., Rialland, A., & Erikstad, S. O. (2022). Optimal ship lifetime fuel and power system selection. *Transportation Research Part D: Transport and Environment*, *102*. https://doi.org/10.1016/j.trd.2021.103145

Lagouvardou, S., Psaraftis, H. N., & Zis, T. (2022). Impacts of a bunker levy on decarbonizing shipping: A tanker case study. *Transportation Research Part D: Transport and Environment*, *106*. https://doi.org/10.1016/j.trd.2022.103257

Lashgari, M., Akbari, A. A., & Nasersarraf, S. (2021). A new model for simultaneously optimizing ship route, sailing speed, and fuel consumption in a shipping problem under different price scenarios. *Applied Ocean Research*, *113*. https://doi.org/10.1016/j.apor.2021.102725

Lindstad, H., & Eskeland, G. S. (2015). Low carbon maritime transport: How speed, size and slenderness amounts to substantial capital energy substitution. *Transportation Research Part D: Transport and Environment*, *41*, 244–256. https://doi.org/10.1016/j.trd.2015.10.006

Lindstad, H., Sandaas, I., & Strømman, A. H. (2015). Assessment of cost as a function of abatement options in maritime emission control areas. *Transportation Research Part D: Transport and Environment*, *38*, 41–48. https://doi.org/10.1016/j.trd.2015.04.018

Machaj, K., Kupecki, J., Malecha, Z., Morawski, A. W., Skrzypkiewicz, M., Stanclik, M., & Chorowski, M. (2022). Ammonia as a potential marine fuel: A review. *Energy Strategy Reviews*, *44*. https://doi.org/https://doi.org/10.1016/j.esr.2022.100926

Man Energy Solution. (2018). *Basic principles of ship propulsion*.

MarineTraffic. (2023). *Ais - history port calls - 2022*.

Maritime Safety Office. (2019). *World port index - pub. 150*. National Geospatial-Intelligence Agency. https://msi.nga.mil/Publications/WPI

McKinlay, C. J., Turnock, S., & Hudson, D. (2020). A comparison of hydrogen and ammonia for future long distance shipping fuels.

McKinlay, C. J., Turnock, S. R., & Hudson, D. A. (2021). Route to zero emission shipping: Hydrogen, ammonia or methanol? *International Journal of Hydrogen Energy*, *46*, 28282–28297. https://doi.org/10.1016/j.ijhydene.2021.06.066

Merien-Paul, R. H., Enshaei, H., & Jayasinghe, S. G. (2019). Effects of fuel-specific energy and operational demands on cost/emission estimates: A case study on heavy fuel-oil vs liquefied natural gas. *Transportation Research Part D: Transport and Environment*, *69*, 77–89. https://doi.org/10.1016/j.trd.2019.01.031

National Fire Protection Association. (2017). *Nfpa 704, standard system for the identification of the hazard of materials for emergency response*.

Nayak-Luke, R. M., & Bañares-Alcántara, R. (2020). Techno-economic viability of islanded green ammonia as a carbon-free energy vector and as a substitute for conventional production. *Energy and Environmental Science*, *13*, 2957–2966. https://doi.org/10.1039/d0ee01707h

OCI. (2022). *Oci n.v. to expand port of rotterdam ammonia import terminal to meet emerging large-scale low-carbon hydrogen and ammonia demand in the energy transition*.

Orsted. (2021). *Ørsted and yara seek to develop a groundbreaking green ammonia project in the netherlands.* https://orsted.com/en/media/newsroom/news/2020/%2010/143404185982536.

Prussi, M., Scarlat, N., Acciaro, M., & Kosmas, V. (2021). Potential and limiting factors in the use of alternative fuels in the european maritime sector. *Journal of Cleaner Production*, *291*. https://doi.org/10.1016/j.jclepro.2021.125849

Pruyn, J., Mourão, Z., Villar, J., Calado, G., da Silva, J. V., & van den Berg, N. (2022). *Deliverable d3.1 transport energy requirements*.

Psaraftis, H. N., Zis, T., & Lagouvardou, S. (2021). A comparative evaluation of market based measures for shipping decarbonization. *Maritime Transport Research*, *2*. https://doi.org/10.1016/j.martra.2021.100019

Salmon, N., & Bañares-Alcántara, R. (2022). A global, spatially granular techno-economic analysis of offshore green ammonia production. *Journal of Cleaner Production*, *367*. https://doi.org/10.1016/j.jclepro.2022.133045

Salmon, N., Bañares-Alcántara, R., & Nayak-Luke, R. (2021). Optimization of green ammonia distribution systems for intercontinental energy transport. *iScience*, *24*. https://doi.org/10.1016/j.isci.2021.102903

Scarbrough, T., Horton, G., Finney, H., Fischer, S., Sikora, I., McQuillen, J., Ash, N., & Shakeel, H. (2022). *Technological, operational and energy pathways for maritime transport to reduce emissions towards 2050*. Ricardo Energy & Environment. https://www.concawe.eu/wp-content/uploads/Technological-Operational-and-Energy-Pathways-for-Maritime-Transport-to-Reduce-Emissions-Towards-2050.pdf

Snaathorst, A. M. (2022). *Alternative marine energy carrier impact on ship pow-ering and the environment a comparative conceptual lca of the operational stage of ship types with alternative marine energy carriers*. http://repository.tudelft.nl/.

Snaathorst, A. M., & Pruyn, J. F. J. (2022). Design and powering impact on ships by alternative marine energy carriers to determine the total environmental impact.

Sommer, A. (2023). *Green shipping program pilot report: Ammonia powered bulk carrier*. GRIEG STAR.

Tuljak-Suban, D. (2019). Mcdm bunkering optimisation in a hub and spoke system: The case of the north adriatic ports. *Promet - Traffic & Transportation*, *31*, 539–547.

UNFCCC. (2015). *Paris agreement*. https://unfccc.int/process-and-meetings/the-paris-agreement

Ursavas, E., Zhu, S. X., & Savelsbergh, M. (2020). Lng bunkering network design in inland waterways. *Transportation Research Part C: Emerging Technologies*, *120*. https://doi.org/10.1016/j.trc.2020.102779

Valera-Medina, A., Amer-Hatem, F., Azad, A. K., Dedoussi, I. C., Joannon, M. D., Fernandes, R. X., Glarborg, P., Hashemi, H., He, X., Mashruk, S., McGowan, J., Mounaim-Rouselle, C., Ortiz-Prado, A., Ortiz-Valera, A., Rossetti, I., Shu, B., Yehia, M., Xiao, H., & Costa, M. (2021). Review on ammonia as a potential fuel: From synthesis to economics. *Energy and Fuels*, *35*, 6964–7029. https://doi.org/10.1021/acs.energyfuels.0c03685

Valera-Medina, A., Xiao, H., Owen-Jones, M., David, W. I., & Bowen, P. J. (2018). Ammonia for power. *Progress in Energy and Combustion Science*, *69*, 63–102. https://doi.org/10.1016/j.pecs.2018.07.001

van Veldhuizen, B. N., van Biert, L., Amladi, A., Woudstra, T., Visser, K., & Aravind, P. V. (2023). The effects of fuel type and cathode off-gas recirculation on combined heat and power generation of marine sofc systems [Dus daarom Ammonia interessant!!]. *Energy Conversion and Management*, *276*. https://doi.org/10.1016/j.enconman.2022.116498

von Westarp, A. G., & Brabänder, C. (2021). Support of the speed decision in liner operation by evaluating the trade-off between bunker fuel consumption and reliability. *Maritime Transport Research*, *2*. https://doi.org/10.1016/j.martra.2021.100009

Wang, S., & Meng, Q. (2015). Robust bunker management for liner shipping networks. *European Journal of Operational Research*, *243*, 789–797. https://doi.org/10.1016/j.ejor.2014.12.049

Wang, S., Meng, Q., & Liu, Z. (2013). Bunker consumption optimization methods in shipping: A critical review and extensions. *Transportation Research Part E: Logistics and Transportation Review*, *53*, 49–62. https://doi.org/10.1016/j.tre.2013.02.003

Wang, Y., Meng, Q., & Kuang, H. (2018). Jointly optimizing ship sailing speed and bunker purchase in liner shipping with distribution-free stochastic bunker prices. *Transportation Research Part C: Emerging Technologies*, *89*, 35–52. https://doi.org/10.1016/j.trc.2018.01.020

Wang, Y., & Wright, L. A. (2021). A comparative review of alternative fuels for the maritime sector: Economic, technology, and policy challenges for clean energy implementation. *World*, *2*, 456–481. https://doi.org/10.3390/world2040029

Wen, M., Pacino, D., Kontovas, C. A., & Psaraftis, H. N. (2017). A multiple ship routing and speed optimization problem under time, cost and environmental objectives. *Transportation Research Part D: Transport and Environment*, *52*, 303–321. https://doi.org/10.1016/j.trd.2017.03.009

Wu, S., Miao, B., & Chan, S. H. (2022). Feasibility assessment of a container ship applying ammonia cracker-integrated solid oxide fuel cell technology. *International Journal of Hydrogen Energy*, *47*, 27166–27176. https://doi.org/10.1016/j.ijhydene.2022.06.068

Yang, M., & Lam, J. S. L. (2023). Operational and economic evaluation of ammonia bunkering – bunkering supply chain perspective. *Transportation Research Part D: Transport and Environment*, *117*, 103666. https://doi.org/10.1016/j.trd.2023.103666

A

Extra Results S4B

The diagrams in this appendix are an extension to the diagram shown in figures 8.6 and 8.7. The annual fuel costs per fleet type in scenario S3B are shown in figure A.1 (run 0 to run 5) and figure A.2 (run 6 to run 10). The annual loss in revenue per fleet type in scenario S3B is shown in figure A.3 (run 0 to run 5) and figure A.4 (run 6 to run 10).

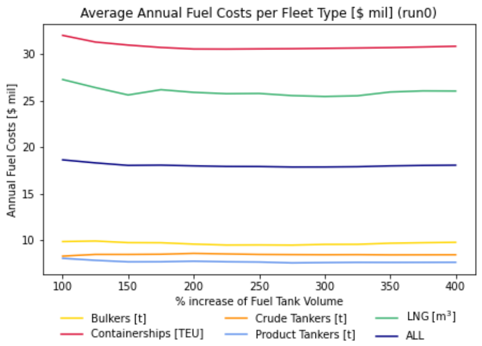

(a) run 0

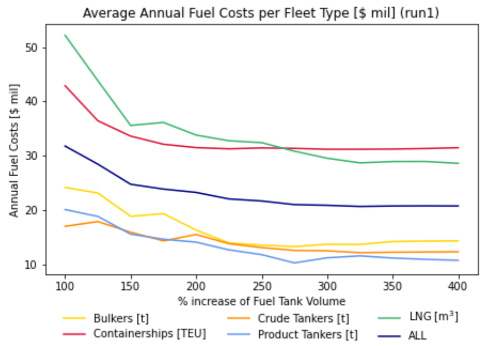

(b) run 1

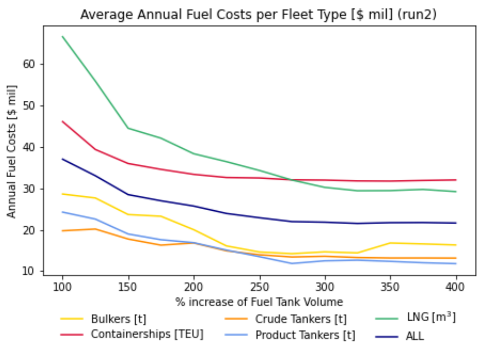

(c) run 2

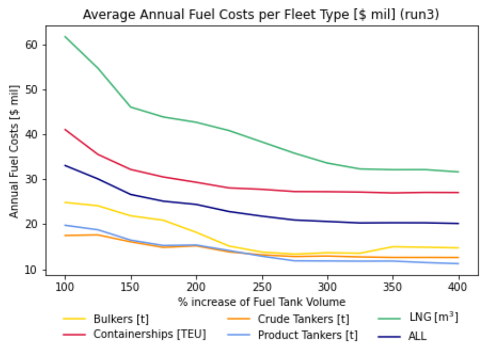

(d) run 3

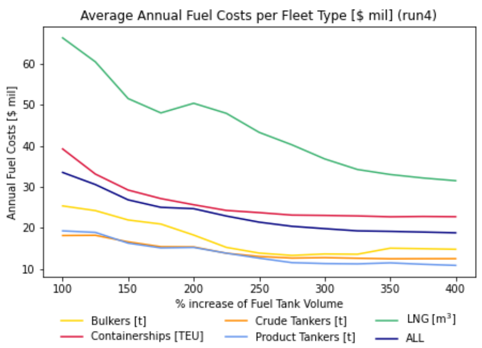

(e) run 4

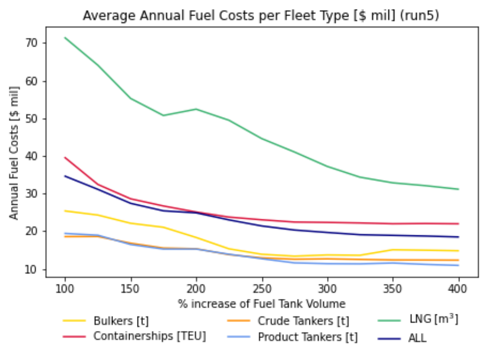

(f) run 5

Figure A.1: Evaluation of the Annual Fuel Costs per Fleet Type in Scenario S3B (run 0 to run 5).

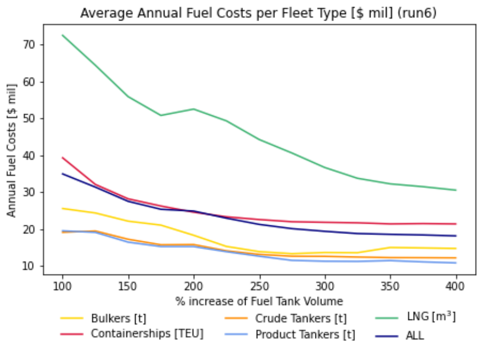

(a) run 6

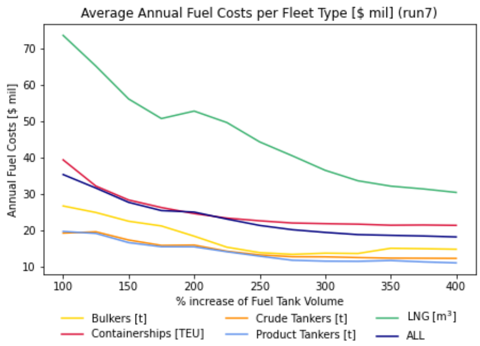

(b) run 7

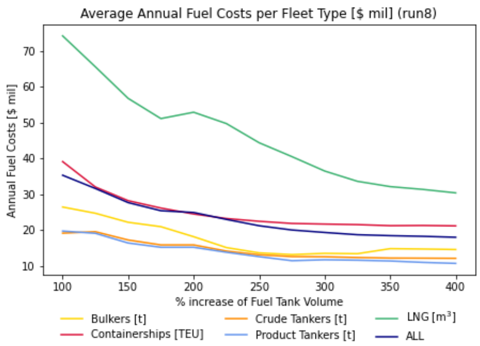

(c) run 8

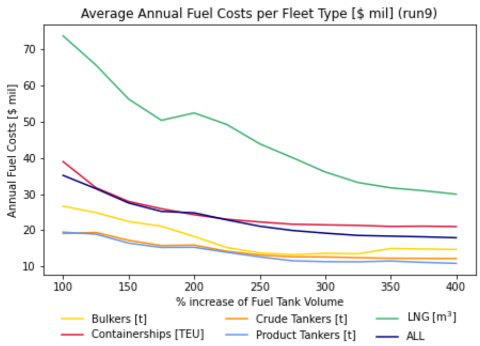

(d) run 9

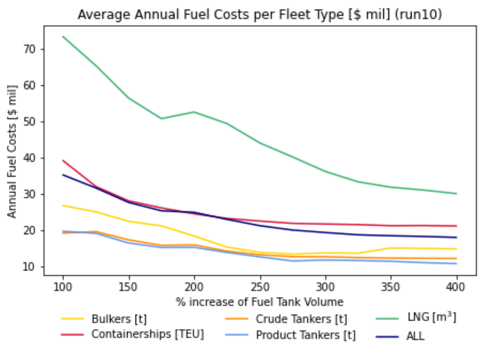

(e) run 10

Figure A.2: Evaluation of the Annual Fuel Costs per Fleet Type in Scenario S3B (run 6 to run 10).

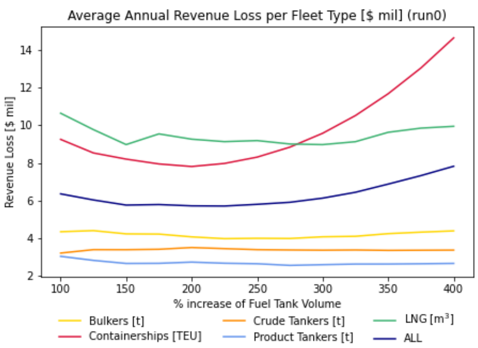

(a) run 0

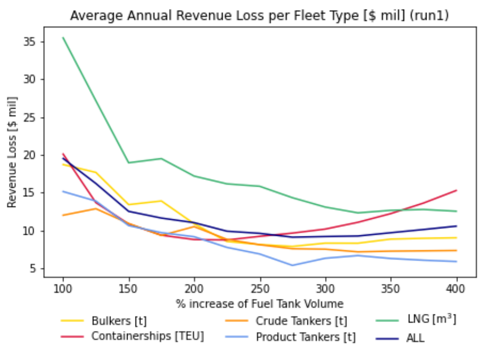

(b) run 1

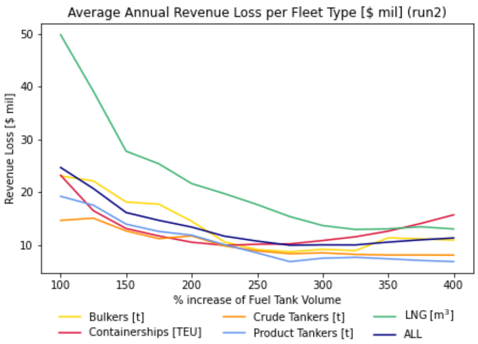

(c) run 2

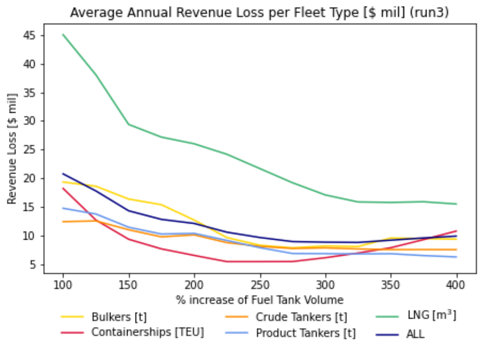

(d) run 3

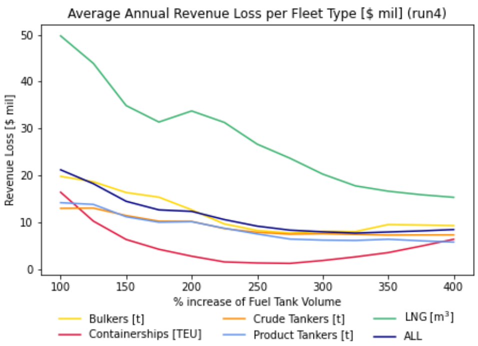

(e) run 4

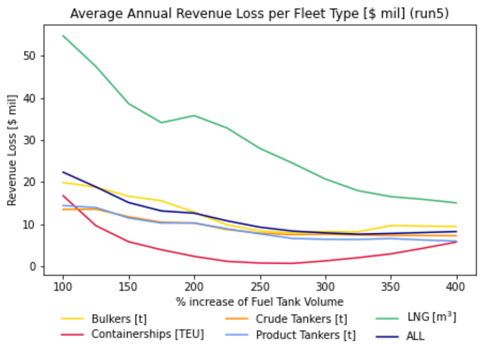

(f) run 5

Figure A.3: Evaluation of the Annual Loss in Revenue per Fleet Type in Scenario S3B (run 0 to run 5).

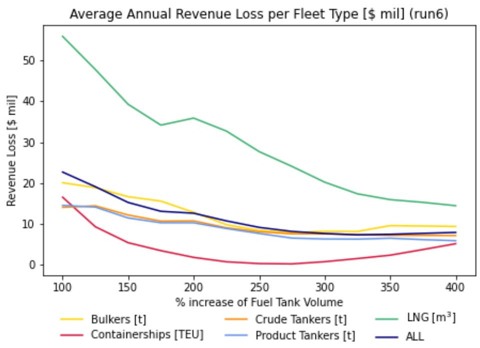

(a) run 6

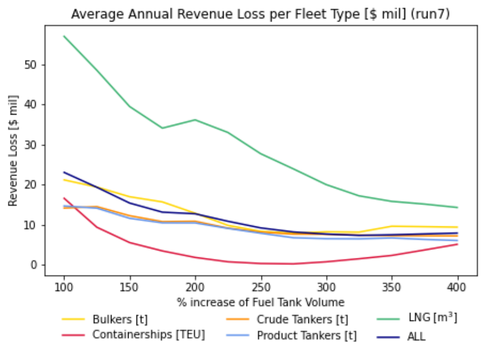

(b) run 7

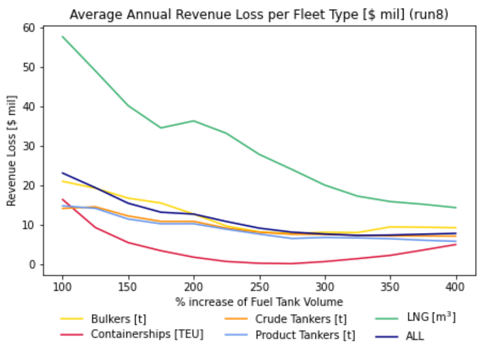

(c) run 8

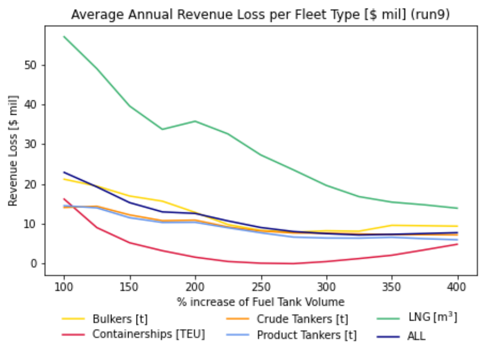

(d) run 9

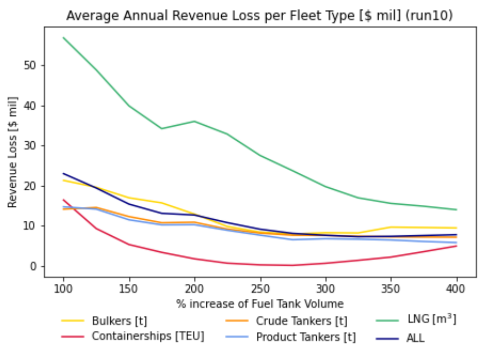

(e) run 10

Figure A.4: Evaluation of the Annual Loss in Revenue per Fleet Type in Scenario S3B (run 6 to run 10).

B

Ship Selection

The tables in this appendix represent the ship selection applied in the case study. The total fleet contains 1025 ships and is divided into five fleet types: 112 bulkers, 300 containerships, 313 crude tankers, 125 product tankers and 176 LNG carriers. The parameters used to identify the ships are included in this appendix. The identification parameters are the shipname, the IMO number, the built year and the deadweight.

B.1. Bulkers

Table B.1: The Bulkers used in the case study of this report.

Name	IMO number	Built Year	DWT [t]
AM Kirti	9832925	2019	180000
AM Tarang	9832913	2019	180000
Apollonius	9718234	2016	180544
Ariadne	9721877	2016	207520
Berge Mawson	9738868	2015	181160
Berge Meru	9855214	2021	210734
Berge Sarstein	9774367	2017	182981
Bosporus	9689691	2016	179177
Bregaglia	9694945	2016	87665
Bulk Ginza	9875111	2020	182868
Bulk Peninsula	9839014	2019	182983
Bulk Santos	9849772	2020	208445
Bulk Sao Paulo	9849760	2020	208445
Bulk Sydney	9849758	2020	208445
Cape Harrier	9860477	2019	183142
Cape Kestrel	9767510	2016	181267
Cape Owl	9729219	2016	179510
Capricorn One	9739018	2015	181319
Capricorn Sigma	9747962	2015	181305
Castillo De Malpica	9722962	2015	119613
Castillo de Navia	9722974	2015	119612
Cheng May	9751028	2017	180008
Chow	9743291	2016	181146

CL Liuzhou	9854533	2020	208775
CL Wuzhou	9854557	2021	208521
CL Yulin	9854545	2020	208611
Contamines	9743277	2016	180922
CSSC Amsterdam	9853890	2020	120566
CSSC Cape Town	9853888	2020	120578
CSSC Gladstone	9853917	2021	120633
CSSC Le Havre	9853931	2021	120000
CSSC Rotterdam	9853905	2021	120640
Diane Oldendorff	9860362	2020	100449
Diavolezza	9694933	2016	87665
Double Delight	9738806	2015	95522
Duhallow	9729207	2016	179481
Fabulous	9861380	2019	180724
Fomento Four	9783320	2019	209951
Fomento Three	9783318	2018	209935
Fortune	9737838	2016	182620
Friedrich Oldendorff	9889265	2020	208822
Genco Resolute	9698977	2015	181060
Golden Aquamarine	9882475	2021	209187
Golden Cirrus	9717395	2018	180487
Golden Competence	9856490	2020	207397
Golden Coral	9842712	2019	208132
Golden Kathrine	9701322	2015	182486
Golden Sapphire	9882463	2021	209182
Golden Savannah	9723538	2017	181044
Golden Surabaya	9723526	2017	181046
Hanna Oldendorff	9731614	2017	208942
Harvest Rain	9643893	2015	95263
Harvest Time	9643881	2015	95263
Heide Oldendorff	9871103	2021	207629
Helena Oldendorff	9718351	2016	209177
Henry Oldendorff	9871086	2020	208194
Hera Oldendorff	9718363	2017	209249
Hermann Oldendorff	9731585	2016	209243
Hille Oldendorff	9731573	2016	209200
Hinrich Oldendorff	9713064	2016	209114
Huge Kumano	9889277	2020	208848
Jubilant Devotion	9760471	2016	117549
Judd	9639476	2015	205855
KLKH Friendship	9875123	2020	182697
KSL Sakura	9719941	2015	181062
KSL Seoul	9723502	2015	181010
KSL Seville	9723540	2015	181003
KSL Stockholm	9723514	2015	181043
Long May	9847085	2020	207997

Lowlands Amber	9866720	2021	100309
Ludolf Oldendorff	9691955	2015	207562
Lydia Oldendorff	9699634	2015	207562
Maharaj	9735165	2015	209472
Maran Excellence	9703241	2016	180940
Maran Horizon	9702699	2016	180940
Maran Unity	9729166	2015	179405
Maran Venture	9703239	2016	180940
Maria D	9689689	2016	179232
Marigo P	9689706	2016	178923
Mineral Edo	9727352	2015	207219
Mineral Yangfan	9738571	2019	206392
Minoas	9721865	2015	207520
Navios Felix	9756743	2016	181221
Navios Mars	9747950	2016	181259
New Admire	9738844	2015	181050
Niseko Queen	9889289	2020	208786
Nordic Nuluujaak	9884966	2021	95758
Nordic Sanngijuq	9895795	2021	95758
Nordic Siku	9895800	2021	95000
NSU Brazil	9837987	2020	399821
Ou May	9751016	2017	180003
Pacific Anouk	9835874	2019	180000
Pacific Myra	9835898	2019	181060
Pacific Sarah	9835886	2019	180000
Samjohn Argonaut	9745938	2017	209756
Samjohn Odyssey	9745940	2019	209801
Seafighter	9686326	2015	181119
Seaforce	9685487	2015	181098
Secretariat	9699701	2015	180848
Shandong De Tai	9872121	2021	180702
Shandong De Yu	9872107	2021	180730
Star Gina 2GR	9735177	2016	209475
Stella Hope	9742209	2016	180007
Thalassini Njord	9757838	2016	181218
True Cardinal	9750828	2016	182631
True Courage	9750830	2016	182644
True North	9713076	2016	209325
Tzoumaz	9694921	2015	87665
United Eternity	9802102	2017	183026
United Grace	9870147	2019	182922
Vitus Bering	9838840	2019	104548
Xin Da Hai	9738155	2017	178438

B.2. Containership

Table B.2: The Containerships used in the case study of this report.

Shipname	IMO number	Built Year	DWT [t]
Afif	9732345	2017	149360
Akadimos	9706308	2015	114856
Al Dahna Express	9708825	2016	199744
Al Dhail	9732307	2016	149360
Al Jasrah	9732321	2016	149360
Al Jmeliyah	9732357	2017	149360
Al Mashrab	9732319	2016	149360
Al Murabba	9708837	2015	149360
Al Muraykh	9708863	2015	199744
Al Nasriyah	9708849	2015	149360
Al Nefud	9708813	2015	199744
Al Zubara	9708875	2015	199744
Alexis	9686900	2015	79274
Atacama	9718947	2016	113227
Barzan	9708851	2015	199744
Callao Express	9777606	2016	123587
Cap San Juan	9717204	2015	123101
Cap San Lazaro	9717216	2015	123101
Cape Akritas	9706190	2016	134869
Cape Kortia	9727613	2017	134869
Cape Pioneer	9719874	2017	79329
Cape Sounio	9727625	2017	134869
Cape Tainaro	9706205	2017	134869
Cartagena Express	9777618	2017	123490
CCNI Andes	9718935	2015	113073
CCNI Angol	9683867	2015	113213
CCNI Arauco	9683843	2015	112588
CMA CGM Arkansas	9722651	2015	104236
CMA CGM Bali	9867827	2021	158999
CMA CGM Benjamin Franklin	9706891	2015	185000
CMA CGM Bougainville	9702156	2015	186528
CMA CGM Carl Antoine	9729087	2017	109808
CMA CGM Champs Elysees	9839131	2020	220868
CMA CGM Columbia	9722663	2015	104236
CMA CGM Concorde	9839208	2021	221250
CMA CGM Estelle	9729116	2018	109808
CMA CGM Ganges	9718117	2015	111034
CMA CGM Georg Forster	9702144	2015	186745
CMA CGM Hermes	9882499	2021	156198
CMA CGM Hope	9897755	2021	154700
CMA CGM Iguacu	9859131	2021	158999
CMA CGM Jacques Joseph	9729104	2017	109808
CMA CGM Jacques Saade	9839179	2020	221250
CMA CGM Jean Gabriel	9729128	2018	109794

CMA CGM Jean Mermoz	9776420	2018	202684
CMA CGM Kerguelen	9702132	2015	186745
CMA CGM Kimberley	9894973	2021	155000
CMA CGM Lisa Marie	9729099	2017	109808
CMA CGM Louis Bleriot	9776432	2018	198580
CMA CGM Louvre	9839143	2020	220868
CMA CGM Mekong	9718105	2015	111040
CMA CGM Mississippi	9679907	2015	115657
CMA CGM Montmartre	9839155	2021	220868
CMA CGM Ohio	9722687	2015	110552
CMA CGM Palais Royal	9839181	2020	221250
CMA CGM Patagonia	9894961	2021	154077
CMA CGM Rhone	9674543	2015	113800
CMA CGM Rio Grande	9722699	2016	104236
CMA CGM Rivoli	9839193	2021	221250
CMA CGM Scandola	9859129	2020	158999
CMA CGM Sorbonne	9839210	2021	221250
CMA CGM Tanya	9722704	2016	104236
CMA CGM Tenere	9859117	2020	158999
CMA CGM Thames	9674567	2015	113800
CMA CGM Trocadero	9839167	2021	220868
CMA CGM Unity	9897767	2021	154700
CMA CGM Vasco De Gama	9706889	2015	185000
CMA CGM Volga	9705081	2015	112063
CMA CGM Zheng He	9706906	2015	185000
Corcovado	9687564	2015	104544
COSCO Shipping Alps	9757864	2018	153500
COSCO Shipping Andes	9757888	2018	153500
COSCO Shipping Aries	9783497	2018	197500
COSCO Shipping Galaxy	9795634	2019	198070
COSCO Shipping Gemini	9783526	2018	202014
COSCO Shipping Himalayas	9757840	2017	153811
COSCO Shipping Leo	9783502	2018	197500
COSCO Shipping Libra	9783538	2018	201823
COSCO Shipping Nebula	9795622	2018	198485
COSCO Shipping Pisces	9789647	2019	196996
COSCO Shipping Rose	9785809	2018	146714
COSCO Shipping Sagittarius	9783473	2018	202133
COSCO Shipping Scorpio	9789635	2018	196913
COSCO Shipping Seine	9731949	2017	111401
COSCO Shipping Solar	9795646	2019	197820
COSCO Shipping Star	9795658	2019	197976
COSCO Shipping Taurus	9783459	2018	201868
COSCO Shipping Universe	9795610	2018	198485
COSCO Shipping Virgo	9783461	2018	201827
COSCO Shipping Volga	9731925	2017	111244

Croatia	9723277	2016	111469
CSCL Arctic Ocean	9695169	2015	184320
CSCL Atlantic Ocean	9695145	2015	184320
Czech	9723241	2015	111595
Ever Ace	9893890	2021	241960
Ever Act	9893905	2021	241960
Ever Aim	9893917	2021	241960
Ever Alp	9893929	2021	241960
Ever Genius	9786815	2018	199692
Ever Gentle	9820922	2019	199489
Ever Gifted	9786827	2018	198886
Ever Given	9811000	2018	199489
Ever Globe	9786841	2019	199692
Ever Glory	9786839	2019	199692
Ever Golden	9811012	2018	199692
Ever Goods	9810991	2018	199692
Ever Govern	9832717	2019	198937
Ever Grade	9820855	2019	199489
Ever Greet	9832729	2019	198937
Guayaquil Express	9777620	2017	123587
HMM Algeciras	9863297	2020	232606
HMM Copenhagen	9863302	2020	232606
HMM Daon	9869227	2021	160927
HMM Dublin	9863314	2020	232606
HMM Gaon	9869174	2021	160927
HMM Garam	9869186	2021	160927
HMM Gdansk	9863326	2020	232606
HMM Hamburg	9863338	2020	232606
HMM Hanbada	9869203	2021	160927
HMM Hanul	9869239	2021	160927
HMM Helsinki	9863340	2020	232606
HMM Le Havre	9868314	2020	232606
HMM Mir	9869198	2021	160927
HMM Nuri	9869162	2021	160927
HMM Oslo	9868326	2020	229039
HMM Raon	9869215	2021	160926
HMM Rotterdam	9868338	2020	229039
HMM Southampton	9868340	2020	229039
Hungary	9723253	2015	111595
Linah	9708801	2015	149360
Maastricht Maersk	9780483	2019	190326
Madrid Maersk	9778791	2017	190326
Maersk Genoa	9739680	2016	118908
Maersk Gibraltar	9739692	2016	119130
Maersk Guatemala	9713375	2015	115177
Maersk Halifax	9784271	2017	178257

Maersk Hamburg	9784312	2018	178257
Maersk Hangzhou	9784300	2018	178257
Maersk Hanoi	9784295	2018	178257
Maersk Havana	9784336	2019	178257
Maersk Herrera	9784324	2018	178257
Maersk Hidalgo	9784283	2017	178257
Maersk Hong Kong	9784257	2017	178257
Maersk Horsburgh	9784269	2017	178257
Maersk Houston	9848950	2019	178257
Maersk Huacho	9848948	2019	178257
Manchester Maersk	9780445	2018	190326
Manila Maersk	9780469	2018	190326
Marchen Maersk	9632143	2015	194898
Margrethe Maersk	9632131	2015	195071
Marit Maersk	9632167	2015	196000
Marseille Maersk	9778844	2018	190326
Mathilde Maersk	9632179	2015	194934
Mette Maersk	9632155	2015	196000
Milan Maersk	9778820	2017	190326
Monaco Maersk	9778832	2017	190326
Moscow Maersk	9778818	2017	190326
MSC Adonis	9706310	2015	114856
MSC Aino	9770751	2019	128688
MSC Alanya	9785483	2021	128877
MSC Aliya	9842097	2019	150893
MSC Allegra	9897028	2021	228406
MSC Ambra	9839480	2020	228149
MSC Amelia	9896995	2021	228406
MSC Amsterdam	9606338	2015	186649
MSC Anna	9777204	2016	185503
MSC Anzu	9710426	2015	109510
MSC Apolline	9896983	2021	228406
MSC Aries	9857169	2020	158097
MSC Arina	9839284	2019	224983
MSC Avni	9756729	2017	120500
MSC Bianca	9770749	2019	128877
MSC Branka	9720495	2016	110000
MSC Brittany	9724049	2016	115639
MSC Brunella	9702106	2015	109832
MSC Carlotta	9756731	2017	120500
MSC Carole	9785445	2021	128877
MSC Caterina	9705005	2015	109510
MSC Chloe	9720483	2016	110442
MSC Clara	9708693	2015	199272
MSC Clea	9720524	2016	110628
MSC Desiree	9745665	2017	109801

MSC Diana	9755933	2016	202036
MSC Diletta	9897004	2021	228406
MSC Ditte	9754953	2016	198700
MSC Domitille	9720201	2015	110699
MSC Elma	9735218	2016	110103
MSC Eloane	9755957	2016	201792
MSC Elodie	9704972	2015	109510
MSC Erica	9755191	2016	199272
MSC Faith	9842085	2019	150893
MSC Febe	9839478	2019	228149
MSC Gayane	9770763	2018	120500
MSC Giselle	9720196	2015	110412
MSC Giulia	9770737	2017	125000
MSC Gulsun	9839430	2019	228149
MSC Hamburg	9647461	2015	186650
MSC Ingy	9755945	2016	202036
MSC Isabella	9839272	2019	224999
MSC Istanbul	9606326	2015	186649
MSC Jade	9762326	2016	199272
MSC Jeongmin	9720471	2016	110628
MSC Julie	9704996	2015	109510
MSC Leanne	9767390	2017	202036
MSC Leni	9839454	2019	228149
MSC Letizia	9702065	2015	110800
MSC Lily	9704960	2015	109510
MSC Madhu B	9778088	2017	134007
MSC Maxine	9720287	2015	110628
MSC Maya	9708679	2015	199272
MSC Meline	9702077	2015	110029
MSC Mia	9839466	2019	228149
MSC Michela	9720512	2016	110531
MSC Michelle	9897016	2021	228406
MSC Mina	9839260	2019	224983
MSC Mirja	9762338	2016	200148
MSC Mirjam	9767376	2016	202376
MSC Naomi	9704984	2015	109510
MSC Nela	9839296	2019	224983
MSC Nitya B	9778117	2017	134007
MSC Oliver	9703306	2015	199273
MSC Palak	9735206	2016	109801
MSC Rayshmi	9785457	2021	128877
MSC Reef	9754965	2016	200148
MSC Rifaya	9767388	2017	202036
MSC Romane	9745653	2017	109801
MSC Samar	9839442	2019	228149
MSC Sasha	9720500	2016	109520

MSC Shreya B	9778105	2017	134093
MSC Shuba B	9778076	2017	134093
MSC Silvia	9720457	2015	110698
MSC Sixin	9839301	2019	224983
MSC Siya B	9793947	2018	132586
MSC Sofia Celeste	9702091	2015	110039
MSC Sveva	9708681	2015	199272
MSC Tina	9762340	2017	200148
MSC Venice	9647473	2016	186649
MSC Vita	9702089	2015	110029
MSC Viviana	9777216	2017	185503
MSC Yashi B	9778090	2018	134007
MSC Zoe	9703318	2015	199272
Mumbai Maersk	9780471	2018	190326
Munich Maersk	9778806	2017	190326
Murcia Maersk	9780457	2018	190326
Olivia I	9686912	2015	79274
ONE Aquila	9806043	2018	138611
ONE Blue Jay	9741372	2016	139335
ONE Columba	9806055	2018	139335
ONE Crane	9741401	2016	139335
ONE Cygnus	9806081	2019	138611
ONE Eagle	9741396	2016	139335
ONE Falcon	9741425	2017	139335
ONE Grus	9806067	2019	139335
ONE Ibis	9741384	2016	139335
ONE Mackinac	9689603	2015	147420
ONE Manchester	9706748	2015	147420
ONE Manhattan	9689615	2015	147420
ONE Milano	9757187	2018	146931
ONE Millau	9706736	2015	147420
ONE Owl	9741449	2017	139335
ONE Swan	9741437	2017	139335
ONE Tradition	9769300	2017	196155
ONE Treasure	9773222	2018	218000
ONE Tribute	9769295	2017	196155
ONE Triumph	9769271	2017	196155
ONE Trust	9769283	2017	196155
ONE Truth	9773210	2017	218000
OOCL Germany	9776183	2017	191688
OOCL Hong Kong	9776171	2017	191422
OOCL Indonesia	9776224	2018	191374
OOCL Japan	9776195	2017	191640
OOCL Scandinavia	9776212	2017	191343
OOCL United Kingdom	9776200	2017	191570
Paranagua Express	9786724	2017	132791

Salahuddin	9708796	2015	149360
Santos Express	9777632	2017	123587
Talos	9728930	2016	151796
Tampa Triumph	9737462	2017	155000
Taurus	9728942	2016	131600
Texas Triumph	9737503	2017	146722
Theseus	9728954	2016	131600
Tihama	9736107	2016	199744
Titan	9728928	2016	131600
Toledo Triumph	9737486	2017	155000
Triton	9728916	2016	151796
Umm Qarn	9732333	2016	149360
Valparaiso Express	9777589	2016	123587
YM Wellness	9704623	2015	145559
YM Wellspring	9757230	2019	147500
YM Wholesome	9704611	2015	145559
YM Winner	9684689	2015	145559
YM Wisdom	9757216	2019	147500
YM Wish	9684641	2015	145559
YM Wreath	9708473	2017	145500
Zeal Lumos	9864241	2021	158097
Zenith Lumos	9864215	2020	158097
Zephyr Lumos	9864227	2021	158097
Zeus Lumos	9864239	2021	158097
ZIM Norfolk	9710220	2015	110903
ZIM Xiamen	9710232	2015	110903

B.3. Crude Tankers

Table B.3: The Crude Tankers used in the case study of this report.

Shipname	IMO number	Built Year	DWT [t]
Adam	9826732	2018	113226
Aegean Dream	9645425	2016	159000
Aegean Marathon	9745225	2016	158914
Aegean Unity	9745237	2016	158932
Aegean Vision	9645437	2017	158871
Agios Fanourios I	9759824	2016	299996
Agitos	9830824	2019	320785
Aigeorgis	9891660	2021	116092
Aitolos	9867619	2020	115521
Albert	9843572	2019	113095
Alexander	9826720	2018	113170
Alfa Alandia	9752797	2016	105898
Alfa Baltica	9696773	2015	106373
Alfa Finlandia	9823041	2019	109089
Almi Atlas	9816323	2018	315221

Almi Titan	9816335	2018	315299
Altera Wave	9863558	2021	103158
Altera Wind	9863560	2021	103118
Amjad	9779800	2017	298886
Amphion	9830795	2019	298998
Andaman	9739501	2016	299392
Andre Reboucas	9453846	2015	156520
Anna Knutsen	9769221	2017	152268
Apache	9749489	2016	158594
Apollonas	9733806	2016	299999
Aquasurazo	9785720	2017	113032
Aquatravesia	9785732	2017	113032
Aristofanis	9867621	2020	115521
Ascona	9828338	2019	299999
Asian Progress VI	9782522	2019	312328
Atromitos	9733818	2016	299999
Aura M	9595333	2020	156245
Aurora Spirit	9837169	2020	129632
Aurviken	9853400	2019	112802
Balla	9749556	2017	113293
Bella Ciao	9872688	2020	156586
Bergen TS	9737400	2017	113039
Breiviken	9817470	2018	112649
Captain Lyristis	9877183	2021	158082
Caspian Sea	9829095	2019	114218
Cherokee	9749491	2016	158594
Chios	9772113	2016	149989
Chios I	9792187	2017	149999
Cobalt Sun	9814428	2019	114396
Cosdignity Lake	9727209	2017	308013
Cosrising Lake	9735737	2016	310595
Crude Levante	9899363	2021	156828
Crude Zephyrus	9899375	2021	156828
Crudemed	9832547	2018	115643
Crudesun	9832559	2018	115643
Current Spirit	9843924	2020	129801
Dali	9787936	2018	115281
Delta Amazon	9748916	2015	319896
Delta Eurydice	9700706	2015	149990
Delta Maria	9700691	2015	149900
DHT Bronco	9822994	2018	317975
DHT Harrier	9762986	2016	299985
DHT Lion	9722895	2016	299629
DHT Tiger	9733959	2017	299629
Diligent Warrior	9750050	2016	149992
Dimitrios	9900007	2021	159159

Eagle Balder	9833113	2020	128427
Eagle Barcelona	9795048	2018	113327
Eagle Barents	9676125	2015	119690
Eagle Bergen	9676137	2015	120567
Eagle Bintulu	9795074	2019	113049
Eagle Blane	9833101	2020	125000
Eagle Brasilia	9795062	2019	113416
Eagle Brisbane	9795050	2018	113458
Eagle San Francisco	9795127	2018	157512
Eagle San Jose	9795139	2018	157579
Ebn Hawkel	9874507	2021	112003
Eco Bel Air	9794056	2019	157285
Eco Beverly Hills	9794068	2019	157285
Eco Seas	9762998	2016	299998
Eco West Coast	9902811	2021	157668
Effie Maersk	9682978	2017	158295
Eikeviken	9818058	2019	113000
Elandra Eagle	9792474	2017	157554
Elandra Falcon	9792486	2017	157553
Elbhoff	9770646	2017	300837
Elias Tsakos	9724075	2016	112700
Elisabeth Maersk	9682980	2017	158295
Eva Maersk	9682992	2017	158468
Faithful Warrior	9750062	2016	149992
Flavin	9787912	2018	115126
Folegandros	9793753	2018	159221
Fontana	9792541	2017	159855
Frankopan	9796731	2017	114305
Freedom Glory	9863417	2020	114122
Freud	9804461	2018	157620
Front Cascade	9769829	2017	157434
Front Challenger	9759745	2016	157407
Front Classic	9759769	2017	157434
Front Clipper	9759771	2017	157351
Front Coral	9743203	2017	157434
Front Cosmos	9769817	2017	157434
Front Crown	9759757	2016	157460
Front Cruiser	9797230	2020	158000
Front Crystal	9743186	2017	157434
Front Discovery	9830109	2019	298952
Front Idun	9600944	2015	156849
Front Nausta	9845714	2019	318744
Front Princess	9788904	2018	301575
Front Samara	9845130	2019	157271
Front Savannah	9831828	2019	157271
Front Seoul	9831854	2019	157271

Front Shanghai	9832262	2019	157271
Front Siena	9832250	2019	157271
Front Silkeborg	9832274	2019	157271
Front Singapore	9832248	2019	157271
Front Sparta	9847114	2019	157271
Gloria Maris	9899997	2021	156620
Goldway	9742900	2016	157781
Grand Ambition	9909807	2021	299988
Grand Bonanza	9915569	2021	299988
Green Attitude	9808156	2018	112532
Green Aura	9808168	2019	112684
Gustavia S	9859399	2020	299995
Harmonic	9819868	2019	159204
Hercules I	9723124	2017	298976
Homeric	9819844	2019	150090
Humble Warrior	9856361	2020	149990
Hunter	9896414	2021	299940
Iberian Sea	9815604	2018	114218
Ionic Althea	9728435	2016	114737
Ionic Anassa	9779795	2016	114718
Ionic Anax	9802152	2017	114720
Ionic Ariadne	9856555	2020	112007
Ithaki Warrior	9765366	2017	159962
Jaarli	9892432	2021	112459
Jatuli	9892444	2021	112459
Kanaris 21	9889942	2021	156921
Kapodistrias 21	9886639	2021	158081
Karekare	9787986	2017	159638
KHK Majesty	9830977	2019	314014
Kimolos	9791145	2018	159159
Kmarin Reliance	9683025	2016	109466
Kmarin Renown	9683013	2016	109854
Kmarin Resource	9683037	2016	109258
Kmarin Rigour	9683049	2016	109475
Korolev Prospect	9826902	2019	113232
Kriti Hero	9887308	2021	158005
Kriti King	9887255	2021	158005
Kyrakatingo	9779965	2017	113563
Lancing	9792046	2018	105898
Landbridge Horizon	9826847	2019	308396
Landbridge Wisdom	9828780	2020	307894
Leontios H	9724336	2016	113611
Lesvos	9772321	2017	149999
Levantine Sea	9815616	2018	114218
Loire	9761516	2016	154998
Lord Byron 21	9889954	2021	156921

Malibu	9776731	2017	158692
Maran Ares	9796872	2017	319398
Maran Artemis	9753002	2016	318850
Maran Aspasia	9879997	2020	157946
Maran Atalanta	9810393	2018	319398
Maran Helen	9779381	2017	156458
Maran Helios	9761358	2017	156458
Maran Hercules	9761360	2017	156458
Maran Hermes	9761346	2017	156458
Maran Hermione	9779379	2017	156458
Maran Homer	9761372	2017	156458
Maran Mars	9858046	2020	300000
Maran Phoebe	9868156	2020	157946
Maran Solon	9881691	2021	157947
Marathi	9772357	2018	149992
Marathon TS	9737371	2017	113737
Marfa	9773478	2017	159513
Marine Hope	9794006	2019	318747
Maritime Glory	9863429	2021	114122
Marlin Santorini	9835836	2019	156587
Marlin Shikoku	9841627	2019	156374
Marlin Sicily	9835848	2019	156563
Matala	9776743	2017	158715
Miaoulis 21	9886641	2021	158081
Minerva Baltica	9728241	2018	112948
Minerva Coralia	9728239	2017	113850
Minerva Eleftheria	9787168	2018	114696
Minerva Evropi	9785237	2018	159055
Minerva Kallisto	9853008	2019	112802
Minerva Kalypso	9785225	2017	159051
Minerva Karteria	9787170	2018	114696
Minerva Olympia	9787194	2019	114661
Minerva Zenobia	9787182	2018	114780
Miracle Hope	9794018	2019	318747
Monte Serantes	9841615	2019	156584
Monte Udala	9785823	2018	156341
Monte Ulia	9803285	2019	156424
Monte Urbasa	9785835	2018	156400
Monte Urquiola	9803273	2019	156400
Morviken	9817494	2018	157583
Neptune Moon	9784013	2019	157162
New Vision	9804459	2018	157617
Nissos Anafi	9856086	2020	318953
Nissos Antimilos	9895226	2021	157447
Nissos Despotiko	9845697	2019	318744
Nissos Donoussa	9853840	2019	318744

Nissos Ios	9886770	2021	157447
Nissos Keros	9856074	2019	318744
Nissos Koufonissi	9895214	2021	157447
Nissos Kythnos	9853852	2019	318744
Nissos Rhenia	9845685	2019	318744
Nissos Tinos	9886782	2021	157447
Nordic Aquarius	9818216	2018	157338
Nordic Cygnus	9818228	2018	157526
Nordic Space	9748681	2017	157582
Nordic Star	9748679	2016	157738
Nordic Tellus	9818230	2018	157000
Nordic Thunder	9797228	2017	157374
Nordindependence	9783019	2018	112052
Nordpenguin	9783007	2018	112038
North Sea	9760495	2016	106340
Olympic Fighter	9745263	2017	149993
Olympic Friendship	9745251	2017	149984
Olympic Lady	9731169	2017	299337
Olympic Laurel	9831804	2019	318676
Olympic Life	9844277	2019	318676
Olympic Lyra	9831816	2019	318676
Oslo TS	9737383	2017	112949
Ottoman Courtesy	9788708	2017	149999
Ottoman Sincerity	9788710	2017	149999
Pacific Emerald	9893022	2021	113306
Pacific Garnet	9893084	2021	113306
Pacific Treasures	9732242	2016	115177
Papalemos	9826110	2018	319191
Parthenon TS	9724348	2016	112700
Paschalis DD	9765378	2018	159812
Patriotic	9819832	2019	159090
Pegasus Star	9891672	2021	116120
Pertamina Prime	9888508	2021	301781
Philotimos	9793997	2018	113247
Phoenix Vantage	9734109	2016	299999
Platanos	9825477	2019	114578
Pluto Moon	9784025	2019	157072
Poliegos	9746621	2017	157539
Primero	9741815	2016	105898
Primeway	9817626	2018	157470
Prometheus Energy	9801988	2019	114459
Prometheus Light	9801976	2019	114601
Pusaka Java	9783899	2018	108667
Rainbow Spirit	9837171	2020	129220
Rava	9796743	2017	114385
Resilient Warrior	9856359	2020	149990

Rhythmic	9819856	2019	158958
Rivera	9777943	2017	112936
RS Tara	9765354	2016	160036
Runner	9749518	2017	158594
Ryman	9777931	2017	112870
Samsara	9792228	2017	159855
San Jacinto	9730373	2016	158658
Saturn Moon	9814430	2020	157115
Sea Amber	9772931	2016	158455
Sea Dragon	9903918	2021	114073
Sea Garnet	9772943	2017	158000
Sea Jade	9852121	2020	300633
Sea Puma	9802176	2019	114560
Sea Ruby	9779616	2017	299284
Sea Turtle	9886718	2021	114085
Sea Urchin	9886720	2021	114072
Seacalm	9773753	2017	112119
Seacharm	9773765	2018	112179
Seaduke	9890965	2021	313051
Seafaith	9843209	2020	111890
Seagalaxy	9847231	2019	114426
Seatribute	9857468	2020	111932
Seavelvet	9843211	2020	111964
Seavigour	9774185	2016	158734
Seaviolet	9790983	2018	158218
Seavision	9790971	2018	158167
Seaways Diamond Head	9727039	2016	301038
Seaways Hatteras	9730414	2017	158432
Seaways Hendricks	9727015	2016	300960
Seaways Liberty	9727027	2016	300973
Seaways Montauk	9779537	2017	158432
Seaways Reyes	9779939	2017	113689
Seaways Triton	9734654	2016	300960
Seaways Tybee	9734642	2015	300960
Serendipity	9905100	2021	299936
Silverstone	9878838	2020	288772
Silverway	9742912	2017	157781
Sola TS	9724350	2017	113737
Solomon Sea	9760500	2016	106340
Sonangol Cazenga	9766310	2017	156899
Sonangol Maiombe	9766322	2017	156935
Speedway	9749506	2017	158594
Spirit II	9645413	2016	114139
Spyros	9877171	2020	158082
Stavanger TS	9737395	2017	113737
Stirling	9901867	2021	112750

Sur	9870824	2020	299997
Sword	9783631	2018	105898
Tamara	9600889	2015	157016
Tateshina	9910117	2021	311979
Thomas Zafiras	9724087	2016	113691
Tide Spirit	9843912	2020	129632
Tigani	9776767	2017	112887
Tilos I	9800271	2018	149999
TRF Horten	9740342	2018	297639
Tyrrhenian Sea	9829100	2019	114218
Universal Winner	9837602	2019	299981
Vernadsky Prospect	9843560	2019	113310
Victory Venture	9773040	2017	113200
Waikiki	9776755	2017	112829
Water Tiger	9858034	2020	299995
Yuan Dong Hai	9843338	2020	158677
Yuan Gui Yang	9843302	2020	319000
Yuan Hua Hu	9723588	2015	308663
Yuan Nan Hai	9843340	2020	158694
Yuan Peng Yang	9847633	2021	310298
Yuan Yue Hu	9681211	2015	308080

B.4. Product Tankers

Table B.4: The Product Tankers used in the case study of this report.

Shipname	IMO number	Built Year	DWT [t]
Abliani	9693068	2015	109999
Advantage Love	9708552	2015	109999
Agios Gerasimos	9693056	2015	109999
Aifanourios	9891696	2021	116015
Al Bateen	9828376	2020	114717
Al Falah	9828388	2021	114756
Al Khtam	9823534	2021	114644
Aldana	9809368	2018	149999
Alkinoos	9792864	2019	109900
Anwaar Benghazi	9888742	2021	114077
Aretea	9711456	2015	114000
Arizona Lady	9831062	2019	111751
Atlantic Blue	9889124	2021	110400
Atlantic Gold	9889136	2021	109997
Burri	9787948	2019	115018
BW Larissa	9800300	2019	109990
BW Neso	9800312	2019	109990
BW Thalassa	9800324	2019	109990
BW Triton	9800336	2019	109990
Clear Stars	9868778	2020	113252

Clearocean Ajax	9850692	2019	113252
Eagle Le Havre	9795103	2017	113809
Eagle Lyon	9795115	2017	113809
Elandra Bay	9821691	2018	109891
Elandra Sound	9821706	2018	109893
Fezzan	9888730	2021	114243
Front Antares	9745926	2017	109896
Front Capella	9790995	2017	109895
Front Castor	9780251	2017	109900
Front Cheetah	9686637	2016	109900
Front Cougar	9686649	2016	109896
Front Favour	9903968	2021	109899
Front Fusion	9887803	2021	109899
Front Jaguar	9703332	2016	109900
Front Leopard	9703320	2016	109900
Front Lynx	9726592	2016	109900
Front Ocelot	9726580	2016	109900
Front Polaris	9791004	2018	109899
Front Pollux	9780263	2017	109899
Front Sirius	9767340	2017	109896
Front Vega	9767338	2017	109895
Hafnia Despina	9796494	2019	109990
Hanover Square	9783992	2019	114366
Hibernian Tide	9800568	2019	109896
Kleon	9730945	2016	109999
Kmarin Reason	9683087	2017	109483
Kmarin Regard	9683063	2016	109543
Kmarin Resolution	9683051	2016	109258
Kmarin Restraint	9683075	2017	109526
LR2 Aphrodite	9742211	2017	109989
LR2 Athena	9784611	2017	109986
LR2 Olivia	9740469	2017	109985
LR2 Ophelia	9740471	2018	109980
Lyric Camellia	9730933	2016	109999
Lyric Magnolia	9734408	2016	109999
Marlin Loreto	9823558	2021	114823
Marlin Luanda	9829899	2018	109991
Minerva Alexandra	9892999	2021	115484
Minerva Astra	9893008	2021	115484
Nan Lin Wan	9783411	2017	109700
Navig8 Passion	9853278	2019	109992
Navig8 Perseverance	9853266	2019	109998
Navig8 Precision	9831294	2018	109994
Navig8 Prestige JKB	9831309	2019	109995
Navig8 Promise	9791298	2019	109992
Navig8 Prosperity	9855496	2019	109997

Nissos Christiana	9694658	2015	114264
Nolde	9787924	2018	115024
Nordmarlin	9779989	2017	113959
ON Peace	9893204	2021	114623
ON Phoenix	9893228	2021	114623
Pantelis	9865104	2020	115468
Perseus Star	9891684	2021	116026
Prostar	9833723	2019	115643
Rong Lin Wan	9783423	2017	109783
Sea Beauty	9806627	2018	156634
Sea Icon	9806615	2017	156634
Sealegend	9906568	2021	115648
Seaodyssey	9740419	2017	113176
Searover	9765017	2017	114049
Searuby	9759795	2017	114034
Searunner	9765029	2017	114129
Seasprite	9711468	2015	113998
Seriana	9732228	2015	109991
SFL Panther	9664782	2015	115054
SFL Puma	9664794	2015	115054
SFL Tiger	9664809	2015	115024
SFL Trinity	9799862	2017	115711
Sparto	9865116	2020	115468
Spetses Lady	9831074	2020	109992
Star Energy	9773935	2016	156634
Stellata	9732230	2016	109990
Stemnitsa	9693070	2015	109999
STI Alexis	9696694	2015	109999
STI Connaught	9697600	2015	109999
STI Gallantry	9712876	2016	109999
STI Gladiator	9722170	2017	109999
STI Grace	9722584	2016	109999
STI Gratitude	9722182	2017	109999
STI Guard	9717101	2016	109999
STI Jermyn	9722596	2016	109999
STI Kingsway	9712852	2015	109999
STI Lavender	9838254	2019	109994
STI Lily	9838242	2019	109994
STI Lobelia	9838228	2019	109994
STI Oxford	9697595	2015	109999
STI Rambla	9730880	2017	109999
STI Solace	9708588	2016	109999
STI Solidarity	9708576	2015	109999
STI Spiga	9708148	2015	109999
STI Stability	9712840	2016	109999
STI Steadfast	9719719	2016	109999

STI Supreme	9719721	2016	109999
STI Symphony	9719692	2016	109999
STI Veneto	9690822	2015	109999
STI Winnie	9696709	2015	109999
Torm Helene	9904871	2021	115575
Torm Herdis	9797981	2018	115109
Torm Hermia	9797993	2018	114000
Torm Hilde	9798014	2018	114751
Torm Kiara	9701554	2015	114322
Torm Kirsten	9701566	2015	114445
Torm Kristina	9694646	2015	114322
Ypapanti	9693082	2016	109999
Yuan Lan Wan	9845946	2020	109844

B.5. LNG Carriers

Table B.5: The LNG Carriers used in the case study of this report.

Shipname	IMO number	Built Year	DWT [t]
Adamastos	9879698	2021	93400
Adriano Knutsen	9831220	2019	96354
Amberjack LNG	9845776	2020	93535
Aristarchos	9862918	2021	93427
Aristidis I	9862906	2021	93369
Asklipios	9884021	2021	93400
Attalos	9862920	2021	93400
Bonito LNG	9845788	2020	93535
Boris Davydov	9768394	2018	96766
Boris Vilkitsky	9768368	2017	96958
British Achiever	9766542	2018	94303
British Contributor	9766554	2018	94442
British Listener	9766566	2019	94494
British Mentor	9766578	2019	94528
British Partner	9766530	2018	94442
British Sponsor	9766580	2019	94360
BW Lesmes	9873840	2021	94167
BW Lilac	9758076	2018	95978
BW Magnolia	9850666	2020	95547
BW Pavilion Aranda	9792606	2019	95876
BW Pavilion Aranthera	9850678	2020	95789
BW Pavilion Leeara	9640645	2015	91496
BW Pavilion Vanda	9640437	2015	91515
BW Tulip	9758064	2018	95785
Castillo de Caldelas	9742819	2018	93241
Castillo de Merida	9742807	2018	93241
Celsius Canberra	9864796	2021	91838
Celsius Carolina	9878723	2021	91838

Celsius Charlotte	9878711	2021	92253
Celsius Copenhagen	9864784	2020	91838
Christophe de Margerie	9737187	2016	96779
Clean Horizon	9655444	2015	89831
Clean Vision	9655456	2016	89863
Cool Discoverer	9861031	2020	93668
Cool Explorer	9640023	2015	81891
Diamond Gas Crystal	9874454	2021	89846
Diamond Gas Metropolis	9862487	2020	96000
Diamond Gas Rose	9779238	2018	94028
Diamond Gas Victoria	9874466	2021	83000
Dorado LNG	9863182	2020	96000
Eduard Toll	9750696	2017	96840
Elisa Larus	9852975	2020	95418
Energy Atlantic	9649328	2015	89766
Energy Endeavour	9854624	2021	94648
Energy Innovator	9758832	2019	88668
Energy Integrity	9859739	2021	94648
Energy Intelligence	9881201	2021	94649
Energy Pacific	9854612	2020	94648
Energy Universe	9758844	2019	88700
Enshu Maru	9749609	2018	83708
Fedor Litke	9768370	2017	96765
Flex Artemis	9851634	2020	95450
Flex Aurora	9857365	2020	93775
Flex Courageous	9825439	2019	95619
Flex Endeavour	9762261	2018	95802
Flex Rainbow	9709037	2018	88564
Flex Ranger	9709025	2018	88684
Flex Resolute	9851646	2020	95450
Flex Vigilant	9862475	2021	93764
Flex Volunteer	9862463	2021	93608
GAIL Bhuwan	9877145	2021	98882
GasLog Galveston	9864928	2021	96000
GasLog Geneva	9707508	2016	87975
GasLog Genoa	9744013	2018	88016
GasLog Georgetown	9864916	2020	96000
GasLog Gibraltar	9707510	2016	87981
GasLog Gladstone	9744025	2019	87595
GasLog Glasgow	9687021	2016	87975
GasLog Greece	9687019	2016	87975
GasLog Hong Kong	9748904	2018	92266
GasLog Salem	9638915	2015	82023
GasLog Wales	9853137	2020	93077
GasLog Warsaw	9816763	2019	92996
GasLog Wellington	9876660	2021	93695

GasLog Westminster	9855812	2020	92800
GasLog Winchester	9876737	2021	93695
GasLog Windsor	9819650	2020	92764
Georgiy Brusilov	9768382	2018	96847
Georgiy Ushakov	9750749	2019	96796
Global Sea Spirit	9880465	2021	93080
Golar Tundra	9655808	2015	87159
Gui Ying	9878888	2021	91497
Hellas Athina	9872999	2021	92850
Hellas Diana	9872987	2021	92850
Hoegh Esperanza	9780354	2018	92008
Hoegh Galleon	9820013	2019	86057
Hoegh Gannet	9822451	2018	92800
Hoegh Giant	9762962	2017	81624
Kinisis	9785158	2018	95673
Kool Baltic	9654878	2015	93508
Kool Boreas	9654880	2015	94700
Kool Firn	9864746	2020	93025
Kool Orca	9870525	2021	92969
La Mancha Knutsen	9721724	2016	92082
La Seine	9845764	2020	93534
LNG Adventure	9870159	2021	87900
LNG Dubhe	9834296	2019	91588
LNG Endeavour	9893606	2021	96000
LNG Endurance	9874492	2021	96000
LNG Enterprise	9874480	2021	96000
LNG Fukurokuju	9666986	2016	83809
LNG Megrez	9834325	2020	91430
LNG Merak	9834301	2020	91451
LNG Phecda	9834313	2020	91451
LNG Rosenrot	9877133	2021	98936
LNG Sakura	9774135	2018	82137
LNG Schneeweisschen	9771913	2018	98747
LNGShips Athena	9872949	2021	93535
LNGShips Empress	9875800	2021	88592
LNGShips Manhattan	9872901	2021	93535
Magdala	9770921	2018	95449
Maran Gas Achilles	9682588	2016	81739
Maran Gas Agamemnon	9682590	2016	81739
Maran Gas Alexandria	9650054	2015	90500
Maran Gas Amorgos	9887217	2021	93080
Maran Gas Andros	9810379	2019	94638
Maran Gas Chios	9753014	2019	94945
Maran Gas Hector	9682605	2016	81739
Maran Gas Hydra	9767962	2019	94985
Maran Gas Ithaca	9892717	2021	93080

Maran Gas Kalymnos	9883742	2021	93080
Maran Gas Mystras	9658238	2015	90300
Maran Gas Olympias	9732371	2017	95194
Maran Gas Pericles	9709489	2016	92776
Maran Gas Roxana	9701229	2017	95194
Maran Gas Sparta	9650042	2015	90392
Maran Gas Spetses	9767950	2018	94945
Maran Gas Troy	9658240	2015	89240
Maran Gas Ulysses	9709491	2017	81514
Maran Gas Vergina	9732369	2016	95194
Maria Energy	9659725	2016	93301
Marvel Crane	9770438	2019	97794
Marvel Hawk	9760770	2018	89432
Marvel Heron	9770440	2019	92659
Marvel Pelican	9759252	2019	83636
Marvel Swan	9880192	2021	88831
Megara	9770945	2018	95212
Minerva Limnos	9854375	2021	94834
Minerva Psara	9854363	2021	94834
Mu Lan	9878876	2021	91497
Murex	9705641	2017	95235
Myrina	9770933	2018	95378
Nikolay Urvantsev	9750660	2019	96779
Nikolay Yevgenov	9750725	2019	96821
Nikolay Zubov	9768526	2019	96865
Nohshu Maru	9796781	2019	97902
Ougarta	9761267	2017	94575
Pan Americas	9750232	2018	88425
Pan Europe	9750244	2018	88407
Pearl LNG	9862346	2020	88592
Prism Brilliance	9810551	2019	97494
Prism Courage	9888481	2021	97494
Qogir	9851787	2020	88592
Rias Baixas Knutsen	9825568	2019	96352
Rioja Knutsen	9721736	2016	92782
Rudolf Samoylovich	9750713	2018	96703
SCF La Perouse	9849887	2020	92923
Seapeak Creole	9681687	2016	95253
Seapeak Glasgow	9781918	2018	91549
Seapeak Oak	9681699	2016	95253
Seapeak Yamal	9781920	2019	91549
Shinshu Maru	9791200	2019	82287
SK Audace	9693161	2017	94656
SK Resolute	9693173	2018	94666
Sohshu Maru	9791212	2019	82254
Tessala	9761243	2016	94575

Traiano Knutsen	9854765	2020	96354
Transgas Force	9861811	2021	94360
Transgas Power	9861809	2021	94414
Vivit Americas LNG	9864667	2020	93534
Vladimir Rusanov	9750701	2018	96844
Vladimir Vize	9750658	2018	96851
Vladimir Voronin	9750737	2019	96840
Woodside Rees Withers	9810367	2019	94732
Yakov Gakkel	9750672	2019	96839
Yiannis	9879674	2021	92619